The Journal of Gemmology

2014 / Volume 34 / No. 3

The Gemmological Association of Great Britain

The Journal of
Gemmology
2014 / Volume 34 / No. 3

COLUMNS

ARTICLES

Feature Articles

Gemmological Briefs

Cover Photo:

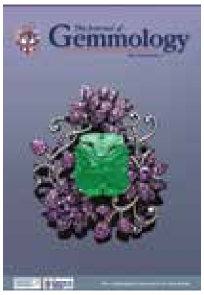

Burmese jadeite is well known for its attractive coloration and transparency. Jadeite-bearing rocks may contain a wide variety of mineral assemblages in fine-grained aggregates that create challenges for the proper characterization and naming of these materials, as discussed in the article by L. Franz et al. on pp. 210–229. The brooch on the cover features a carved piece of Burmese jadeite (6.40 × 5.30 cm) that is set with amethyst and diamonds in platinum and silver. Courtesy of Carnet by Michelle Ong, Hong Kong; photo by Tino Hammid.

The Journal is published by Gem-A in collaboration with SSEF and with the support of AGL and GIT.

ISSN: 1355-4565, http://dx.doi.org/10.15506/JoG.2014.34.3

The Journal of Gemmology

Editor-in-Chief
Brendan M. Laurs
brendan.laurs@gem-a.com

Production Editor
Mary A. Burland
mary.burland@gem-a.com

Marketing Consultant
Ya'akov Almor
bizdev@gem-a.com

Executive Editor
James H. Riley

Editor Emeritus
Roger R. Harding

Assistant Editor
Michael J. O'Donoghue

Associate Editors
Edward Boehm, *RareSource, Chattanooga, Tennessee, USA;* Alan T. Collins, *King's College London;* John L. Emmett, *Crystal Chemistry, Brush Prairie, Washington, USA;* Emmanuel Fritsch, *University of Nantes, France;* Rui Galopim de Carvalho, *Portugal Gemas, Lisbon, Portugal;* Lee A. Groat, *University of British Columbia, Vancouver, Canada;* Thomas Hainschwang, *GGTL Gemlab–Gemtechlab Laboratory, Balzers, Liechtenstein;* Henry A. Hänni, *GemExpert, Basel, Switzerland;* Jeff W. Harris, *University of Glasgow;* Alan D. Hart, *The Natural History Museum, London;* Ulrich Henn, *German Gemmological Association, Idar-Oberstein;* Jaroslav Hyršl, *Prague, Czech Republic;* Brian Jackson, *National Museums Scotland, Edinburgh;* Stefanos Karampelas, *Gübelin Gem Lab Ltd., Lucerne, Switzerland;* Lore Kiefert, *Gübelin Gem Lab Ltd., Lucerne, Switzerland;* Hiroshi Kitawaki, *Central Gem Laboratory, Tokyo, Japan;* Michael S. Krzemnicki, *Swiss Gemmological Institute SSEF, Basel;* Shane F. McClure, *Gemological Institute of America, Carlsbad, California;* Jack M. Ogden, *Striptwist Ltd., London;* Federico Pezzotta, *Natural History Museum of Milan, Italy;* Jeffrey E. Post, *Smithsonian Institution, Washington DC, USA;* Andrew H. Rankin, *Kingston University, Surrey;* George R. Rossman, *California Institute of Technology, Pasadena, USA;* Karl Schmetzer, *Petershausen, Germany;* Dietmar Schwarz, *AIGS Lab Co. Ltd., Bangkok, Thailand;* Menahem Sevdermish, *GemeWizard Ltd., Ramat Gan, Israel;* Guanghai Shi, *China University of Geosciences, Beijing;* James E. Shigley, *Gemological Institute of America, Carlsbad, California;* Christopher P. Smith, *American Gemological Laboratories Inc., New York;* Evelyne Stern, *London;* Elisabeth Strack, *Gemmologisches Institut, Hamburg, Germany;* Tay Thye Sun, *Far East Gemological Laboratory, Singapore;* Pornsawat Wathanakul, *Gem and Jewelry Institute of Thailand, Bangkok;* Chris M. Welbourn, *Reading, Berkshire;* Joanna Whalley, *Victoria and Albert Museum, London;* Bert Willems, *Gilching, Germany;* Bear Williams, *Stone Group Laboratories LLC, Jefferson City, Missouri, USA;* J.C. (Hanco) Zwaan, *National Museum of Natural History 'Naturalis', Leiden, The Netherlands.*

Content Submission

The Editor-in-Chief is glad to consider original articles, news items, conference/excursion reports, announcements and calendar entries on subjects of gemmological interest for publication in *The Journal of Gemmology*. A guide to the preparation of manuscripts is given at www.gem-a.com/publications/journal-of-gemmology.aspx, or contact the Production Editor.

Subscriptions

Gem-A members receive *The Journal* as part of their membership package, full details of which are given at www.gem-a.com/membership.aspx. Laboratories, libraries, museums and similar institutions may become Direct Subscribers to *The Journal* (see www.gem-a.com/publications/subscribe.aspx).

Advertising

Enquiries about advertising in *The Journal* should be directed to the Marketing Consultant. For more information, see www.gem-a.com/publications/journal-of-gemmology/advertising-in-the-journal.aspx.

Copyright and Reprint Permission

Abstracting with credit to the source, photocopying isolated articles for noncommercial classroom use, and photocopying by libraries for private use of patrons, are permitted. Requests to use images published in *The Journal* should be directed to the Editor-in-Chief. Give the complete reference citation and the page number for the image(s) in question, and please state how and where the image would be used.

The Journal of Gemmology is published quarterly by Gem-A, The Gemmological Association of Great Britain. Any opinions expressed in *The Journal* are understood to be the views of the contributors and not necessarily of the publisher.

Printed by DG3 (Europe) Ltd.
© 2014 The Gemmological Association of Great Britain
ISSN: 1355-4565

Mixed Sources
Product group from well-managed forests and other controlled sources
www.fsc.org Cert no. TT-COC-002454
© 1996 Forest Stewardship Council

Gem-A
THE GEMMOLOGICAL ASSOCIATION OF GREAT BRITAIN

21 Ely Place
London EC1N 6TD
UK

t: +44 (0)20 7404 3334
f: +44 (0)20 7404 8843
e: information@gem-a.com
w: www.gem-a.com

Registered Charity No. 1109555
Registered office: Palladium House,
1–4 Argyll Street, London W1F 7LD

President
Harry Levy

Vice Presidents
David J. Callaghan, Alan T. Collins, Noel W. Deeks, E. Alan Jobbins, Michael J. O'Donoghue, Andrew H. Rankin

Honorary Fellow
Emmanuel Fritsch

Honorary Diamond Member
Martin Rapaport

Honorary Life Members
Anthony J. Allnutt, Hermann Bank, Terence M.J. Davidson, Peter R. Dwyer-Hickey, Gwyn M. Green, Roger R. Harding, John S. Harris, J. Alan W. Hodgkinson, John I. Koivula, C.M. (Mimi) Ou Yang, Evelyne Stern, Ian Thomson, Vivian P. Watson, Colin H. Winter

Chief Executive Officer
James H. Riley

Council
Jason F. Williams – Chairman
Mary A. Burland, Jessica M. Cadzow, Steven J.C. Collins, Paul F. Greer, Nigel B. Israel, Jonathan Lambert, Richard M. Slater, Miranda E.J. Wells, Stephen Whittaker

Branch Chairmen
Midlands – Georgina E. Kettle
North East – Mark W. Houghton
South East – Veronica Wetten
South West – Richard M. Slater

Understanding Gems™

What's New

INSTRUMENTS AND TECHNIQUES

Gem Spectra Database

Images and descriptions of absorption and emission spectra (the type collected with a handheld or desktop spectroscope) have been compiled into a useful database by John Harris FGA at www.gemlab.co.uk. According to notes on the website, "This database is mainly for use by students studying gemmology in the courses offered by the Gemmological Association of Great Britain and the National Association of Goldsmiths."

As of September 2014, the spectra database covers gem materials of the following colour groups: colourless, red, pink, orange, yellow, green, brown and blue. The spectra are available as downloadable Excel files for gems of specific colour ranges, such as the following for blue stones: BL1 Blue, BL2 Greenish Blue and BL3 Lavender and Indigo Blue. Work on the final gem colour group (violet and purple) is in progress, and should be completed within a few months.

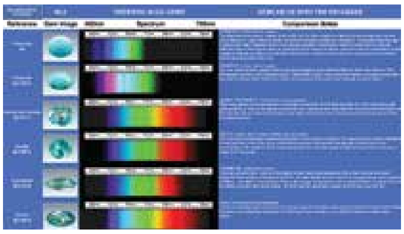

Users may also view spectra according to gem variety. As of September 2014, these include beryl (emerald), chrysoberyl (including alexandrite), corundum (ruby, blue sapphire and synthetic colour-change corundum), diamond, garnet (almandine), glass (cobalt blue), jadeite (green), peridot, spinel (red, green, blue and synthetic blue spinel) and zircon (high and low types).

Sarine DiaMension Axiom

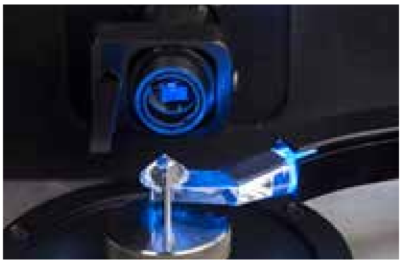

In the 1990s Sarine (then Sarin) Technologies introduced the first system to measure the cut characteristics of polished diamonds based on shadow technology, becoming a standard in most well-equipped gemmological labs and cutting workshops. In August 2014, Sarine added a new breakthrough to the measuring technology using an automatic microscopic dimension. The result is the DiaMension Axiom, which includes a sophisticated new illumination technology combined with a highly accurate optical system and a state-of-the-art motion system, resulting in micron-scale accuracy. The instrument makes direct measurements of a faceted diamond's geometry, in addition to the traditional three-dimensional modelling of cut characteristics. This gives complementary symmetry measurements that are not obtained with shadow mapping, while enabling full automatic symmetry grading. In light of the instrument's accuracy, the measurement results are repeatable regardless of where or how many times a diamond is measured. The DiaMension Axiom also offers the user important visual microscopic information as required for evaluating the cut perfection of a diamond.

Tamar Brosh (tamar.brosh@sarine.com)
Sarine Technologies Ltd., Kfar Saba, Israel

NEWS AND PUBLICATIONS

Gem Testing Laboratory (Jaipur, India) Newsletter

The latest Lab Information Circular (Vol. 70, July 2014), available at www.gtljaipur.info/Lab%20Information%20Circular.asp, describes microscopic features in emeralds fracture-filled with resin and oil, quartz coated with diamond chips, 'Bumble-

GEM TESTING LABORATORY

LAB INFORMATION CIRCULAR

bee' jasper, Raman spectroscopy with a 375 nm UV laser, Ti-diffused synthetic sapphires, beads and faceted stones composed of a ceramic material imitating hematite, and coated and/or dyed mollusc shell.

GSA Gem Session Abstracts

A session titled 'Gemological Research in the 21st Century: Exploration, Geology, and Characterization of Diamonds and Other Gem Minerals' will take place at the 2014 Geological Society of America Annual Meeting in Vancouver, British Columbia, Canada (19–22 October 2014), and abstracts for this session are available at https://gsa.confex.com/gsa/2014AM/webprogram/Session 35272.html and https://gsa.confex.com/gsa/ 2014AM/webprogram/Session36607.html.

GSA 2014

GIA Reports on Mozambique Rubies and Nigerian Sapphires

The Gemological Institute of America posted reports describing the location, geology and gemmology of corundum from these two localities in October 2013 and August 2014, respectively. 'Rubies from the Montepuez Area (Mozambique)' can be accessed at www.gia.edu/gia-rubies-from-montepuez-area, and 'Blue sapphires from the Mambilla Plateau, Taraba State, Nigeria' at www.gia.edu/gia-news-research-nigerian-source-blue-sapphire.

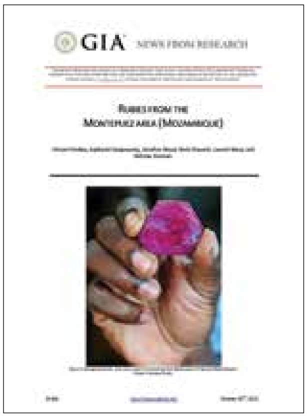

GIA NEWS FROM RESEARCH

RUBIES FROM THE
MONTEPUEZ AREA (MOZAMBIQUE)

GIA NEWS FROM RESEARCH

Blue sapphires
from the Mambilla Plateau,
Taraba State, Nigeria

Goldsmiths' Review 2013/2014

In July 2014, The Goldsmiths' Company released the 2013/2014 issue of the *Goldsmiths' Review*. The issue features articles on history, jewellery design, objets d'art and a new line of replica Cheapside Hoard jewellery, as well as an overview of the Company's activities. The issue costs £6 within the UK and £10 for locations elsewhere. Visit www.thegoldsmiths.co.uk/library/goldsmiths'-review.

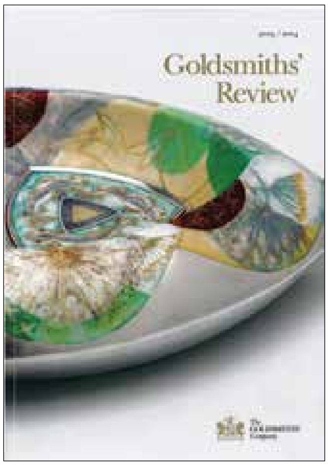

Goldsmiths' Review

ICA Congress 2013 Speaker Presentations

The International Colored Gemstone Association has posted PDF files of presentations from the 15th ICA Congress held in Changsha, China, on 12–16 May 2013. Some presentations are in Chinese and some are in English. Visit http://tinyurl.com/pg4x5zm.

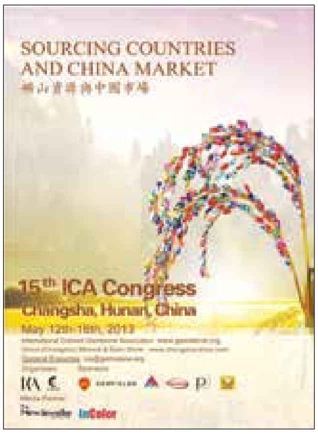

SOURCING COUNTRIES
AND CHINA MARKET

15th ICA Congress
Changsha, Hunan, China
May 12th-16th, 2013

ICGL Newsletter

The International Consortium of Gem-Testing Laboratories has released Newsletter No. 3, Summer

2014, available at http://icglabs.org. It includes two reports on CVD synthetic diamonds and descriptions of treated-colour black diamond earrings, a 10 ct asteriated diamond and pieces of topaz fashioned to look like diamond crystals.

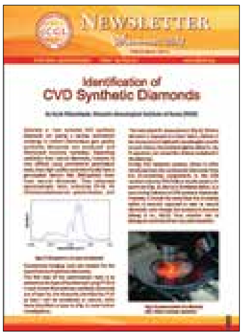

'World of Color' Communication System

In September 2014, GemWorld International Inc. released its new colour communication system, based on the Munsell system. It has more than 1,500 colours represented on 40 individual hue pages, accompanied by overlay charts showing universal scientific nomenclature for all the colour names. Also included is a proprietary simulated gemstone crown for use when comparing the colour of an actual gem, and a companion guide that includes an explanation of colour science, how to grade coloured stones, and grading charts for approximately 50 stones relating the colour system to GemGuide's 1–10 grading scale. The colour system is available for US$495; visit http://gemguide.com/products-page.

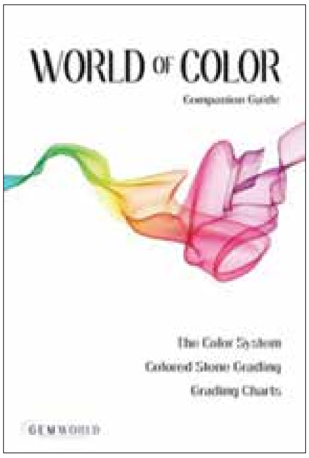

Updated *Fei Cui* Testing Standards in Hong Kong

In July 2014, The Gemmological Association of Hong Kong (GAHK) finalized updates to the document *Standard Methods for Testing Fei Cui for Hong Kong*, which is available for download at www.gahk.org/attachment/fcteststd2.pdf. The report defines the term *fei cui,* lists properties for jadeite jade, omphacite jade and kosmochlor jade, and briefly reviews the types of treatment used on this material. The main part of the document gives recommended methods for testing *fei cui* for gem laboratories. GAHK developed these updated standards in consultation with *fei cui* experts, gemmologists and academia in mainland China and overseas.

World Gold Council's Gold Demand Trends

Every quarter, the World Gold Council releases a report on gold demand trends, and each issue includes a section on jewellery. The Q2 report was released in August 2104. For free downloads, visit www.gold.org/supply-and-demand/gold-demand-trends.

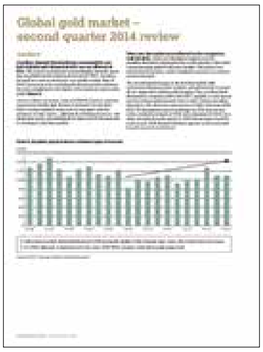

The Journal of Gemmology Indexes: Vols. 29–33

In November 2014, Gem-A will release indexes for Vols. 29–33 (covering 2004–2013). As with previous volume indexes, each will contain a contents listing followed by a detailed subject index. Use these valuable tools to take full advantage of the large amount of information available within these back issues of *The Journal*. A limited number of hard copies will be available, and PDF files will be freely downloadable from *The Journal's* website at www.gem-a.com/publications/journal-of-gemmology.aspx.

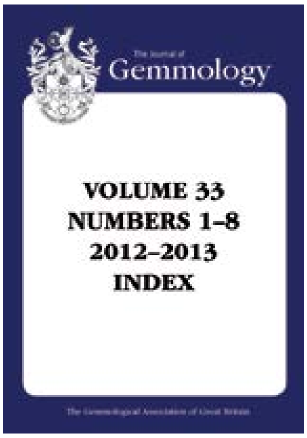

What's New provides announcements of new instruments/technology, publications, online resources and more. Inclusion in What's New does not imply recommendation or endorsement by Gem-A. Entries are prepared by Brendan Laurs unless otherwise noted.

Use of Stacking Software for Expanding Depth-of-Field in Inclusion Photomicrography

Nick Prince

Photomicrographers often desire the ability to capture full scenes (rather than just individual objects) that are completely in focus. This may be important for aesthetic reasons, and also for scientific purposes to give photographic subjects additional context and scale. This is difficult at best with single-shot photography due to depth-of-field limitations, particularly at higher magnifications. However, a photographic method called image stacking can virtually eliminate depth-of-field issues and therefore provide tremendous flexibility for photomicrographers. This process involves taking a series of images of the scene with slightly overlapping depths of field so that all desired elements are captured in focus in the complete photo series. These images are then processed with special 'stacking' software to produce a single photo that represents the entire scene in sharp detail.

For my inclusion photography I use a digital SLR camera, bellows, focusing rail, tripod and extension tubes as necessary. Although high-end equipment may make things easier and add flexibility, I believe that a photographer's technique is more important to the quality of the final image.

Figure 1: This polished crystal of quartz (reportedly from Brazil) contains a series of inclusions (outlined by the red box) that were photographed and processed using image-stacking software. The specimen is 5.6 cm tall and 5.0 cm wide at its base. Photo by N. Prince.

To illustrate my technique for photographing inclusions over a large depth of field, this article provides a case study of the quartz specimen in Figure 1. I obtained this polished quartz crystal many years ago and, although I did not realize it at the time, it contained a series of inclusions that proved wonderful for photography.

To search large specimens such as this quartz crystal for areas of photographic interest, I usually begin at the base and work my way up each face. Lighting is critical, and patience is key when discovering and capturing inclusion scenes that may span several millimetres in depth. Once a scene is identified, I begin the task of positioning the specimen and the lighting for best effect. Lighting does not have to be expensive; I often use Ikea Jansjö LED lamps that sell for about US$10. LEDs minimize heat issues, and the light heads are mounted on goosenecks so several can be easily positioned around a specimen. If the light is too bright or direct, it can be diffused with lens-cleaning sheets or facial tissues attached to the light heads with rubber bands. (However, care should be exercised using this method on hot light sources due to fire

Figure 2: The left image is the first picture in a series of 84 images, showing a large negative crystal at the deepest point photographed in the inclusion scene. The haze across the dark area is created by the out-of-focus series of negative crystals that are shown in the image on the right, which represents the shallow end of the image stack. Photomicrographs by N. Prince; image width 12 mm.

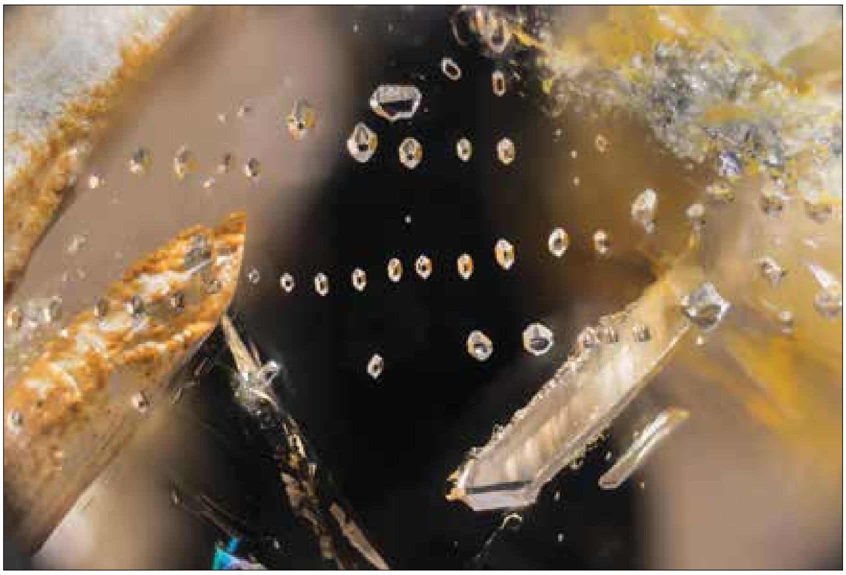

Figure 3: After processing the 84 photos with photo stacking software, the final image, called 'Stars in Alignment', shows the various inclusion features in sharp detail. Photomicrograph by N. Prince; image width 12 mm.

danger.) Although most LEDs produce 'cool' light, the white balance of your photos can be adjusted in-camera or when the image is processed.

When I am ready to 'frame up' the shot, I find the nearest and farthest points in the scene that I want to be in focus. In Figure 2, notice how little of the view is in focus in these photos taken at the 'top' and 'bottom' of the scene, covering a depth of ~10 mm. To capture the complete scene, I shot a series of 84 images, each one after moving the camera so that the focus was slightly shallower in the scene. I suggest 'over shooting' several shots at the beginning and end to compensate for mechanical tolerances in the camera rig. Out-of-focus frames are easily removed before the stacking process, and this is better than having to reshoot the scene for lack of a clean shot or two. Note that when photographing typical inclusion scenes in faceted gemstones, the total depth of field is substantially smaller than in this example, so fewer images will be required to capture a crisp photo. When using a gemmological microscope, the focus knob performs the same function as the focusing rail, and a bellows (or extension tube) is also not necessary.

After all of the photos have been taken, I transfer them to my computer for processing with the stacking software. (I use Zerene Stacker.) The result for this case study, which I call 'Stars in Alignment', is shown in Figure 3.

For readers who desire more information on photo stacking technology, there are a variety of useful articles and online resources (e.g., Piper, 2010; Thiérya and Green, 2012; and http://en.wikipedia.org/wiki/Focus_stacking).

References

Piper J., 2010. Software-based stacking techniques to enhance depth of field and dynamic range in digital photomicrography. In T.D. Hewitson and I.A. Darby (Eds.), *Histology Protocols, Methods in Molecular Biology*, Vol. 611, Humana Press, New York, New York, USA, 193–210, http://dx.doi.org/10.1007/978-1-60327-345-9_16.

Thiérya V. and Green D.I., 2012. The multifocus imaging technique in petrology. *Computers & Geosciences*, **45**, 131–138, http://dx.doi.org/10.1016/j.cageo.2011.10.027.

Nick Prince is a mineral collector and photomicrographer in Atlanta, Georgia, USA. Email: pndpapl@mindspring.com

Gem Notes

COLOURED STONES

Adularia (Including Moonstone) from Austria

For decades, gem and mineral collectors have appreciated gem-quality adularia (a hydrothermal low-temperature variety of orthoclase) from the Zillertal Alps, Tirol, Austria. However, presently it is rare to encounter faceted material from this historic deposit. In February 2012, gem dealer Dudley Blauwet (Dudley Blauwet Gems, Louisville, Colorado, USA) purchased a 947 g rough parcel of this adularia that was reportedly mined during or before the 1980s. Cutting of this material has so far produced numerous stones in the 2–5 ct range, and approximately 10 large gems weighing ~15–30 ct. When the cutting is complete, Blauwet anticipates obtaining more than 1,000 carats. A small proportion of this material shows adularescence, and would therefore be considered moonstone.

Blauwet loaned two of the larger oval-cut gems (18.69 and 27.56 ct; Figure 1) to the American Gemological Laboratories for examination. When viewed with strong transmitted light, both stones showed a distinctive white adularescence with a slight blue component that is typical of moonstone. The RIs of 1.520–1.530 (birefringence 0.008–0.010) and SG of 2.57 were consistent with orthoclase (O'Donoghue, 2006). The stones fluoresced weak blue to long-wave UV radiation and weak orange to short-wave UV. Both samples were highly transparent, and microscopic examination revealed only a few elongate, centipede-like inclusions in one of them (Figure 2); similar features are well known in moonstone (e.g. Gübelin and Koivula, 1986). Chemical analysis by energy-dispersive X-ray fluorescence (EDXRF) spectroscopy showed the expected major-to-minor amounts of K, Si, Al, Ba and Sr.

Figure 1: These oval-cut moonstones (27.56 and 18.69 ct) from Austria display noticeable adularescence. Photo by Bilal Mahmood and Alex Mercado.

Figure 2: Elongate, centipede-like inclusions are seen in one of the Austrian moonstones. Photomicrograph by M. Chaipaksa; magnified 70×.

The majority of alkali feldspar possessing adularescence is semi-transparent and has a somewhat 'milky' appearance. It is uncommon to find samples that have both an attractive adularescence and a high degree of transparency.

Monruedee Chaipaksa
(mchaipaksa@aglgemlab.com)
American Gemological Laboratories
New York, New York, USA

References

Gübelin E.J. and Koivula J.I., 1986. *Photoatlas of Inclusions in Gemstones*. ABC Edition, Zurich, Switzerland, 135.

O'Donoghue M. (Ed.), 2006. *Gems*, 6th edn. Butterworth-Heinemann, Oxford, 248–251.

Cat's-eye Apatite from Namibia

In March 2013, this author obtained a parcel of yellow gem rough from a small informal market on the road leading to the Spitzkoppe beryl and topaz area in west-central Namibia. At first glance the material appeared to be heliodor, which is well-known from Klein Spitzkoppe (e.g. Cairncross et al., 1998). The parcel consisted of ~500 g of mostly small fragments (<1 g each), as well as one larger piece that showed obvious chatoyancy.

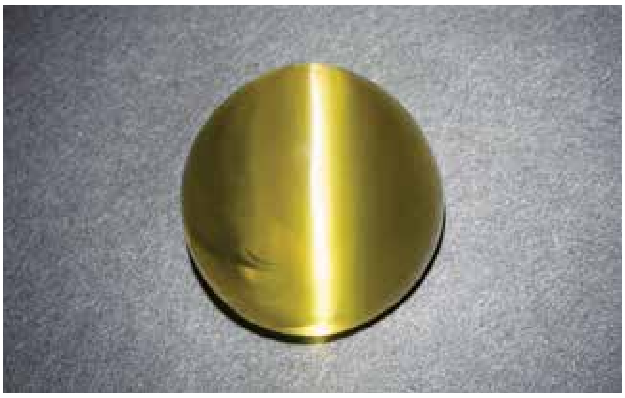

Figure 3: Namibia is the source of this 26.10 ct chatoyant apatite, which resembles fine cat's-eye chrysoberyl. Photo by C. L. Johnston.

To clean the parcel prior to a closer examination, the material was placed in a rock tumbler (together with some aquamarine obtained from the same dealer), and it soon became apparent that the 'heliodor' was actually yellow apatite. There are several apatite localities in Namibia, but the origin of this particular material is unknown. Cutting of the single chatoyant apatite yielded a 26.10 ct round cabochon measuring 15.8 mm in diameter (Figure 3). It is the best Namibian cat's-eye apatite known to this author, with both a sharp eye and an attractive 'golden' yellow colour that are strongly reminiscent of cat's-eye chrysoberyl.

Christopher L. Johnston
(chris@johnstonnamibia.com)
Johnston Namibia c.c., Omaruru, Namibia

Reference

Cairncross B., Campbell I.C. and Huizenga J.M., 1998. Topaz, aquamarine, and other beryls from Klein Spitzkoppe, Namibia. *Gems & Gemology*, **34**(2), 114–125, http://dx.doi.org/10.5741/gems.34.2.114.

Colour-change Axinite-(Mn) from Tanzania

During the June 2014 JCK show in Las Vegas, Nevada, USA, gem dealer Mark Kaufman (Kaufman Enterprises, San Diego, California, USA) informed one of us (BML) about an interesting colour-change stone from Tanzania that he had recently faceted. Kaufman obtained the rough material, represented as magnesioaxinite [renamed axinite-(Mg) after the scheme proposed by Burke (2008)], from a supplier who had purchased it in Tanzania in late April 2014. The rough consisted of a large crystal that was broken into several pieces, two of which were facetable. Kaufman cut a 4.48 ct oval stone that showed a distinct colour change, from greenish blue in daylight to lavender purple in incandescent light (Figure 4). He loaned the gem to authors CW and BW for examination and confirmation of its identity.

Figure 4: This 4.48 ct axinite-(Mn) appears greenish blue in daylight and lavender purple in incandescent light. Composite photo by B. Williams.

Members of the axinite group typically exhibit trichroism, and this sample showed pleochroic colours of violet-blue, pink and yellow (with some green appearing at certain angles, presumably due to the facet arrangement creating a blending of the yellow and blue directions

Figure 5: The only internal features seen in the axinite-(Mn) consisted of thin blade-like inclusions. One of them (top-centre) contains fluid and a vapour bubble. Photomicrograph by C. Williams; magnified 40×.

when viewed from certain angles). The gem was eye-clean. Microscopic examination revealed a few thin colourless blade-like inclusions; one of them contained fluid and a vapour bubble (Figure 5). The RIs were 1.672–1.687, yielding a birefringence of 0.015. Hydrostatic SG was 3.27. When viewed with the Chelsea colour filter, the stone appeared distinctly purplish pink. It fluoresced moderately strong orangey red to long-wave UV radiation, and weak green to short-wave UV. EDXRF spectroscopy showed major amounts of Si and Ca, a significant Mn component, and only traces of Fe and V. (Although no Mg was recorded, this relatively light element is not easily detected by EDXRF.) Taken together, the physical and chemical properties identify the stone as axinite-(Mn) [or manganaxinite, $Ca_2MnAl_2BSi_4O_{15}(OH)$] rather than axinite-(Mg), and this was consistent with the Raman spectrum. The presence of significant Mn was also evident with simple magnetic testing, in which the stone was easily pulled across the desk by a rare-earth magnet.

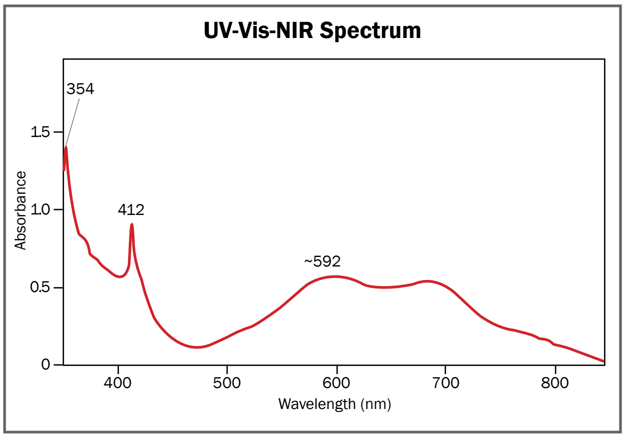

Figure 6: UV-Vis-NIR spectroscopy of the axinite-(Mn) shows features that may be ascribed to Mn^{2+} and V^{3+}.

An ultraviolet-visible–near infrared (UV-Vis-NIR) absorption spectrum of the axinite-(Mn) collected with an Ocean Optics USB4000 spectrometer showed sharp peaks at 354 and 412 nm, and a broad absorption centred at ~592 nm (Figure 6). Similar features were documented in a fragment of pale blue axinite-(Mn) by Arlabosse et al. (2008): a broad band centred at ~597 nm due to V^{3+} and several features that could be due to Mn^{2+}, including sharp peaks at 355, 368, 413 and 421 nm and two broad bands at 515 and 733 nm.

Cara and Bear Williams (info@stonegrouplabs.com)
Stone Group Laboratories
Jefferson City, Missouri, USA

Brendan M. Laurs

References

Arlabosse J.-M., Rondeau B. and Fritsch E., 2008. Gem News International: A blue manganaxinite. *Gems & Gemology*, **44**(1), 81.

Burke E.A.J., 2008. Tidying up mineral names: An IMA-CNMNC scheme for suffixes, hyphens and diacritical marks. *Mineralogical Record*, **39**(2), 131–135.

Green Fluorite from Stak Nala, Pakistan

Pegmatites at Stak Nala in northern Pakistan are famous for producing exceptional specimens of tourmaline, as well as a variety of other minerals (e.g. Laurs et al., 1998). Particularly coveted by mineral collectors are matrix specimens consisting of tricolour tourmaline with white albite and green fluorite. According to gem dealer Dudley Blauwet, there has been sporadic production of small amounts of gem fluorite from Stak Nala since 1982. In June 2013, he obtained a parcel

Figure 7: These fluorites from Stak Nala, Pakistan, weigh 24.07, 28.68 and 17.98 ct, from left to right. Photo by Dirk van der Marel.

of broken fragments of Stak Nala fluorite while visiting Skardu, Pakistan. He sent the 12 cleanest pieces totalling 249.6 g to his cutting factory, and in January 2014 he received 44 stones weighing 226.70 carats that ranged from sub-carat sizes to nearly 30 ct. On a return trip to Skardu in November 2013, Blauwet purchased another similar parcel weighing 243 g from the same dealer, and those pieces will be faceted in the future.

Blauwet loaned three Stak Nala fluorites to this author for examination. The stones weighed 17.98–28.68 ct (Figure 7) and showed an attractive light, strong, bluish green colour. The gemmological properties were consistent with fluorite: RI of 1.434, singly refractive, and a hydrostatic SG of 3.18. The stones appeared green under the Chelsea filter, and showed weak, dark grey anomalous birefringence with the polariscope. They luminesced a weak yellowish 'mustard' green to long-wave UV radiation, and a strong greenish yellow to short-wave UV. After switching off the short-wave UV lamp, the stones showed weak green phosphorescence for a few seconds. All three gems were eye-clean, and microscopic examination of each stone revealed a few rounded to euhedral, transparent, colourless crystal inclusions (Figure 8) that were doubly refractive. The inclusions could not be identified with Raman analysis due to the strong fluorescence of the fluorite and their positions deep inside the stones.

Figure 8: Euhedral mineral inclusions were seen in all three of the fluorites. Photomicrograph by J. C. Zwaan; image width 0.9 mm.

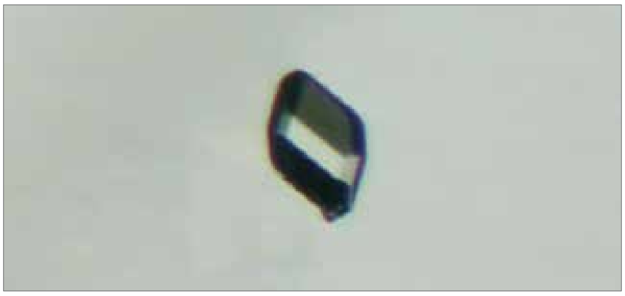

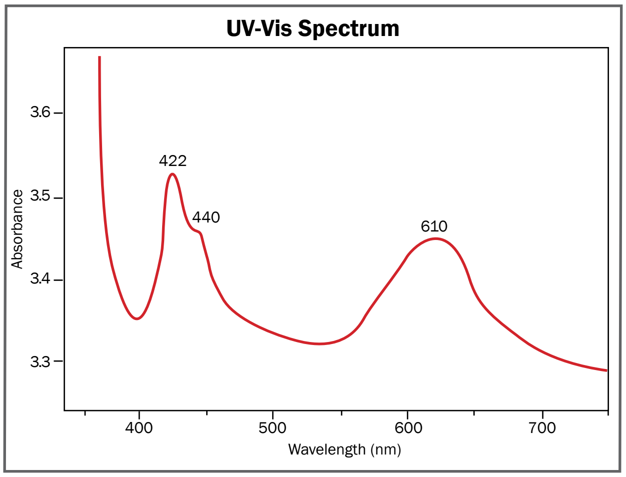

Figure 9: UV-Vis spectroscopy of the fluorite reveals bands at 422, 440 and 610 nm that are associated with Sm^{2+}, which is responsible for the green coloration.

In all three stones, EDXRF analyses revealed traces of Y (~0.7-0.9 wt.% Y_2O_3), Yb (~0.2 wt.% Yb_2O_3) and Mn (~0.04–0.05 wt.% MnO). UV-Vis spectra showed absorptions at 422 nm (with a shoulder at 440 nm) and at 610 nm (Figure 9). These features are reportedly associated with Sm^{2+} ions in light to 'emerald' or 'bright' green fluorite (e.g. from Brazil and from Weardale, England: Bill and Calas, 1978; http://minerals.gps.caltech.edu). Although Sm was not detected by EDXRF, only small concentrations (ppm level) of divalent rare-earth elements such as Sm^{2+} are needed to cause colour in fluorite (cf. Marchand et al., 1976). Yttrium is commonly known to associate with F-centres (produced when an electron is trapped in a vacancy that occupies the position of a fluorine ion) within fluorite to produce various colours. Y-associated F-centres are known to cause blue colour in fluorite, with absorptions at 400 and 590 nm, and may also produce a bluish green colour, with bands at 350, 400 and 600 nm (Kim et al., 2012). However, comparing the latter spectrum with the Sm^{2+}-related features in the Stak Nala fluorites, the position of the peaks is slightly shifted, the shoulder at 440 nm is absent, and the absorption at 400 nm is much stronger than at 600 nm.

J. C. (Hanco) Zwaan (hanco.zwaan@naturalis.nl)
National Museum of Natural History 'Naturalis'
Leiden, The Netherlands

References

Bill H. and Calas G., 1978. Color centres, associated rare-earth ions and the origin of coloration in natural fluorites. *Physics and Chemistry of Minerals,* **3**(2), 117–131, http://dx.doi.org/10.1007/bf00308116.

Kim M., Yoon Y., Kang M. and Shin D., 2012. Spectroscopic characteristics of natural fluorite induced by electron-beam irradiation. *Journal of Ceramic Processing Research,* **13**(5), 541–546.

Green Fluorite from Vietnam

On three separate trips to Luc Yen, Vietnam, in May 2008 and in May and November 2012, gem dealer Dudley Blauwet obtained some interesting dodecahedral crystals of green fluorite. According to his supplier, the fluorite was mined from Cao Bang Province, northeast of Yen Bai. The crystal surfaces were corroded with dendritic grooves and appeared blackish, much different than the 'emerald' green colour of their interior. Black string-like inclusions were visible in some of the material. From the crystal he purchased in 2008, Blauwet had a 55.24 ct stone cut that he donated in 2010 to the National Gem Collection at the Smithsonian National Museum of Natural History in Washington D.C., USA (http://geogallery.si.edu/index.php/en/10209869/fluorite). The rough material he obtained in 2012 consisted of 11 pieces weighing a total of ~430 g. After having them faceted at his cutting factory, in January 2013 he received 62 stones weighing ~480 ct, ranging from sub-carat pieces to nearly 30 ct.

Figure 10: This 29.05 ct fluorite is reportedly from Cao Bang Province in northern Vietnam. Photo by Bilal Mahmood.

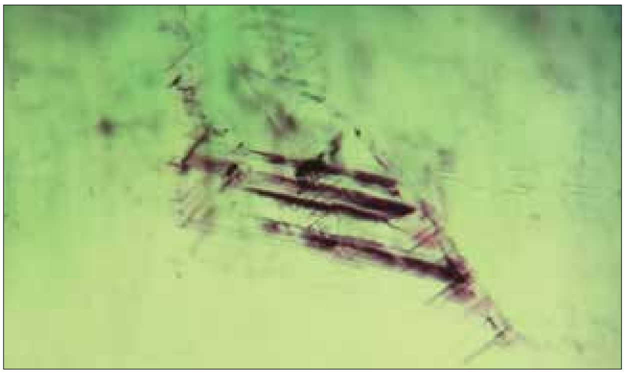

Figure 11: The dark 'inclusions' in the fluorite actually consist of purple colour concentrations. Photomicrograph by M. Chaipaksa; magnified 50×.

Blauwet loaned a 29.05 ct cushion-cut fluorite (Figure 10) to American Gemological Laboratories for examination. The RI of 1.437 and hydrostatic SG of 3.18 were consistent with fluorite (O'Donoghue, 2006). The stone was inert to UV radiation (both long- and short-wave). EDXRF analysis showed only the presence of Ca, and Raman spectroscopy confirmed it was fluorite.

When observed with the unaided eye, the stone displayed an assortment of dark inclusions (Figure 10). Microscopic examination revealed that they actually consisted of angular patterns of dark purple colour concentrations (Figure 11). Other internal features in the fluorite were primary (Figure 12) and secondary two-phase (liquid-gas) inclusions and fluid 'fingerprints' along partially healed fractures (Figure 13). In addition, the stone displayed conspicuous colour banding (green to near-colourless) when viewed through the pavilion with diffused lighting.

In three subsequent trips to Luc Yen, Blauwet has not encountered any more of this fluorite. The angular patterns of dark colour concentrations are quite distinctive, and may be unique to green fluorite from this locality.

Monruedee Chaipaksa

Reference

O'Donoghue M. (Ed.), 2006. *Gems,* 6th edn. Butterworth-Heinemann, Oxford, 411–412.

Figure 12: *Primary two-phase (liquid-gas) inclusions display various jagged forms in the Vietnamese fluorite. Photomicrographs by M. Chaipaksa; magnified 70×.*

Figure 13: *This partially healed fracture in the fluorite consists of a plane of fluid inclusions. Photomicrograph by M. Chaipaksa; magnified 50×.*

Bicoloured Grossular from Kambanga, Kenya

Light yellow-green grossular from Kambanga, Taita-Taveta District, Voi, Kenya, is notable for having a significantly lighter colour than the tsavorite that is commonly known from this part of East Africa (Jang-Green and Beaton, 2009). Recently, some additional production of grossular from this area has included some interesting bicoloured stones. In September 2013, gem dealer Dudley Blauwet received a shipment of rough from his East African supplier that included a small parcel of grossular. Of the 67 small pieces it contained, about 26 of them weighing a total of 6.1 g were strongly colour zoned in green and near-colourless. Blauwet instructed his cutting factory to facet some of the stones as step-cuts to show their distinctive coloration. Of the 38 gems that were faceted from the parcel in January 2014, 10 were bicoloured; these had a total weight of 2.80 carats and the stones ranged from 0.04 to 0.61 ct.

Two bicoloured emerald-cut stones that weighed 0.42 and 0.61 ct (Figure 14) were examined by this author. The pronounced colour zoning exhibited by each stone consisted of two shades of a pure green: (1) a medium, strong green; and (2) a very light green. Face-up, the very light green portion appeared very slightly yellowish. The two stones showed RIs of 1.739 and 1.740, were singly refractive, and had a hydrostatic SG value of 3.64. These properties are consistent with grossular, and are comparable with those obtained by Jang-Green and Beaton (2009) except those authors reported somewhat lower SG values of 3.58–3.60.

Figure 14: *These bicoloured grossulars (0.61 and 0.42 ct) are from Kambanga, Kenya. Photo by Dirk van der Marel.*

The darker parts of the stones fluoresced very weak dark red to long-wave UV radiation and very weak dark orange to short-wave UV. The lighter parts luminesced weak red to long-wave and weak orange to short-wave UV. The stones were moderately to heavily included. Partially healed fissures were most prominent, consisting of randomly positioned voids (Figure 15, left) or of smaller voids arranged in linear arrays (Figure 15, centre); many of the voids contained transparent to whitish solid phases. Raman spectroscopy of these solids in about 10 voids identified calcite; a few voids also contained sulphur. An isolated inclusion of titanite (sphene) also was found in the 0.61 ct grossular (Figure 15, right).

Chemical analysis with EDXRF spectroscopy identified Ca, Al and Si as the main elements, indicating a pure grossular composition, with traces of Mn (~0.2–0.6 wt.% MnO), Fe (~0.1 wt.% FeO) and Ti (~0.3–0.4 wt.% TiO_2). Traces

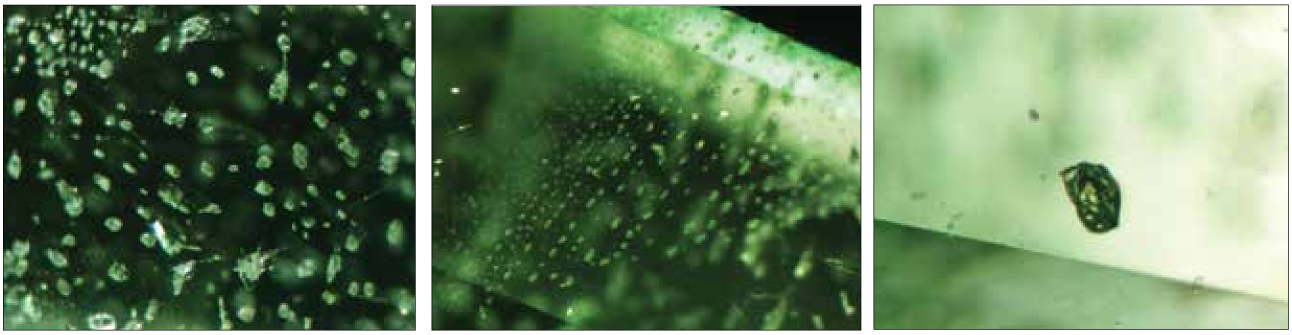

Figure 15: Partially healed fissures were prominent in the grossulars, consisting of randomly arranged voids (left) or smaller voids arranged in linear arrays (centre). Solid inclusions in some of the voids were identified as calcite, with sulphur in a few cases. Also present in one of the stones was an isolated titanite inclusion (right). Photomicrographs by J. C. Zwaan; image width 1.3 mm (left and centre) and 1.2 mm (right).

Table I: Range of trace elements in bicoloured grossular from Kenya, measured by EDXRF.[a]

Oxide (wt.%)	Medium green	Very light green
TiO_2	0.26–0.35	0.25–0.39
V_2O_3	0.32–0.38	0.04–0.08
Cr_2O_3	0.41–0.47	0.09–0.14
MnO	0.51–0.59	0.17–0.48
FeO	0.09–0.10	0.08–0.09

[a] Ranges are based on 20 spot analyses.

of V and Cr also were present, with greater concentrations in the darker green portions (Table I), indicating that both of these elements play a role in causing the green colour (cf. Muije et al., 1979).

UV-Vis-NIR spectra (Figure 16) showed large asymmetrical absorption bands at about 430 and 605 nm, with the most intense absorption at the blue end of the spectrum. The spectra of the darker green portions showed more intense absorption peaks than the lighter green parts, which created a more pronounced and narrower transmission window (centred at about 520 nm). Fourier-transform infrared (FTIR) spectra recorded bands at 3642, 3598, 3564 and 3544 cm^{-1} (Figure 17), which indicate the presence of hydroxyl groups in the garnet structure (Rossman and Aines, 1991).

The chemical composition and UV-Vis-NIR and FTIR spectroscopic features correspond to 'type 4' tsavorites (Mn-bearing chromian-vanadian grossular, with Mn>Cr>V), as

Figure 16: These UV-Vis-NIR spectra of the medium green and light green areas of a bicolour grossular show greater absorption for the darker area, with a more pronounced transmission window centred at about 520 nm, resulting in the darker green colour.

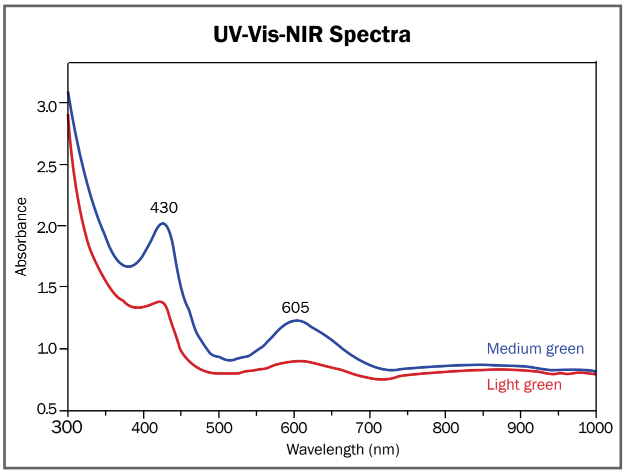

Figure 17: This FTIR spectrum shows the presence of structural OH⁻ in the grossular.

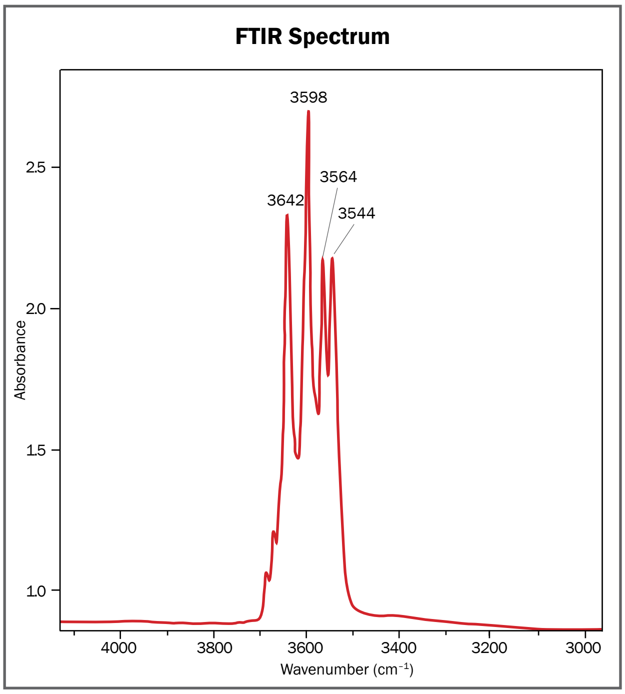

distinguished by Feneyrol et al. (2014). The V/Cr ratio of the samples ranged from 0.7 to 0.9, similar to the ratio in tsavorite from Baraka, Kenya. Also the FTIR spectra, with a main peak at 3598 cm^{-1}, are consistent with tsavorites from this area. In the UV-Vis-NIR region, the absorption bands at 430 and 605 nm are both produced by V^{3+} and Cr^{3+}, but their concentrations were too low to create noticeable features at 697 and 701 nm. In addition, small peaks related to Mn at about 408 and 418 nm were not visible, because they only show up at values greater than ~1.2 wt.% MnO (Feneyrol et al., 2014).

J. C. (Hanco) Zwaan

References

Feneyrol J., Giuliani G., Ohnenstetter D., Rondeau B., Fritsch E., Fallick A.E., Ichang'i D., Omito E., Rakotondrazafy M., Ranatsenho M. and Lallier F., 2014. New typology and origin of tsavorite based on trace-element chemistry. *European Journal of Mineralogy,* **26**, 293–308, http://dx.doi.org/10.1127/0935-1221/2014/0026-2367.

.Jang-Green H. and Beaton D., 2009. Gem News International: Light yellow-green grossular from Kenya. *Gems & Gemology,* **45**(1), 65–66.

Muije P., Muije C.S. and Muije L.E., 1979. Colourless and green grossularite from Tanzania. *Gems & Gemology,* **16**(6), 162–173.

Rossman G.R. and Aines R.D., 1991. The hydrous components in garnets: Grossular-hydrogrossular. *American Mineralogist,* **76**, 1153–1164.

Jade-like Jewellery Materials Sold in Myanmar

A portion of the Myanmar Gems Museum in Yangon consists of the Gems Mart, where numerous gem and jewellery stalls sell various items such as bracelets, bangles, necklaces, rings and decorative objects to tourists as souvenirs (e.g. Figure 18). These materials are also offered at the Myanmar Gems Emporium in Naypyidaw (as rough stones, partially cut pieces, cabochons and bangles), and at the Yangon airport. The jewellery is manufactured in Mandalay, Sagaing and Naypyidaw, using a variety of materials from both the jadeite mining area in north-central Myanmar and the Myitsone area near Myitkyina (located ~10 km east of the jadeite deposits). The colour of these items includes white, yellow, orange to brown, and green to blue (e.g. Figures 19 and 20).

The items sold at the Emporium are tested by gemmologists from the Myanmar Gems Enterprise, and according to a 2013 catalogue the non-jade materials consisted of quartzite, albite, amphibole, serpentine and petrified wood. Approximately 70% of the Emporium parcels consisted of quartzite, and they were bought by foreign merchants from China and Hong Kong. For the experienced gemmologist, it is not difficult to separate the various non-jade materials by their appearance (colour, lustre, and texture) and specific gravity (heft). There was

Figure 18: There are approximately 50 stalls like this one at the Gems Mart within the Myanmar Gems Museum in Yangon. Photo by U Tin Hlaing.

Figure 19: These bangles consist of jadeite (left, 5.5 cm in diameter) and quartzite (right, 6.5 cm). Photo by U Tin Hlaing.

Figure 20: All of the beads in these bracelets are quartzite. Each bracelet is ~6 cm in diameter. Photo by U Tin Hlaing.

no visual evidence of dyeing, waxing, or other treatments in the non-jade materials.

Since the items offered at the Gems Mart are for the tourist souvenir market, they are not labelled with their identities (jadeite or otherwise), but they are priced according to the type and quality of the material and its polish. For example, the asking price for quartzite cabochons was €0.5–1 and bangles ranged from €23 to €350. Bracelets made of round quartzite beads were €0.8–1.5. Petrified wood bangles were €2, and jadeite bangles were €230–765.

U Tin Hlaing (p.tinhlaing@gmail.com)
Dept. of Geology (retired), Panglong University
Myanmar

Blue Kyanite from Tanzania

Tanzania has been known as a source of gem-quality kyanite for many years (e.g. Quinn and Laurs, 2004). While the material documented previously was light greenish blue or very dark blue, some additional kyanite was recently produced that shows a particularly attractive blue colour. Gem dealer Dudley Blauwet obtained two pieces of this material from his supplier in Kenya in September 2013. The combined weight of the pieces was 6.17 g, and they were reportedly mined from the Umba area in Tanzania. Blauwet stated that they were fairly well crystallized (for kyanite), and each had a deep blue stripe along its centre that extended the length of the crystal. After the material was cut in January 2014, he obtained nine stones weighing a total of 6.47 carats that ranged from 0.19 to 1.68 ct.

Two of the kyanites were examined by this author. They weighed 0.19 and 1.68 ct, and showed a medium light, moderately strong, slightly greenish blue coloration (Figure 21). RI readings were 1.716–1.730, yielding a birefringence of 0.014, and the hydrostatic SG was 3.67. These values are typical for kyanite.

Figure 21: These attractive blue kyanites from Tanzania weigh 1.68 and 0.19 ct. Photo by Dirk van der Marel.

Viewed with the dichroscope, both stones showed distinct trichroism in strong, slightly greenish blue, light violetish blue and colourless. They fluoresced weak red to long-wave UV radiation and chalky green-white to short-wave UV. The stones appeared bright red under the Chelsea filter. Using a prism spectroscope, two sharp dark lines were observed in the deep red region, with a red fluorescent line between them. A grey band partly absorbed the green region between about 550 and 610 nm, and the spectrum showed a cut-off in the blue at about 430 nm.

Microscopic examination revealed that the kyanites mainly contained cleavage planes (oriented in two directions) and needle-like tubes (in the larger stone, mainly along the longitudinal direction). Some were connected in such a way that they looked like icicles (e.g. Figure 22). The girdle of the round stone displayed small parallel-oriented incipient cleavage breaks that were reminiscent of the 'bearding' observed in bruted diamonds.

Raman spectra gave an excellent match with the kyanites in the RRUFF database (http://rruff.info/Kyanite). Besides the main elements Al and Si, EDXRF analyses indicated traces of Cr (0.14–0.16 wt.% Cr_2O_3), V (0.09–0.14 wt.% V_2O_3) and Ti (0.02–0.03 wt.% TiO_2). Remarkably, no Fe was detected. FTIR spectra showed features at 3437, 3409, 3386 and 3276 cm^{-1}, confirming the presence of OH^- in the crystal structure of these kyanites (cf. Bell et al., 2004).

Figure 22: The intersection of these needle-like tubes with subtle cleavage planes (nearly horizontal in this view) resembles icicles hanging from a roof in this kyanite. Photomicrograph by J. C. Zwaan; image width 4.2 mm.

The UV-Vis-NIR spectra showed two main absorptions, centred at 400 and 590 nm, with smaller sharp features at 371, 690 and 710 nm (Figure 23). A transmission window centred at 470 nm is responsible for the slightly greenish blue coloration. The feature at 371 nm is known to be associated with Fe^{3+} (Henn and Schollenbruch, 2012), although it must be present in very low concentrations since Fe could not be detected by EDXRF. The peaks at 690 and 710 nm are attributed to Cr^{3+} (Pradat and Choudhary, 2014). This spectrum differs from those reported for 'sapphire'-blue kyanite from Nepal (Henn and Schollenbruch, 2012) that show small peaks at 370, 380, 435 and 445 nm (related to Fe^{3+}), as well as a dominant band centred at 610 nm and a large shoulder at 800 nm, which are attributed to Fe^{2+}-Ti^{4+} and Fe^{2+}-Fe^{3+} intervalence charge transfer, respectively. It also differs from the spectra of blue kyanite from India (Pradat and Choudhary, 2014), which showed features at 690 and 710 nm due to Cr^{3+}, as well as a band centred at 590–610 nm, and smaller peaks at 370, 380, 417, 431 and 446 nm, attributed to Fe^{2+}-Ti^{4+} and Fe^{3+}, respectively. It is also unlike an East African kyanite with a colour change ('alexandrite') effect, probably caused by the presence of chromium and iron, or chromium alone (Bosshart, 1982). On the contrary, the spectrum of this kyanite from Tanzania looks very similar to that of the Cr,V-bearing grossular documented on pp. 195–197 of this issue, except

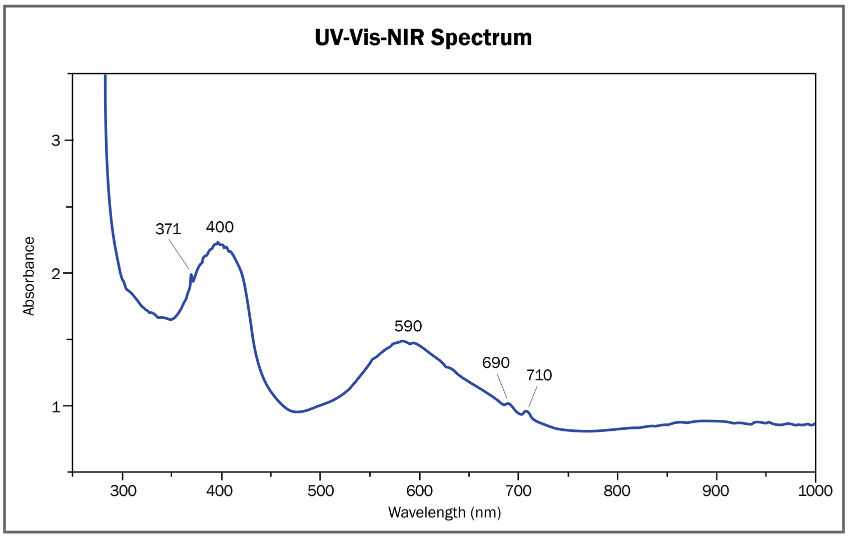

Figure 23: The UV-Vis-NIR spectrum of the kyanite suggests that Cr^{3+} and V^{3+} are the cause of the blue colour, and not Fe^{2+}-Ti^{4+} intervalence charge transfer as in blue kyanite from most other localities. The very small feature at 371 nm does indicate the presence of Fe^{3+}, although iron must be at low concentration since it was not detected by EDXRF.

that the major bands are shifted to 400 and 590 nm, resulting in a slightly greenish blue colour. Together with the fact that Cr and V were the only trace elements detected in these samples, this strongly suggests that both Cr^{3+} and V^{3+} are the colour-causing elements, rather than Fe^{2+}-Ti^{4+} charge transfer. However, more analytical work needs to be done to confirm this hypothesis for the blue kyanite from this locality.

J. C. (Hanco) Zwaan

References

Bell D.R., Rossman G.R., Maldener J., Endisch D., Rauch F., 2004. Hydroxide in kyanite: A quantitative determination of the absolute amount and calibration of the IR spectrum. *American Mineralogist,* **89**, 998–1003.

Bosshart G., 1982. Blue colour-changing kyanite from East Africa. *Journal of Gemmology,* **18**(3), 205–212, http://dx.doi.org/10.15506/jog.1982.18.3.205.

Henn U. and Schollenbruch K., 2012. Saphirblauer Disthen (Kyanit) aus Nepal. *Gemmologie: Zeitschrift der Deutschen Gemmologischen Gesellschaft,* **61**(3-4), 91–98.

Pradat T. and Choudhary G., 2014. Gem News International: Gem-quality Cr-rich kyanite from India. *Gems & Gemology,* **50**(1), 87–88.

Quinn E.P. and Laurs B.M., 2004. Gem News International: Kyanite from Tanzania. *Gems & Gemology,* **40**(4), 341–342.

Rainbow Moonstone from Malawi

Rainbow moonstone is a trade name that has been used for colourless labradorite (a plagioclase feldspar) that displays iridescent colours in the form of labradorescence. This phenomenal behaviour appears quite different from the billowy blue or white glow (adularescence) that is displayed by typical *moonstone* (alkali feldspar). Gem dealer Mark Kaufman recently encountered an old parcel of rainbow moonstone from an unusual locality—Malawi. According to him, Malawi has occasionally produced this material for several years, but the deposit has not proved economically viable due to the small amount of cuttable rough. Nevertheless, some impressive stones have been cut, including a 28.8 ct gem (Figure 24). The parcel seen by Kaufman consisted of ~100 kg of rough, but only 2 kg were of facetable quality. The best stone that he has cut from this lot is a 12.22 ct cushion (Figure 25), which he loaned to Stone Group Labs for examination.

The gem showed pronounced spectral colours when viewed from all angles. The RIs of 1.553–1.566 (birefringence 0.013) were within the expected range for labradorite, and the hydrostatic SG was 2.69. A moderately strong chalky purplish pink fluorescence was observed

Figure 24: Malawi is reportedly the source of this exceptional 28.8 ct rainbow moonstone. Courtesy of James Zigras; photo by Jeff Scovil.

Figure 25: Bright iridescence is displayed by this 12.22 ct rainbow moonstone from Malawi, which was studied for this report. Photo by B. Williams.

under long-wave UV radiation and a weaker greenish yellow luminescence was seen under short-wave UV. This fluorescence behaviour is quite different from that reported for rainbow moonstone from other localities, including India (Johnson and Koivula, 1997), Madagascar (Ito, 2012) and Zambia (Win and Moe, 2012).

Inclusions are to be expected in this type of feldspar, with loupe-clean stones being rare. The only eye-visible inclusion in this stone appeared to consist of a small fracture oriented along a cleavage direction. Microscopic observation revealed lamellar twin planes with needle-like interfaces oriented parallel to the crystal axes. In addition, a tiny surface-reaching fissure appeared to be due to cleavage and contained minor polishing residues.

The distinctive UV fluorescence may help separate Malawi labradorite from other localities, although more samples will need to be examined to confirm this.

Cara and Bear Williams

Brendan M. Laurs

References

Ito C., 2012. Gem News International: Rainbow moonstone from Madagascar. *Gems & Gemology,* **48**(3), 223–224.

Johnson M.L. and Koivula J.I. (Eds.), 1997. Gem News: Blue- and multicolor-sheen moonstone feldspar from India. *Gems & Gemology,* **33**(2), 144–145.

Win W.L. and Moe K.S., 2012. Gem News International: Rainbow moonstone from Zambia. *Gems & Gemology,* **48**(2), 146–147.

Recent Smoky-Citrine Quartz and Tourmaline Discoveries at the Oceanview Mine, Pala, California, USA

During the past several years, a number of important gem-bearing pockets have been found at the Oceanview mine in Southern California, USA (e.g. Mauthner, 2011). These finds have yielded beryl (morganite and aquamarine), spodumene (kunzite and triphane), tourmaline and other minerals. Recently, mine owner Jeff Swanger and his crew have made some interesting discoveries of quartz and pink tourmaline. Since early 2013, a series of pockets have produced some large and clear quartz crystals with an attractive smoky-citrine colour. One of these crystals was polished by gem artist Lawrence Stoller to showcase its clarity and coloration (Figure 26). In addition, some large gemstones have been cut from this material, including a 1,030 ct Portuguese cut (Figure 27) and a 615 ct Mikan cut that was faceted by Philip Osborn, one of Oceanview's miners.

Most recently, in late July 2014, Swanger and his crew found a small pocket in a part of the mine known as Osborn Alley that contained pink tourmaline crystals with flat blue terminations (e.g. Figure 28). This find generated a lot of excitement since the crystals resembled the famous 'blue-cap' tourmalines found in 1972 at the Tourmaline Queen mine, also in the Pala District (e.g. Larson, 2012). So far, approximately three dozen of these tourmalines have been recovered—from both

Figure 26: This crystal of smoky citrine from the Oceanview mine was polished by Lawrence Stoller and measures 31 cm tall and 18 cm wide. Courtesy of James Zigras; photo by Gary Alvis and Lawrence Stoller.

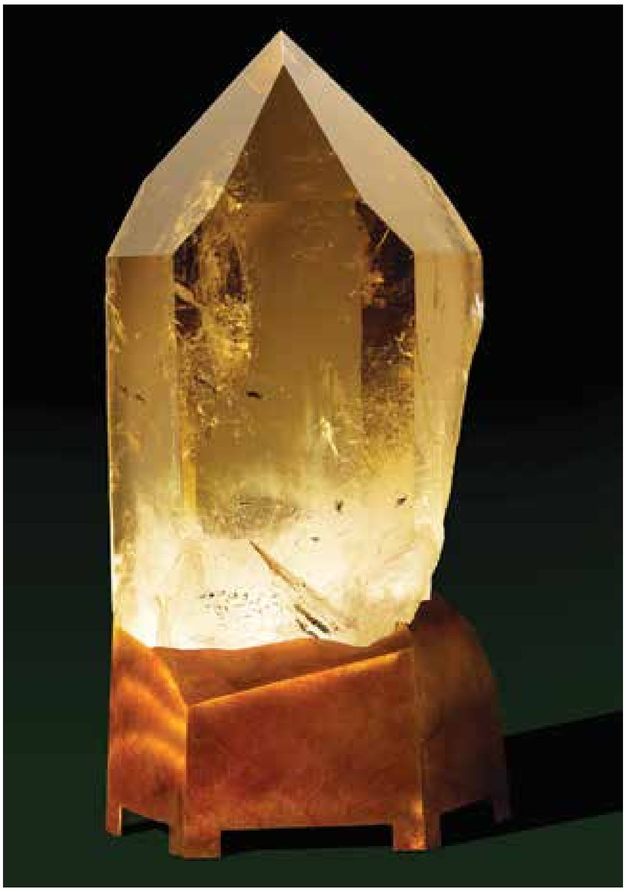

Figure 27: Some large gems have been faceted from smoky citrine produced at the Oceanview mine, such as this 1,030 ct Portuguese cut by Joel Baskin. Courtesy of James Zigras; photo by Jason Baskin.

Figure 28: The Oceanview mine is also the source of these 'blue-cap' tourmalines (each 3.3 cm tall). Courtesy of Oceanview Mines LLC; photo by Mark Mauthner.

the underground workings and from the mine tailings by fee diggers—and the largest crystal measured 4.2 × 3.3 cm. Additional small pockets in this area of the mine have produced a few crystals of morganite and kunzite.

Swanger recently completed a new haulage tunnel that will significantly decrease the distance for removing material from the mine. This will increase efficiency and hopefully bring the miners closer to more gem finds in the near future.

Brendan M. Laurs

References

Larson W.F., 2012. "Blue-caps" find 40th anniversary. *Minerals—The Collector's Newspaper*, **5**, pp. 1 and 7–12, http://spiriferminerals.com/foto_artyk/minerals/minerals5-net.pdf.

Mauthner M., 2011. Recent finds at the Oceanview mine, Pala District, San Diego County, California. *Rocks & Minerals*, **86**(1), 41-49, http://dx.doi.org/10.1080/00357529.2011.537174.

Scheelite from Inner Mongolia

During the 2014 gem shows in Tucson, Arizona, USA, one of us (BML) was informed about an unusual gem originating from Inner Mongolia, China. Gem dealer Mark Kaufman reported that in 2012 some colourless crystals were found at the Huanggang mine that were represented by his Chinese supplier as powellite [$Ca(MoO_4)$]. Powellite forms the molybdenum-rich end member of an isomorphous series with scheelite [$Ca(WO_4)$], which is the tungsten-rich end member. Kaufman obtained one of the crystals in late 2013 that measured about 10 cm long and 3 cm wide, and was broken at its base. He used strong transmitted lighting to detect a facetable area through the naturally etched surface of the crystal, near its termination. He cut a 41.38 ct square cushion, measuring 17.4 × 17.2 mm (Figure 29), and the stone was loaned to authors CW and BW for examination and confirmation of its identity.

The colour of the gem was so white as to appear 'silvery' white, presumably due to the high lustre and refraction. The RI could not be measured since it was over the limit of the refractometer (>1.81). The stone's hydrostatic SG was 5.71. It fluoresced strong chalky yellow to

Figure 29: This scheelite weighs 41.38 ct and is reportedly from Inner Mongolia. Photo by B. Williams.

long-wave UV radiation and moderate chalky yellowish pink to short-wave UV. These properties are largely consistent with those reported for scheelite by O'Donoghue (2006), except that the SG values in that publication are slightly higher. However, this would be expected for scheelite that contains some Mo (i.e. some of the powellite end member). The stone was free of any eye-visible inclusions, and microscopic examination revealed only a few small 'fingerprint' inclusions. In addition, the use of darkfield lighting and higher magnification showed some mist-like diffuse lines of pinpoint dots.

UV-Vis spectroscopy revealed a narrow weak absorption at 378 nm and a broad weak absorption centred at 700 nm. EDXRF spectroscopy showed major amounts of Ca and W, as expected for scheelite, as well as moderate Mo and some Yb. Raman analysis confirmed the stone was scheelite.

Facetable scheelite is considered a collectors' stone due to its rarity and low hardness (4½–5 on the Mohs scale). This 41.38 ct stone is the first faceted scheelite from Inner Mongolia that is known to these authors, and its large size and eye-clean transparency are particularly notable for a gem from a new locality.

Cara and Bear Williams

Brendan M. Laurs

Reference

O'Donoghue M. (Ed.), 2006. *Gems,* 6th ed. Butterworth-Heinemann, Oxford, 446.

PEARLS

Aging Silver-treated Cultured Pearl

The Laboratoire Français de Gemmologie (LFG) recently received a round dark brown pearl for analysis that was taken from a necklace composed entirely of pearls with the same appearance. The owner stated that the necklace was bought in the 1950s and was represented to consist of natural black pearls from the Red Sea region.

The pearl measured 6.8 mm in diameter and was very dark brown with no secondary colour. Magnification revealed an inhomogeneous coloration, as well as a darker area around the drill hole (Figure 30). These features strongly suggest colour treatment.

The pearl was then analysed with X-ray microradiography to observe its inner structures and determine its natural or cultured origin. A round bead was clearly seen inside (Figure 31), establishing that it is a beaded cultured pearl. However, the most interesting aspect of the X-radiograph was a bright-appearing layer surrounding the nucleus. This feature is typically seen within pearls treated with silver nitrate (Webster, 1949; Crowningshield, 1950). In this treatment, pearls are immersed in a silver nitrate solution in the dark. Then the pearls are exposed to light or treated with hydrogen sulphide to precipitate dark-coloured colloidal silver. It is well known that this treatment is used to blacken Akoya cultured pearls. Because the silver nitrate reacts more intensely with organic material, a greater concentration of silver precipitates in the tiny space surrounding the nucleus. Since silver has a much higher opacity to X-rays than the $CaCO_3$ composing the pearl, the X-rays are blocked, producing the bright layer around the nucleus.

Figure 30: The inhomogeneous colour and darker area concentrated around the drill hole of this 6.8 mm cultured pearl are indications of colour treatment. Photo by O. Segura.

Figure 31: With microradiography, a round bead is clearly visible, identifying the sample as a beaded cultured pearl.

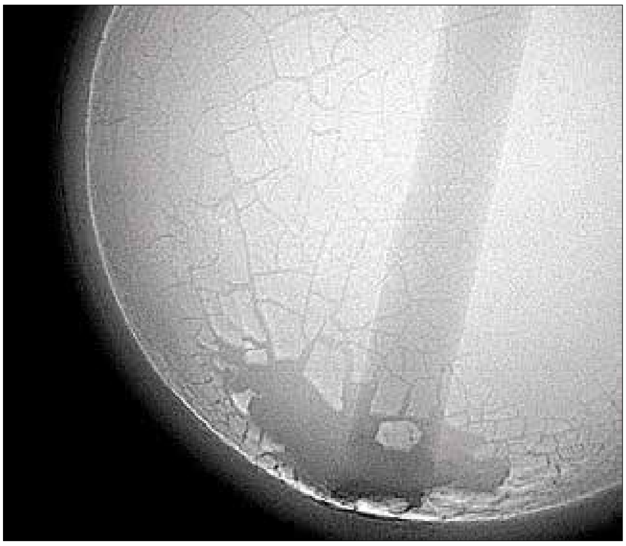

Figure 32: At higher magnification, desiccation cracks are easily seen with microradiography in the aged silver-treated cultured pearl.

As the pearl was rotated and the area near the drill hole inspected and magnified, an unusual fracture pattern was observed in the radiographs. The cultured pearl exhibited a network of desiccation cracks (Figure 32), as commonly seen in mud when it dries and contracts. Near the drill hole, some of the cracked material appeared to be missing, possibly ejected by the movements of the cultured pearl in the necklace. To the authors' knowledge, this has not been previously reported in old untreated cultured pearls of similar nature. Hence, we suggest that the silver nitrate provoked or accelerated the drying of the layer of organic matter present around the nucleus. This eventually resulted in cracking, then flaking. It is likely that similar patterns might be observed if more old treated cultured pearls of a similar nature are observed with high-resolution X-ray microradiography. However, the relatively unattractive nature of such aged, treated cultured pearls makes it unlikely that they would be submitted for detailed inspection by a well-equipped gemmological laboratory.

Olivier Segura (o.segura@bjop.fr)
Laboratoire Français de Gemmologie, Paris, France

Emmanuel Fritsch
Institut des Matériaux Jean Rouxel CNRS
Team 6502, University of Nantes, France

References

Webster R., 1949. Stained pearls and X-rays. *Journal of Gemmology*, **11**(2), 51–54, http://dx.doi.org/10.15506/jog.1949.2.2.51.

Crowningshield R., 1950. Gemological Digests: Reverse pattern noted on half drilled black pearls. *Gems & Gemology*, **6**(11), 353.

TREATMENTS

Dyed Hessonite as a Ruby Imitation

Ruby imitations consisting of dyed-red quartz, sillimanite and corundum are known in the gem trade (e.g. Schmetzer et al., 1992; Singbamroong, 2005). Recently we encountered a different imitation in a parcel of rubies submitted for testing at our laboratory. According to the client, the stones (both faceted and cabochons) had been removed from an old piece of jewellery.

At first glance, the cabochons in the parcel appeared typical of ruby (e.g. Figure 33). Most of the stones had inclusions consisting of short rutile needles and negative crystals, as are commonly

Figure 33: The largest cabochon (2.68 ct) shown here proved to be dyed hessonite. Its appearance closely resembles the accompanying ruby cabochons (0.56, 0.69 and 1.10 ct). Photo by J. Panjikar.

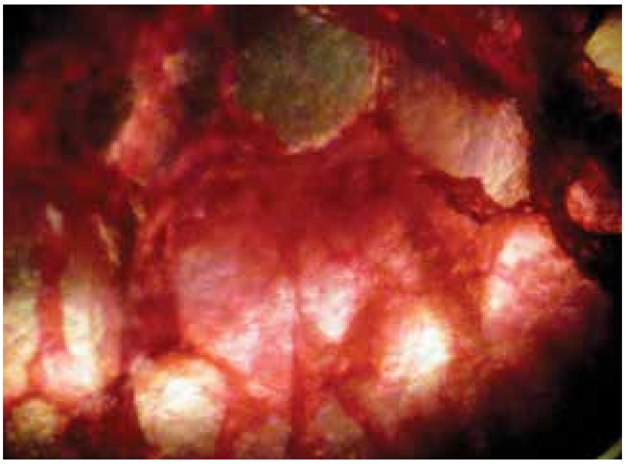

Figure 34: The hessonite showed a typical roiled appearance, as well as red dye concentrations along fractures. Photomicrograph by J. Panjikar; magnified 60×.

seen in rubies from Mogok, Myanmar. However, one of the cabochons proved much different, with the following gemmological properties: isotropic optic character, spot RI of 1.74 and hydrostatic SG of 3.68. Microscopy revealed a roiled appearance with red dye concentrations along fractures (Figure 34), as well as small transparent crystals. These properties identified the stone as dyed hessonite. UV-Vis spectroscopy confirmed that there was no chromium present, and the material was indeed hessonite.

This example serves as a reminder for gemmologists to remain vigilant about detecting imitations in gem parcels, even in those represented as 'old' stones.

Jayshree Panjikar (jayshreepanjikar@gmail.com)
Pangem Testing Laboratory, Pune, India

References

Schmetzer K., Hänni H.A., Jegge E.P. and Schupp E.-J., 1992. Dyed natural corundum as a ruby imitation. *Gems & Gemology*, **28**(2), 112–115, http://dx.doi.org/10.5741/gems.28.2.112.

Singbamroong S., 2005. Gem News International: Fibrolite (sillimanite) dyed and impregnated to imitate ruby. *Gems & Gemology*, **41**(3), 274.

MISCELLANEOUS

The Mirasety Ring: An Ethiopian 'Rainbow' Opal Set with a Hologram

During the 2014 Tucson gem shows, these authors briefly exhibited a unique jewel for the first time: the Mirasety ring, named *FS01*. The ring is shaped like a flying saucer and features an opal bead from Wollo, Ethiopia, that is set over a hologram embedded within a glass disc (Figure 35). This ring is the first embodiment of a new concept by a group of designers, jewellery

Figure 35: Mirasety ring FS01 (42×42 mm) is shown here resting on a dichromate gelatine hologram created by Michael E. Crawford. Photo by F. Mazzero.

Figure 36: A 26.60 ct 'rainbow' opal bead from Wollo, Ethiopia, is set with gold and diamonds for the Mirasety ring. Although not visible in the photo, when this opal is viewed in person the rainbows appear to extend well outside of the stone. The diameter of the bead is 19 mm. Photo by F. Mazzero.

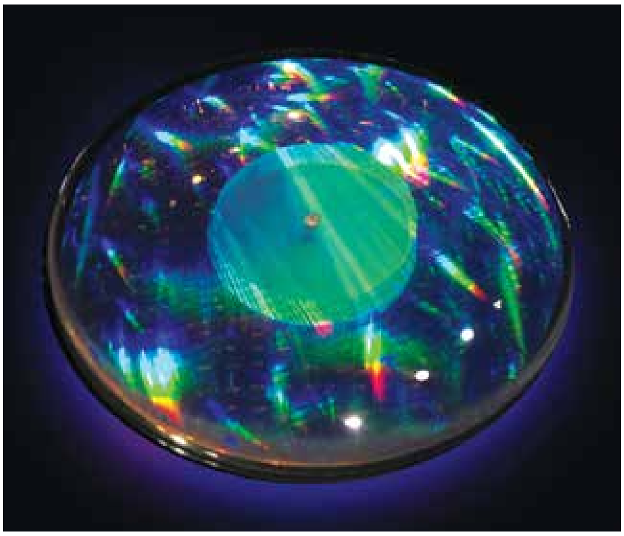

Figure 37: A hologram is embedded in a 38×8 mm round glass disc that in profile forms an ellipse. The upper surface has been drilled and flattened to accommodate the mounted opal in Figure 36. The hologram is registered in a dichromate gelatine emulsion, and was created by one of the authors (AM). Photo by F. Mazzero.

manufacturers, holographers and opal experts, in which jewels associate opals with holographic optical elements. The origin of the concept comes from the unique optical properties displayed by some Ethiopian opals (Gauthier et al., 2004; Fritsch and Rondeau, 2009), as described below.

Play-of-colour opal is composed of a regular three-dimensional grid of isodiametric spheres or lepispheres of hydrated silica ranging from about 150 to 250 nm in diameter; this grid diffracts white light into single spectral colours, producing play-of-colour (Sanders 1964, 1968). The hydrated silica composing the spheres is not crystalline, so therefore opal is not crystalline either. However, their regular and uniform stacking resembles the arrangement of atoms in a crystal. Therefore, play-of-colour opal can be considered a pseudo-crystal, and since it diffracts light in a visible fashion it can also be thought of as an 'optical crystal'.

Sometimes Ethiopian opals show beautiful full rainbows generated by diffraction, as seen in the bead used in the Mirasety ring (Figure 36). The phenomenon is still not well understood, as it contradicts the model of diffraction into single spectral colours (Rondeau et al., 2010; Gauthier et al., 2013). These gems are quite rare, constituting less than 1% of Wollo opals, and this phenomenon has not been observed in opal from any other deposit. The rainbows actually appear to float in space as they project above the surface of the stone. Although this effect is impossible to capture in photos or videos without three-dimensional viewing capability, readers wishing to learn more can access a video that has been placed in the online data depository on *The Journal*'s website.

For this line of jewellery, the holograms are created using an argon laser (488 nm wavelength) in a dichromate-sensitized emulsion with a thickness of only 10 μm that is coated on glass. The emulsion is protected with another glass plate on top. Then this assemblage is cut with high precision to a shape matching the requirements of the designer (e.g. Figure 37). In the Mirasety ring, the hologram generates rainbows that add to those produced by the opal (Figure 38).

Some Ethiopian opals display remarkable optical effects. By combining these 'optical' opals with holograms in jewellery, designers exploring this new field can create unusual pieces that act to sculpt colour and unveil dancing lights which appeal to our emotions.

Francesco Mazzero (mazzero@opalinda.com)
Opalinda, Paris, France

August Muth
The Light Foundry, Santa Fe, New Mexico, USA

Figure 38: The completed Mirasety ring FS01 consists of 54.68 g of 18 carat gold, a 26.60 ct Ethiopian 'rainbow' opal, a 16.3 g hologram set in glass, and four diamonds that have a total weight of 0.61 ct. Photo by F. Mazzero.

References

Fritsch E. and Rondeau B., 2009. Gem News International: Rare optical phenomenon in play-of-color opal. *Gems & Gemology,* **45**(2), 147–148.

Gauthier J.P., Mazzero F., Mandaba Y. and Fritsch E., 2004. L'opale d'Ethiopie: Gemmologie ordinaire et caractéristiques exceptionnelles [Opal from Ethiopia: Typical gemmology and unusual characteristics]. *Revue de Gemmologie,* **149**, 15–23.

Gauthier J.P., Mazzero F., Rondeau B. and Fritsch E., 2013. De l'originalité des opales éthiopiennes [Originality of Ethiopian opals]. *Revue de Gemmologie,* **184**, 11–16.

Rondeau B., Fritsch E., Gauthier J.-P., Mazzero F., Cenki-Tok B., Bekele E. and Gaillou E., 2010. Play-of-color opal from Wegel Tena, Wollo Province, Ethiopia. *Gems & Gemology,* **46**(2), 90–105, http://dx.doi.org/10.5741/GEMS.46.2.90.

Sanders J.V., 1964. Colour of precious opal. *Nature,* **204**(4964), 1151–1153, http://dx.doi.org/10.1038/2041151a0.

Sanders J.V., 1968. Diffraction of light by opals. *Acta Crystallographica Section A,* **24**(4), 427, http://dx.doi.org/10.1107/S0567739468000860.

Errata

1. The Gem Note on Emerald Essence triplets (Vol. 34, No. 2, 2014, p. 109) should have indicated that some of the gems were assembled using colourless beryl for the pavilion and petalite (not phenakite) for the crown. According to Anil Dholakia, petalite was used because of its brighter appearance than beryl.
2. The conference report on the 12th Annual Sinkankas Symposium (Vol. 34, No. 2, 2014, pp. 156–157) should have reported that US$10 billion in Burmese jadeite has been traded since 2006 (not annually). For additional Burmese jadeite production data, see www.palagems.com/gem_news_burma_stats.php.

Shine Bright

Celebrating 20 Years of Opening the World of Jewelry and Gemstones to Everyone!

As the largest retailer of loose gemstones in the world, Jewelry Television is committed to offering more of the naturally beautiful treasures that our customers adore.

Education, Expertise & Entertainment

We take pride in our longstanding commitment to education. With programs like our web-based GEM-A course and our on-air Jewel School® series, our partnerships bring industry luminaries straight into the homes of jewelry and gemstone aficionados everywhere.

Educational videos, professional tools of the trade, plus live programming with knowledgeable hosts place Jewelry Television and jtv.com at the forefront of a dynamic learning and shopping environment.

Into the Future

At the heart of our vision is a continuing quest to deliver the rarest of gemstones, plus educational resources and world-class gemstone authorities to our customers. We believe this is the ultimate way to enlighten, inform and entertain, as we take flight into our next decade.

JTV Your Way

To order call 800-619-3000 or visit jtv.com

20 yrs
jewelrytelevision.

A Comparative Study of Jadeite, Omphacite and Kosmochlor Jades from Myanmar, and Suggestions for a Practical Nomenclature

Leander Franz, Tay Thye Sun, Henry A. Hänni, Christian de Capitani,
Theerapongs Thanasuthipitak and Wilawan Atichat

Jadeitite boulders from north-central Myanmar show a wide variability in texture and mineral content. This study gives an overview of the petrography of these rocks, and classifies them into five different types: (1) jadeitites with kosmochlor and clinoamphibole, (2) jadeitites with clinoamphibole, (3) albite-bearing jadeitites, (4) almost pure jadeitites and (5) omphacitites. Their textures indicate that some of the assemblages formed syn-tectonically while those samples with decussate textures show no indication of a tectonic overprint. Backscattered electron images and electron microprobe analyses highlight the variable mineral chemistry of the samples. Their extensive chemical and textural inhomogeneity renders a classification by common gemmological methods rather difficult. Although a definitive classification of such rocks is only possible using thin-section analysis, we demonstrate that a fast and non-destructive identification as *jadeite jade, kosmochlor jade* or *omphacite jade* is possible using Raman and infrared spectroscopy, which gave results that were in accord with the microprobe analyses. Furthermore, current classification schemes for jadeitites are reviewed.

The Journal of Gemmology, 34(3), 2014, pp. 210–229, http://dx.doi.org/10.15506/JoG.2014.34.3.210

Introduction

The word *jade* is derived from the Spanish phrase for *piedra de ijada* (Foshag, 1957) or 'loin stone' from its reputed use in curing ailments of the loins and kidneys. In former times, jade simply included nephrite (Werner, 1774) and jadeite (Damour, 1863); therefore, its nomenclature was rather simple. Jadeite jade is usually a green massive rock consisting of jadeite ($NaAlSi_2O_6$; see Ou Yang, 1999; Ou Yang and Li, 1999; Ou Yang and Qi, 2001). Nephrite jade, a rock mainly composed of the amphibole tremolite [$Ca_2(Mg,Fe)_5Si_8O_{22}(OH)_2$], shows a similar colour and massive structure, and can be difficult to visually separate from jadeite

Figure 1: The Hutton-Mdivani necklace sold for US$27.44 million at Sotheby's Hong Kong auction in April 2014—a world-record price for a piece of jadeite jade jewellery. It features 27 colour-matched beads (15.4–19.2 mm in diameter) that consist of translucent bright green Imperial jadeite. Photo by Luc Phan, © Swiss Gemmological Institute SSEF.

jade. Microscopically, jadeite jade shows a mixed texture of granular and fibrous polycrystalline aggregates, while nephrite mainly shows a fibrous structure. International bodies such as CIBJO have agreed to use the terms *jadeite jade* or *nephrite jade* for the two materials (CIBJO, 2013). Serpentine and other green rocks are not accepted under the jade umbrella. The most valuable jade variety is so-called *Imperial jadeite,* consisting of pure intense green translucent material from Myanmar (e.g. Figure 1).

In the 1960s, Dr Eduard Gübelin described an interesting new gem material also originating from the Burmese jadeitite area: Maw-sit-sit (Figure 2). It is a rock composed of many minerals, and ranges from white to green and black (Gübelin, 1964–1965, 1965). It was later found that maw-sit-sit contained the first terrestrial occurrence of ureyite ($NaCrSi_2O_6$; cf. Harlow and Olds, 1983), later renamed kosmochlor (Ou Yang, 1984; Harlow and Olds, 1987; Hänni and Meyer, 1997). It became evident that jadeite-related rocks are often composed principally of both pyroxenes and amphiboles, and frequently represent members of solid-solution series. Isovalent ionic substitution such as $Al^{3+} \leftrightarrow Cr^{3+}$ and coupled substitution such as $Na^+ + Al^{3+} \leftrightarrow Ca^{2+} + (Mg^{2+} + Fe^{2+})$ are both common. In addition, samples may contain a variety of non-pyroxene minerals, such as clinoamphibole (mainly sodic and sodic-calcic amphiboles), albite, chromite and others (cf. Harlow and Olds, 1987; Htein and Naing, 1994; Shi et al., 2005a, 2012). Furthermore, individual mineral grains may show pronounced chemical zoning (e.g. Harlow and Olds, 1987; Shi et al., 2005a, 2009, 2012). These factors pose a major problem to gem testing laboratories, firstly for the identification of the mineral constituents and their amounts by straightforward non-destructive procedures, and secondly due to the absence of

Figure 2: Kosmochlor is one of the many constituents of maw-sit-sit, a rock that also commonly contains chromian jadeite, albite, clinochlore, amphibole and chromite. The cabochon shown here weighs 12.09 ct and the polished cobble is 128.02 g (65.7 × 45.3 mm). Photo by Tay Thye Sun.

a. Jadeitites with Kosmochlor and Clinoamphibole (JKC)

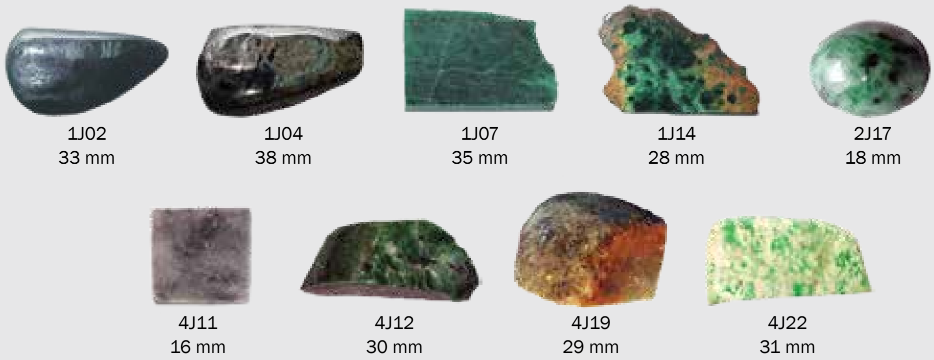

b. Jadeitites with Clinoamphibole (JC)

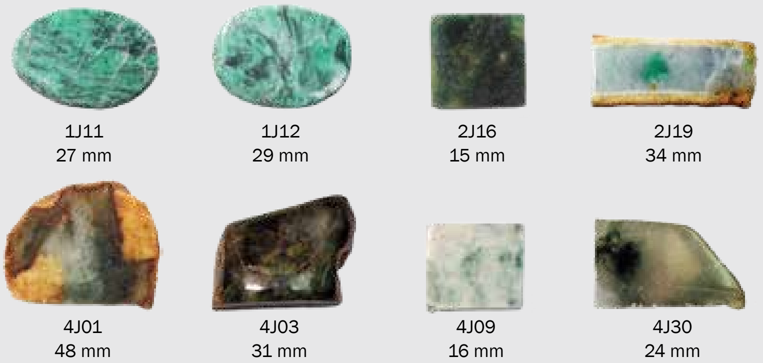

c. Albite-bearing Jadeitites (ABJ)

d. Jadeitites (J)

e. Omphacitites (O)

Figure 3: The samples studied for this report are grouped here according to their classification into five groups based on thin-section investigations. The longest dimension of each piece is shown under the sample number. Photos by Tay Thye Sun.

a simple terminology that can be applied to such a complex gem material.

In 2006, the term *fei cui* was officially implemented by the Hong Kong government to cover jadeitite* gemstones. This umbrella term is used for jadeite, omphacite and kosmochlor jades (Ou Yang et al., 2003; Prosperi et al., 2011). The expression *fei cui* or 翡翠, when used in the course of any trade or business to describe an object, means it is a granular to fibrous polycrystalline aggregate that is composed solely or principally of jadeite, omphacite and/or kosmochlor, or any combination of these minerals (cf. www.gahk.org/attachment/fcteststd2.pdf). However, under this regulation, any rock containing one or more of these three minerals can now be sold in the same category as jadeite jade.

Most jadeite jade in the market comes from the classic Uru River area (Kyaukseinmyo) in northern Myanmar (Chhibber, 1934; Bender, 1983; Hughes et al., 2000; Harlow et al., 2014). For the trade it should not be a problem to communicate to consumers that such material may fall into a number of categories, including some that are more rare and others that are more common. However, for the gemmologist and research scientist, the questions arise: What do these Burmese jades consist of, and how common are omphacite, kosmochlor and mixed members of these pyroxenes? These questions have become even more pertinent with the recognition that there is material circulating in the trade with the appearance, colour and gemmological properties of fine-quality jadeite jade, but it is actually omphacite jade (e.g. McClure, 2012).

Materials and Methods

Eighty-eight samples of rough and cut (slabs and cabochons) 'Burmese jade' were collected in jade markets in Myanmar, Singapore and Hong Kong. From these, petrographic thin sections were cut and polished for 39 of the samples that we considered representative of what one would expect to encounter as cut jades in the marketplace (Figure 3).

Mineral abbreviations used in this article are after Whitney and Evans (2010), except for the following: Q = quadrilateral pyroxenes (diopside-hedenbergite-enstatite-ferrosilite), Cr-Jd = chromian jadeite and Cr-Omp = chromian omphacite. *Chromian* is used to refer to material with <0.01 Cr^{3+} per formula unit (cf. Morimoto et al., 1988).

Gemmological and Petrographic Methods

All 88 samples were visually examined, and their refractive indices were determined by either the spot method or by normal readings from flat-polished surfaces. Specific gravity was determined hydrostatically for all of these samples, and they also were examined with a desk-model prism spectroscope.

The mineralogy and micro-textures of the 39 petrographic thin sections were studied using a Leica DMRX polarized light microscope.

Chemical Analysis

The compositions of rock-forming minerals in the 39 thin sections were quantitatively measured by electron microprobe. The main focus of this investigation was the various types of clinopyroxene. Chemical analyses were performed with a JEOL JXA-8600 electron microprobe at the University of Basel, Switzerland. The instrument was equipped with an ultra-dry silicon energy-dispersive X-ray detector (Noran System 7 spectral imaging system by Thermo Scientific). The accelerating voltage was 15 kV and beam current was 20 nA, and we used a peak counting time of 30 seconds for all elements. Data correction was performed using the Proza ($\varphi\varrho Z$) method. To avoid volatilization of Na we chose a beam size of 10 μm. As the analyses were performed without the use of standards, an overall error of 2% is assumed. Ferric iron in the clinopyroxenes was estimated according to stoichiometry, following the method of Droop (1987). Ferric iron in amphibole was calculated using the min-max method (see Appendix 2 of Leake et al., 1997) using the intermediate value of Fe^{3+}. The quantitative results obtained with the microprobe permit calculation of the end-member percentages in solid solutions (e.g. from the jadeite-kosmochlor series).

---

* *Jadeite* is the name of a mineral, while *jadeitite* is the petrographic name for a rock composed predominantly or entirely of jadeite (synonymous with *jadeite jade*). Likewise, *omphacite* is a mineral name and *omphacitite* is a rock composed primarily of that mineral.

Following the recommendation of S. I. Liu (pers. comm., 2013), backscattered electron (BSE) imaging was done at low magnification in a scanning electron microscope at the University of Basel to investigate the mineralogical composition of the samples. With this technique, the amount of non-jadeite constituents in a polymineralic rock can be quickly estimated, since a relatively higher mean atomic weight (e.g. due to Ca, Fe or Cr) shows up as a brighter image. For example, in the BSE image of sample 4J12, which consists of jadeitite with kosmochlor and clinoamphibole, pure jadeite appears dark grey and omphacite as well as chromian jadeite appear distinctly brighter (Figure 4).

Chemical data obtained by the electron microprobe are very precise and quantitative, but the instrument is expensive and needs a professional technician to operate it, making it impractical for gem labs. Energy-dispersive X-ray fluorescence (EDXRF) spectroscopy used in gem labs has an excitation spot that is too large to resolve individual components of Burmese jade, and also it is only a qualitative technique (without a careful and painstaking standardization procedure). Furthermore, Na is too light an element for measuring with this technique. However, EDXRF is suitable to check for the presence of Ca, to give an indication of the presence of omphacite or sodic-calcic amphibole.

Raman Spectroscopy

Confocal Raman micro-spectroscopy was used to non-destructively characterize individual mineral grains in all 39 of the polished thin sections. We used a Bruker Senterra Raman dispersive microscope spectrometer equipped with a green laser (532 nm). The high resolution of this method (measurement of spots with diameters of 1–3 µm is possible) even allows the identification of complex mineral intergrowths and mineral zoning. For clinopyroxenes, we only measured spots that had been previously analysed by the electron microprobe, to have an absolutely certain identification of the mineral and to avoid sub-microscopic intergrowths or exsolution lamellae. Measurements were performed at 20 mW with a 100 second counting time; we used objective lenses with 50× and 100× magnification, and an aperture of 25 µm. Mineral identification was performed using the RRUFF database (Downs, 2006) and our own Raman database at the mineralogical institute in Basel.

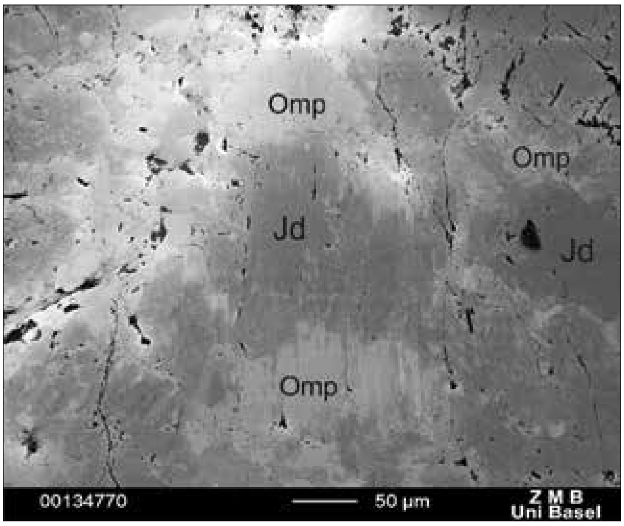

Figure 4: Backscattered-electron imagery of sample 4J12 (jadeitite with kosmochlor and clinoamphibole) shows a jadeite grain (Jd; appears dark) mantled by omphacite (Omp; appears bright). Note also the presence of omphacite along jadeite grain boundaries and fractures. Image by Marcel Düggelin.

Infrared Spectroscopy

Mineral identification also was accomplished using Fourier-transform infrared (FTIR) spectroscopy, performed with a Bruker Lumos FTIR microscope at Bruker's laboratories in Fällanden, Switzerland. Two samples (2J17 and 4J22) were analysed, as well as four additional cabochons from author HAH's collection. Data were collected in the range of 7000–650 cm^{-1} with a resolution of 4 cm^{-1}. The accuracy was ≤0.05 cm^{-1} at 1576 cm^{-1}, and the spectral resolution was <2 cm^{-1}. A mercury-cadmium-telluride (MCT) detector cooled with liquid nitrogen was used. Time-resolved measurements were performed by averaging eight interferograms per spectrum, for a total acquisition time of 8 seconds. Reflection IR measurements of two polished thin sections containing jadeite + omphacite (section 4J12) and chromian jadeite + kosmochlor (2J17) also were undertaken. The size of the measured spots ranged from 15 × 40 µm to 60 × 100 µm. We measured several spots with minerals showing different crystallographic orientations, which had little effect on the main IR bands.

Results

Gemmological Data

The gemmological and petrographic data for each of the 39 samples that were also cut into thin sections are reported in an online data depository on *The Journal*'s website. The colour of the samples ranged from light to dark green (coloured by Cr), lavender (coloured by Mn and/or Fe; see Harlow and Shi, 2011), yellow to brown (coloured by Fe) and black. Kosmochlor-bearing samples were spotted dark green within a lighter green and white matrix. Our samples of omphacitite appeared black, and only the use of transmitted light revealed a dark to very dark green colour.

For our jadeitite samples, spot RI values mostly ranged from 1.65 to 1.66, whereas the omphacitites had a slightly higher RI (1.67–1.68). The SG of our jadeitites was variable but most values fell in the range 3.27–3.35, while the omphacitites varied from 3.26 to 3.36. The large variations in SG can be explained by mineral compositional zoning and the presence of impurities such as clinoamphibole and kosmochlor.

The absorption spectra of the jadeitites revealed a typical sharp line at 437 nm, which was sometimes masked in green chromian jadeite jade, the latter showing absorption lines at 630, 655, and 690 nm (as documented by Liddicoat, 1981). The omphacitites showed no distinctive absorption line (as mentioned by Okano et al., 2009).

Petrographic Examination

Microscopic examination allowed us to visually identify the mineral content and study the micro-textures in the samples. The following groups of jadeite-bearing rocks could be distinguished.

Jadeitites with Kosmochlor and Clinoamphibole (JKC): Samples belonging to this category are 1J02, 1J04, 1J07, 1J14, 2J17, 4J11, 4J12, 4J19 and 4J22 (Figure 3a). These rocks consist mainly of jadeite (modal vol.% estimated at 60–75%; some with additional chromian jadeite) and variable amounts of kosmochlor (1–25%), omphacite (0–10%), clinoamphibole (10–39%), phlogopite (up to 3%), and chromite, as well as other rare accessories like titanite (<1%). In hand specimen, they ranged from green to dark green with nearly opaque spots (2J17). Some samples were entirely dark green (1J07), while others showed dark green veins. A wide variety of different micro-textures were observed. Sample 2J17, for example, contained aggregates of radiating kosmochlor formed around chromite grains, which were embedded in a matrix of randomly oriented short-prismatic jadeite crystals (Figure 5a), similarly described by Shi et al. (2005a, 2009). Long-prismatic, faintly yellow (in thin section) clinoamphibole prisms formed isolated crystals and some sheaf-like clusters. Other samples like jadeitite schist 1J02 showed compositional banding with jadeite-rich, clinoamphibole-rich and kosmochlor-bearing layers. The minerals were aligned parallel to the compositional banding, with fractures oriented oblique to the layering. Secondary limonite and zeolite were found in some specimens, and biotite (appearing 'olive' green in thin section) rimmed and filled fractures in larger jadeite crystals.

Jadeitites with Clinoamphibole (often with Chromian Jadeite; JC): Samples in this category are 1J11, 1J12, 2J16, 2J19, 4J01, 4J03, 4J09 and 4J30 (Figure 3b). These rocks consist of jadeite and chromian jadeite (60–99%), omphacite (0–10%), clinoamphibole (10–40%), and accessory opaques and titanite (<1%). They looked quite variable in hand specimen, such as white with small green spots (4J09), dark green (2J16), and striped green and dark grey (1J11 and 1J12), which was due to the presence of chromian jadeite (bright green in 1J11), omphacite (4J30) or dark amphibole (4J03). In thin section, a distinct compositional banding of jadeite- and clinoamphibole-rich layers and lenses was visible. The main foliation, which was oriented parallel to this banding, experienced an intense micro-folding with partially isoclinal fold structures (Figure 5b). Polygonal arc structures of minerals in fold hinges point to pre-crystallization folding and mimetic crystallization (i.e. recrystallization that reproduces pre-existent textures; Spry, 1969; see also Hibbard, 1995, p. 297). There were a number of jadeitites that lacked chromian jadeite (e.g. 2J19, 4J01, 4J03, 4J09 and 4J30). According to our Raman investigation, the clinoamphiboles in these rocks consisted of sodic-calcic (richterite) and sodic (arfvedsonite) varieties.

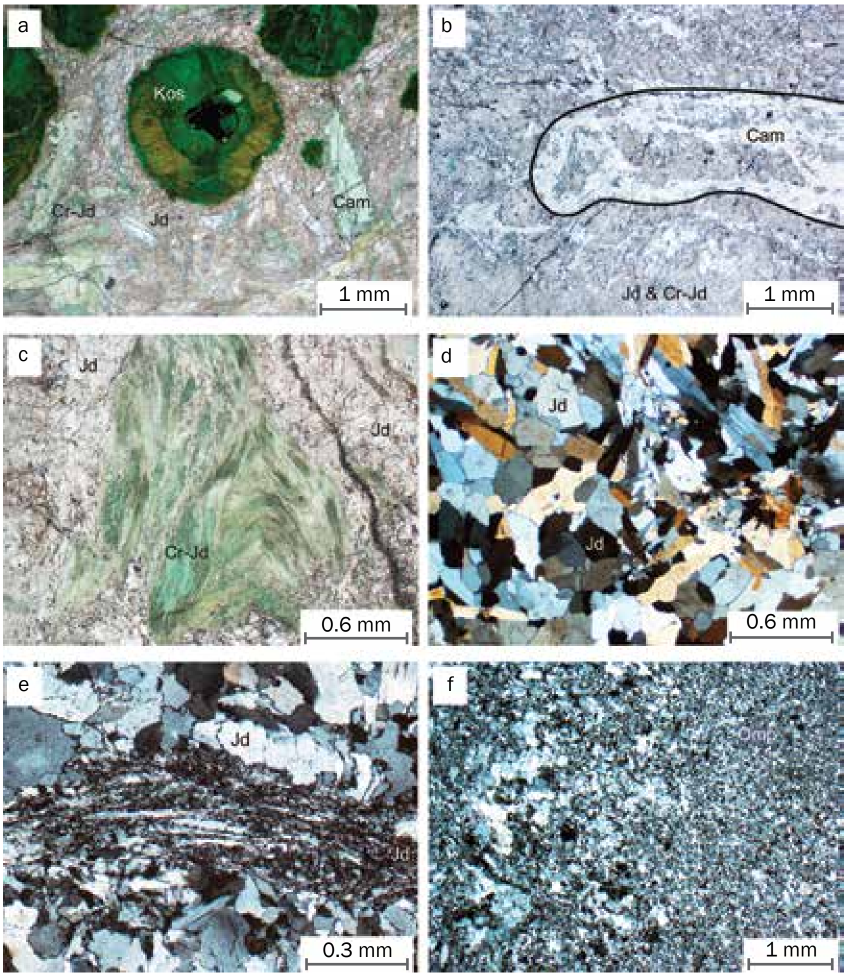

Figure 5: These photomicrographs show the texture and mineralogy of selected samples. (a) Dark green radiating aggregates of kosmochlor with chromite cores are surrounded by a matrix of jadeite, chromian jadeite and clinoamphibole in JKC-type sample 2J17. (b) An isoclinally folded layer of clinoamphibole (low-relief mineral Cam; folding is shown by the black line) is surrounded by jadeite and chromian jadeite in JC sample 1J12. (c) Green chromian jadeite prisms show intense micro-folding and are bordered by colourless jadeite in ABJ sample 2J18. (d) Jadeite prisms show a decussate texture in J sample 2J03. (e) An ultramylonitic shear zone with dynamically recrystallized jadeite grains (centre) cuts through randomly oriented, larger jadeite grains in J sample 4J13. (f) Patchy sections of larger omphacite grains are present in a fine-grained matrix of omphacite crystals in O sample J274. Photos a–c are in plane-polarized light, and d–f are in cross-polarized light. Photos by L. Franz.

Albite-bearing Jadeitites (with Chromian Jadeite or Omphacite; ABJ): Samples of this category (1J05, 2J18 and 4J27; Figure 3c) show wide petrographic variability. Sample 1J05, for example, consisted of almost pure jadeite (99%) with <1% albite and omphacite. Other samples showed darker green veins and irregular spots due to the presence of chromian jadeite (e.g. 2J18). Macroscopically, the albite-bearing jadeitites often resembled the darker samples from the second group, however they contain no amphibole. Thin-section examination showed a distinct compositional banding of medium-grained jadeite-rich layers alternating with fine-grained layers rich in chromian jadeite, with the latter displaying a distinct mineral alignment and local micro-folding (Figure 5c). The semi-polygonal arc structures in the fold hinges point to syn-crystallization folding according to Misch (1969). Accessory minerals were albite (forming angular inclusions in jadeite) and rare titanite. Secondary limonite was found as brownish staining at the rim and along fractures in the samples.

Jadeitites (without Chromian Jadeite; J): Fourteen samples (1J03, 1J06, 1J09, 1J13, 2J03, 2J07, 2J12, 4J04, 4J06, 4J10, 4J13, 4J21, 4J26 and 4J28; Figure 3d) consisting of pure and almost pure jadeitites (92–100%) are grouped into this category. Macroscopically, these rocks often appeared homogeneous with a broad range of colour, from yellowish white to distinctly green or brown. Besides jadeite, the samples contained minor amounts of omphacite (2J07 and 4J06), vesuvianite (4J04), amphibole (4J04; grunerite/cummingtonite according to Raman spectroscopy), analcime (4J06 and 4J13) and phlogopite (4J13). Accessory minerals were disordered graphite (identified by Raman spectroscopy in 4J10 and 4J13) occurring as tiny inclusions in jadeite and also rare titanite. Secondary minerals consisted of biotite and limonite present along the rim and in fractures of jadeite (1J03). Furthermore, tiny fibres with a low RI were zeolite (probably natrolite) that formed at the expense of analcime (4J06). Viewed with the microscope (e.g. Figure 5d), the jadeitite fabrics were rather variable, with most of them showing a medium-grained decussate texture (i.e. the axes of contiguous jadeite crystals lie in diverse, crisscross directions without any alignment; Spry, 1969; see also Yardley et al., 1990, p. 89). Some of the rocks showed a fine-grained foliated texture with aligned jadeite prisms and microfolds, while others contained shear bands made up of dynamically recrystallized jadeite neoblasts surrounding coarser-grained porphyroclastic rock fragments (Figure 5e).

Omphacitites (O): The omphacitites (J270–J274) in this study were easily distinguished from the jadeitites by their very dark green colour and almost opaque appearance (Figure 3e). Thin sections of two samples (J271 and J274) proved to be monomineralic omphacitite without any accessory minerals or secondary alteration. While sample J271 displayed a homogeneously fine-grained texture, sample J274 showed an inhomogeneous size distribution with patchy sections yielding larger, irregular omphacite crystals in a matrix of tiny omphacite prisms (Figure 5f).

Electron Microprobe Analysis

Chemical data for eight representative samples are plotted in jadeite-aegirine–quadrilateral pyroxene (Jd-Ae-Q) diagrams following Morimoto et al. (1988) and in a kosmochlor–(jadeite+aegirine)–quadrilateral pyroxene diagram to highlight the wide variability of the mineral composition within the rocks (Figure 6).

In all the investigated samples, jadeite and omphacite crystals revealed distinct chemical inhomogeneities due to zoning or variations from crystal to crystal, which are described in detail below. Selected microprobe analyses of clinopyroxenes are listed in Table I. The entire dataset is available via *The Journal*'s online data depository.

Jadeitites with Kosmochlor and Clinoamphibole: Clinopyroxenes from these rocks show obvious chemical variations, which is particularly evident for jadeite from sample 2J17. The BSE image (Figure 6a) shows distinct zoning with dark, Na-rich sections (cf. spot 3; $Jd_{90.6}Ae_{4.3}Q_{5.2}$), bright, Na-poor sections (cf. spot 2; $Jd_{74.3}Ae_{15.2}Q_{10.4}$) and intermediate sections (cf. spot 1; $Jd_{85.6}Ae_{8.9}Q_{5.4}$; see Table I). Such a pronounced mineral zoning in jadeitites from Myanmar was already described by Harlow and Olds (1987). Jadeite from sample 4J12 showed a compositional range of $Jd_{71.6-96.8}Ae_{8.6-0.1}Q_{19.8-3.1}$ while omphacite yielded a composition of $Jd_{34.9-50.8}Ae_{8.8-6.8}Q_{56.3-42.4}$ (plotted in Figure 6a).

When data for these two samples are plotted in Figure 6b, it becomes evident that Cr-bearing pyroxene in sample 4J12 is mainly chromian omphacite (represented in the diagram by the Jd+Ae apex), whereas sample 2J17 contains major amounts of both chromian jadeite and kosmochlor. The data reveal a distinct compositional gap between kosmochlor and chromian jadeite as well as between chromian jadeite and jadeite, which suggests a solvus between these phases similar to the jadeite-omphacite–Ca-Mg-Fe-pyroxene solvi (Davidson and Burton, 1987; Green et al., 2007). (A *solvus* separates a homogeneous solid solution from a field of several phases that may form by exsolution.) Electron microprobe analyses furthermore showed that the clinoamphibole in sample 2J17 is mainly katophorite and subordinately winchite according to the classification of Hawthorne et al. (2012).

Jadeitite with Clinoamphibole: Sample 4J30 contained jadeite with a compositional range of $Jd_{83.5-97.5}Ae_{2.3-0.2}Q_{14.2-2.3}$, including some crystals revealing a distinct decrease in Na from core to rim. Omphacite in this sample formed solitary grains in contact with clinoamphibole (katophorite and richterite) and showed an intense irregular zoning pattern. Its composition ranged from $Jd_{41.8-62.8}Ae_{8.4-4.2}Q_{49.8-33.0}$ (plotted in Figure 6c).

Albite-bearing Jadeitites: Sample 1J05 contained jadeite with patchy Na-rich and Na-poor sections showing a compositional variation of $Jd_{82.6-96.5}Ae_{4.4-0.2}Q_{13.0-3.3}$. Omphacite formed inhomogeneous rims on jadeite and showed a compositional range of $Jd_{40.3-55.8}Ae_{1.1-5.1}Q_{58.7-39.1}$ (plotted in Figure 6d). The albite in sample 1J05 was close to the end member ($Ab_{97.9-99.9}An_{0-2}Or_{0-0.1}$).

Jadeitites: Samples 4J06 and 4J26 contain clinopyroxenes that have a very similar composition to the foregoing samples, with jadeite ranging from $Jd_{83.0-98.0}Ae_{1.6-0}Q_{15.5-2.0}$ and omphacite varying from $Jd_{36.8-55.5}Ae_{6.5-1.7}Q_{56.7-42.7}$ (plotted in Figure 6e). Similar to the albite-bearing jadeitites,

a. Jadeitites with Kosmochlor and Clinoamphibole

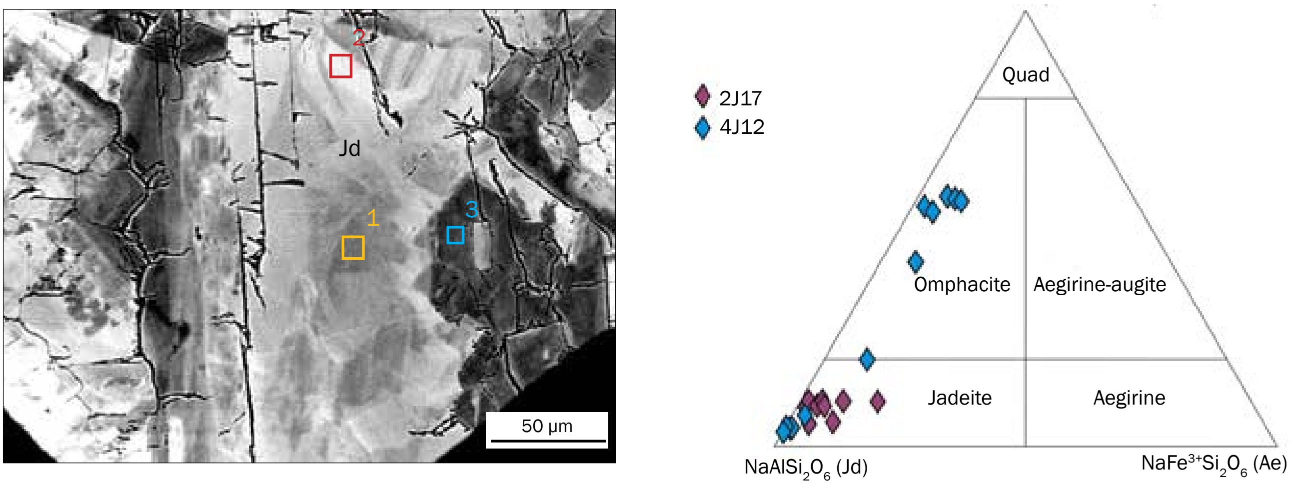

b. Jadeitites with Kosmochlor and Clinoamphibole

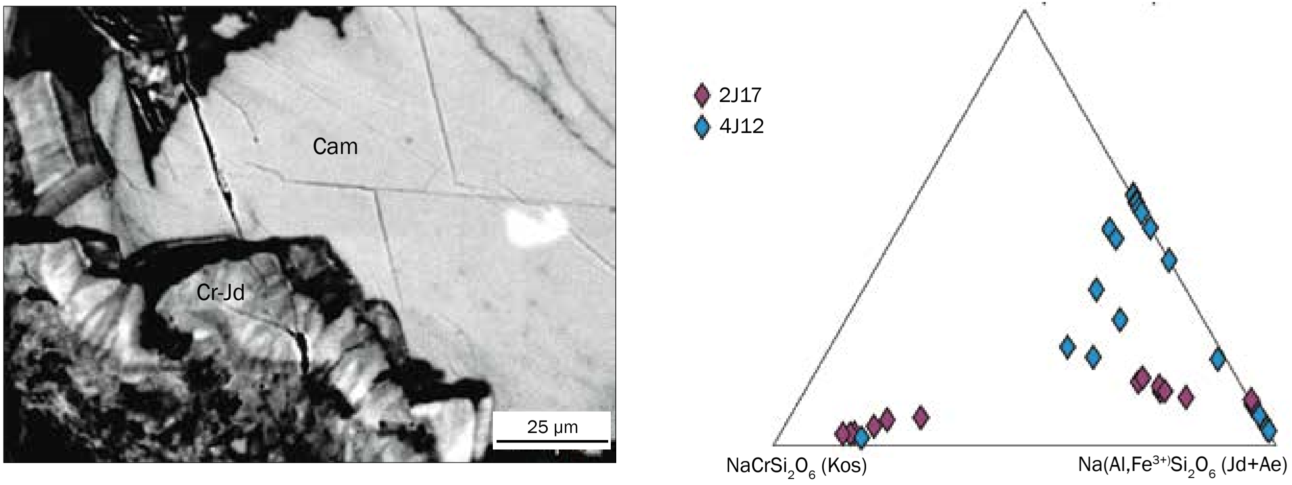

c. Jadeitites with Clinoamphibole

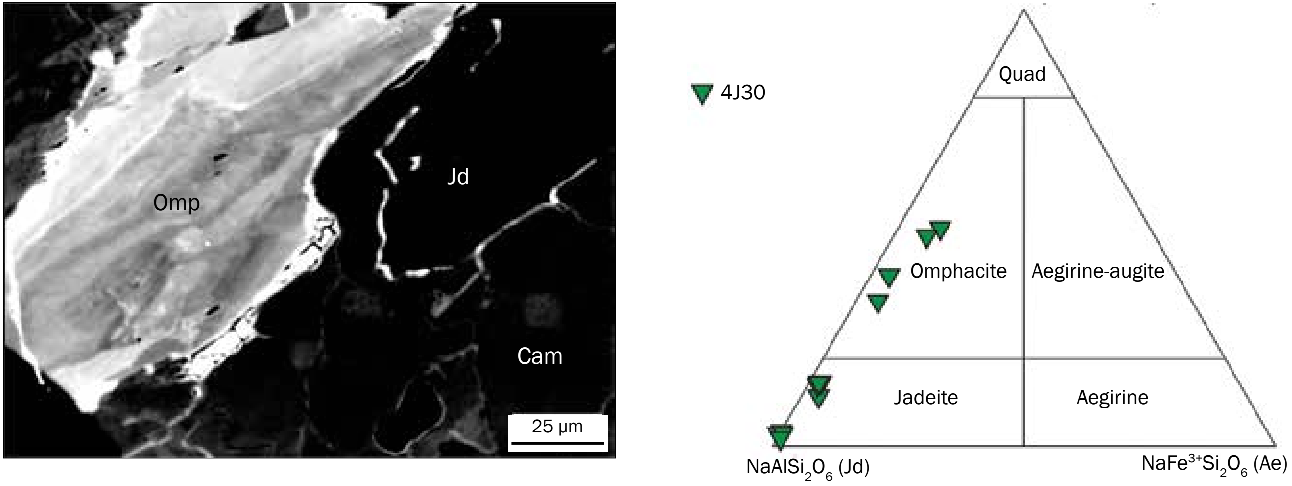

Figure 6: Electron microprobe data of pyroxenes are shown with BSE images of some of the corresponding areas that were analysed. The microprobe data are plotted in the Jd-Ae-Q diagram of Morimoto et al. (1988), except for Figure 6b which shows a Kos-(Jd+Ae)-Q diagram. The data for all samples demonstrate distinct compositional gaps between jadeite and omphacite, except for omphacitite sample (f) which does not contain any jadeite. BSE images: (a) JKC-type sample 2J17 shows distinct

d. Albite-bearing Jadeitites

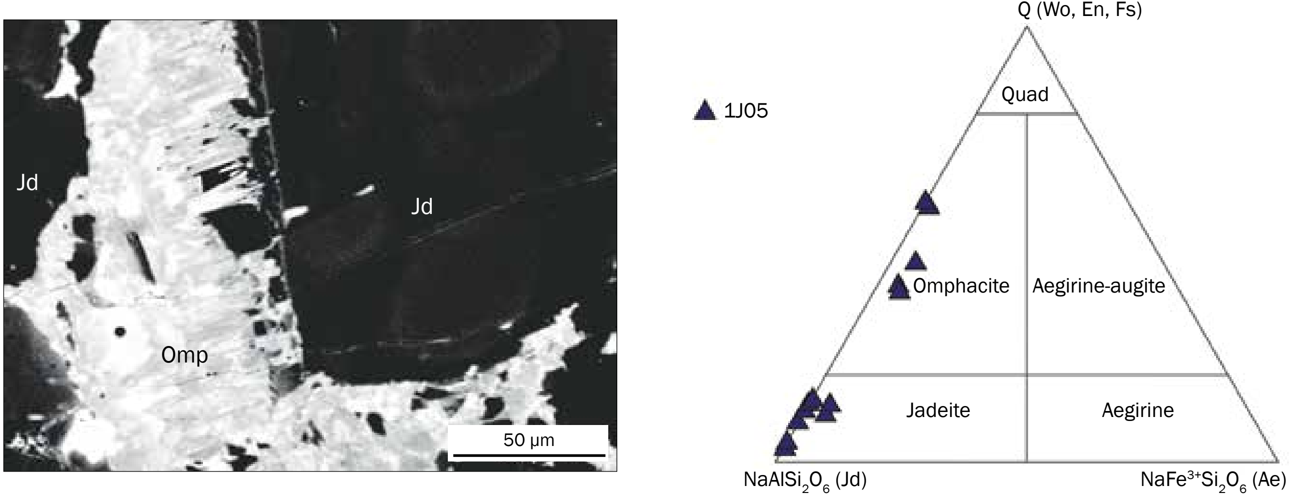

e. Jadeitites

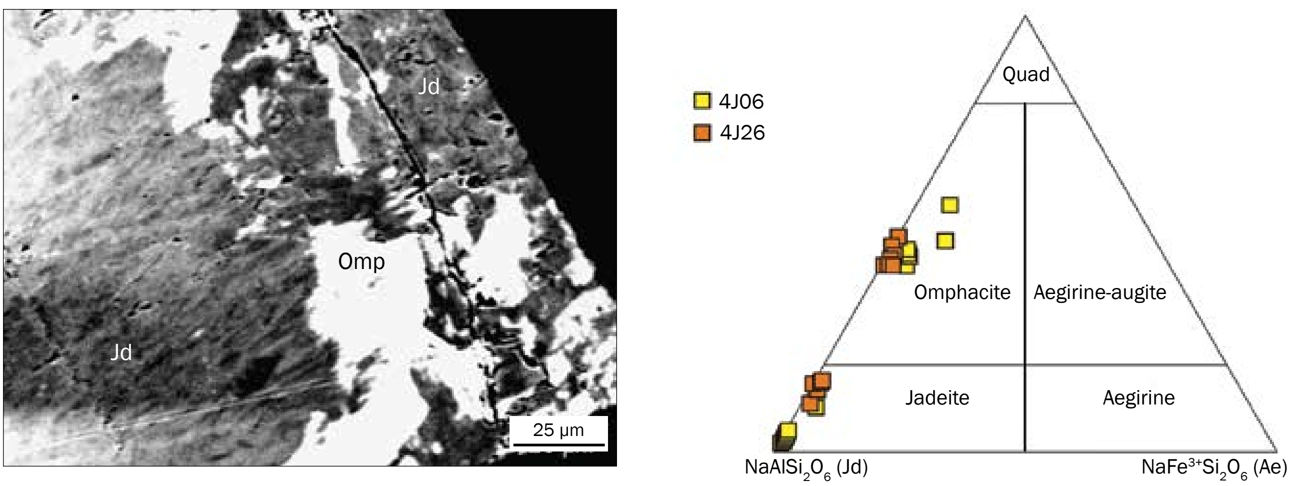

f. Omphacitites

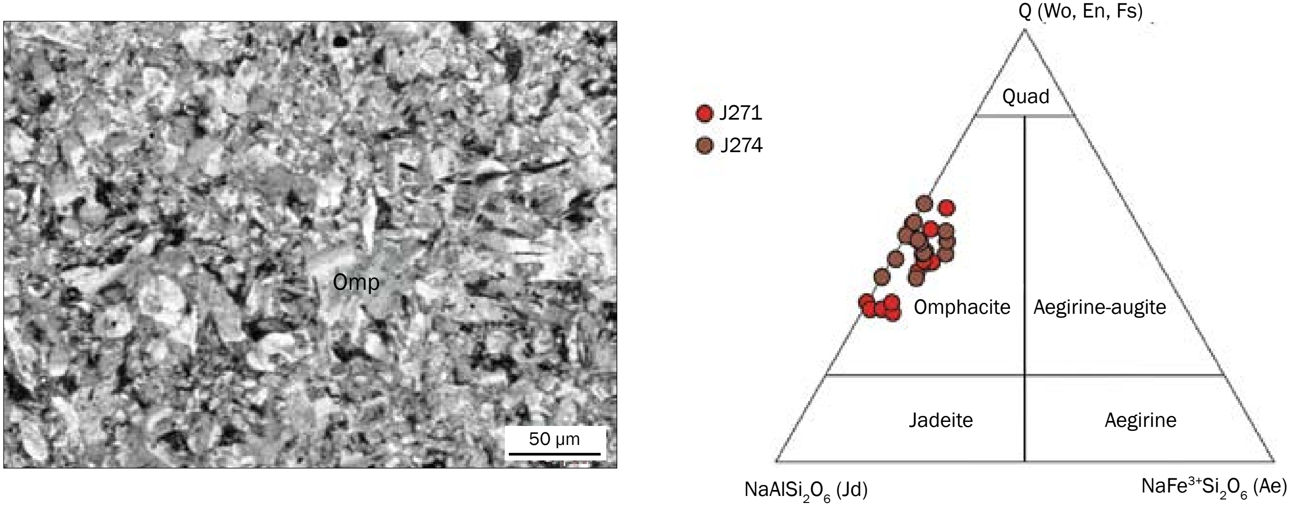

chemical zoning within a jadeite crystal. (b) This portion of sample 2J17 consists of a clinoamphibole crystal that is rimmed by chromian jadeite. (c) JC sample 4J30 shows an inhomogeneous omphacite next to jadeite and clinoamphibole crystals. (d) In ABJ sample 1J05, a jadeite crystal is rimmed by irregularly zoned omphacite. (e) J sample 4J26 displays a patchy replacement of jadeite by omphacite. (f) O sample J271 consists of an intergrowth of small omphacite crystals. Images by C. de Capitani.

Table I: *Selected microprobe analyses of clinopyroxenes from jadeitites with kosmochlor and clinoamphibole (JKC), jadeitites with clinoamphibole (JC), albite-bearing jadeitites (ABJ), jadeitites (J) and omphacitites (O).**

Sample No.	**2J17**						**4J12**		
Rock type	JKC						JKC		
Spot	F2 1	F2 2	F2 3	F2 K 1	F2 K 6	F2 K2 2	F3 1	F3 3	F1 1
Mineral	Jd			Kos		Cr-Jd	Cr-Omp	Omp	Jd
SiO_2	57.59	57.12	58.42	53.35	53.79	56.22	54.66	55.57	58.55
TiO_2	nd	0.07	nd	0.03	0.02	0.01	3.24	0.07	0.03
Al_2O_3	22.78	19.43	23.59	2.90	5.24	12.93	3.54	9.78	25.13
Cr_2O_3	0.02	nd	0.02	29.55	23.86	6.26	5.10	0.03	0.01
Fe_2O_3	3.56	5.96	1.70	nd	1.54	7.08	8.39	2.95	0.06
MgO	1.91	2.76	1.81	0.71	1.45	2.80	7.44	10.50	1.23
CaO	0.29	1.79	0.30	0.05	0.68	2.33	7.40	13.54	nd
MnO	nd	0.12	nd	0.03	nd	0.10	nd	0.23	0.01
FeO	nd	nd	nd	0.16	0.57	0.29	1.59	1.43	nd
Na_2O	14.20	13.35	14.33	13.21	13.01	12.70	9.48	6.21	14.99
Total	**100.35**	**100.60**	**100.17**	**99.99**	**100.15**	**100.72**	**100.84**	**100.31**	**100.01**
Cations (O=6)									
Si	1.959	1.964	1.976	1.988	1.981	1.984	1.981	1.967	1.973
Ti	nd	0.002	nd	0.001	0.001	nd	0.088	0.002	0.001
Al	0.913	0.787	0.940	0.127	0.227	0.538	0.151	0.408	0.998
Cr	0.001	nd	0.001	0.871	0.695	0.175	0.146	0.001	nd
Fe^{3+}	0.091	0.154	0.043	nd	0.043	0.188	0.229	0.079	0.001
Mg	0.097	0.141	0.091	0.039	0.080	0.147	0.402	0.554	0.062
Ca	0.011	0.066	0.011	0.002	0.027	0.088	0.287	0.514	nd
Mn	nd	0.003	nd	0.001	nd	0.003	nd	0.007	0.000
Fe^{2+}	nd	nd	nd	0.005	0.017	0.008	0.048	0.042	nd
Na	0.936	0.890	0.940	0.955	0.929	0.869	0.666	0.426	0.980
Total	**4.007**	**4.008**	**4.002**	**3.989**	**4.000**	**4.000**	**4.000**	**4.000**	**4.016**
End-members (mol%) after Morimoto et al. (1988)									
Jd	85.6	74.3	90.6	97.6	77.9	64.5	23.6	35.9	96.8
Ae	8.9	15.2	4.3	0	15.9	23.2	40.8	7.5	0.1
Q	5.4	10.4	5.2	2.4	6.2	12.3	35.6	56.6	3.1

* Ferric iron is calculated according to Droop (1987). Potassium was analysed for, but not detected in any of these samples.
Abbreviation: nd = not detected.

omphacite formed rims around jadeite but also appeared as relatively homogeneous crystals in sheared zones. A distinct compositional gap exists between jadeite and omphacite (e.g. Figure 6e; see also Green et al., 2007), which has been observed in other jadeitites but curiously not mentioned in the literature for those from Myanmar.

Omphacitites: The fine-grained omphacitites show a decussate intergrowth of omphacite crystals with distinctly variable composition. The BSE image of sample J271 (Figure 6f) shows an aggregate of bright, Na-poor and darker, Na-rich omphacite crystals. Similar mineral intergrowth phenomena were observed in sample J274. The composition of omphacite in these rocks ranged from $Jd_{36.4-63.6}Ae_{4.9-0}Q_{58.7-36.4}$ (plotted in Figure 6f).

Raman Spectroscopy

With this method a reasonably good identification of the different pyroxenes was possible. Jadeite shows a prominent band at 700 cm^{-1}, with weaker bands at 1039, 991, 575, 524, 374 and 203 cm^{-1} (Figure 7a). In contrast, omphacite shows a main band at 684 cm^{-1}, and weaker

4J30		1J05		4J06		4J26		J271		J274	
JC		ABJ		J		J		O		O	
F1 1	F3 3	F2 7	F1 9	F2 7	F2 1	F1 4	F1 8	F3 xt 4	F1 4	F2 4	F3 1
Jd	Omp	Jd	Omp	Jd	Omp	Jd	Omp	Omp		Omp	
59.05	57.30	58.65	56.57	58.70	56.82	57.87	57.27	56.35	55.44	56.16	56.98
0.02	0.05	nd	0.05	0.01	0.29	0.09	0.13	0.16	0.05	0.15	0.15
25.03	16.24	25.24	15.19	24.77	13.04	21.94	14.16	15.71	10.27	10.21	14.77
nd	0.03	nd	0.02	0.01	0.01	nd	0.01	nd	0.01	0.02	nd
0.07	1.67	0.09	2.03	0.24	1.15	0.62	0.67	1.94	1.89	2.91	nd
0.91	7.20	1.29	8.27	1.58	9.35	3.89	9.22	7.81	12.41	10.47	8.54
nd	7.69	nd	9.16	0.20	10.94	2.96	9.88	8.61	13.93	12.43	9.52
nd	0.04	nd	0.01	0.02	0.01	0.05	nd	0.14	0.13	nd	nd
nd	nd	nd	nd	nd	0.56	nd	0.25	nd	nd	1.13	1.58
14.92	9.95	14.74	8.89	14.49	7.97	12.64	8.48	9.45	6.06	6.81	8.45
100.00	**100.17**	**100.01**	**100.19**	**100.02**	**100.14**	**100.06**	**100.07**	**100.17**	**100.19**	**100.29**	**99.99**
1.987	1.976	1.974	1.960	1.977	1.979	1.966	1.983	1.954	1.949	1.978	1.979
0.001	0.001	nd	0.001	0.000	0.008	0.002	0.003	0.004	0.001	0.004	0.004
0.993	0.660	1.001	0.620	0.983	0.535	0.878	0.578	0.642	0.426	0.424	0.605
nd	0.001	nd	0.001	0.000	0.000	nd	0.000	nd	0.000	0.001	nd
0.002	0.043	0.002	0.053	0.006	0.030	0.016	0.017	0.051	0.050	0.077	nd
0.046	0.370	0.065	0.427	0.079	0.485	0.197	0.476	0.404	0.650	0.550	0.442
nd	0.284	nd	0.340	0.007	0.408	0.108	0.367	0.320	0.525	0.469	0.354
nd	0.001	nd	0.000	0.001	0.000	0.001	nd	0.004	0.004	nd	nd
nd	0.000	nd	nd	nd	0.016	nd	0.007	nd	nd	0.033	0.046
0.974	0.665	0.962	0.597	0.946	0.538	0.832	0.569	0.635	0.413	0.465	0.569
4.002	**4.003**	**4.005**	**4.000**	**4.001**	**4.000**	**4.001**	**4.001**	**4.013**	**4.018**	**4.000**	**3.999**
97.5	62.8	96.5	55.8	95.0	51.2	83.0	55.5	58.7	36.4	39.4	57.5
0.2	4.3	0.2	5.1	0.6	3.0	1.6	1.7	5.0	4.9	7.6	0
2.3	33.0	3.3	39.1	4.4	45.8	15.5	42.7	36.3	58.7	53.1	42.5

bands at 1016, 567, 382, 144 and 76 cm^{-1} (Figure 7b). Chromian jadeite has its maximum band at 364 cm^{-1} and two prominent bands at 1025 and 685 cm^{-1} (Figure 7c). Kosmochlor shows a main band at 418 cm^{-1} and four characteristic bands between 1058 and 951 cm^{-1} (Figure 7d). Although the Senterra Raman spectrometer was not equipped with a depolarizer, crystal orientation had only a small effect on the intensity of these bands and almost no effect on their position, according to our measurements taken with the beam parallel to the a-, b- and c-axes of the crystals.

Many of the jadeite crystals in the investigated samples had dark, elongate inclusions in their core that were identified as graphite by Raman spectroscopy.

Infrared Spectroscopy

Figure 8 shows the FTIR spectra of jadeite, omphacite, chromian jadeite and kosmochlor, which can be distinguished easily by the relative height of their prominent absorption bands at 689–665 cm^{-1} and 643–623 cm^{-1}. The jadeite spectrum (Figure 8a) shows a distinctly greater absorbance at 643 cm^{-1} than at 689 cm^{-1}, which is the opposite for omphacite (Figure 8b). Here, the band at 629 cm^{-1} shows a weaker absorbance than the one at 665 cm^{-1}. For chromian jadeite (Figure 8c) the bands at 671 and 631 cm^{-1} show almost identical absorption, while kosmochlor (Figure 8d) reveals a pronounced absorption at 671 cm^{-1} and a distinctly smaller absorption at 623 cm^{-1}. These results could also be reproduced for the four additional cabochons from author HAH's collection.

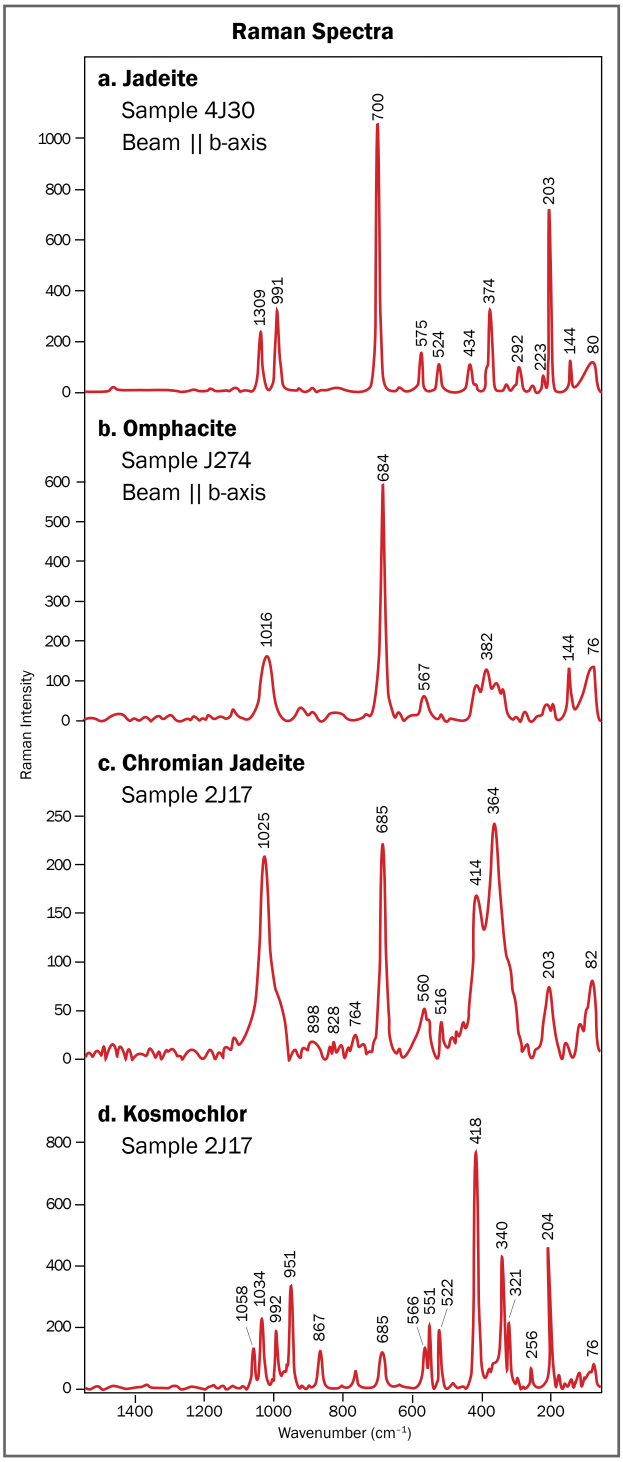

Figure 7: Raman spectra of selected minerals are shown for: (a) jadeite, (b) omphacite, (c) chromian jadeite and (d) kosmochlor.

Discussion

Pyroxene Mineralogy and the Genesis of Burmese Jadeite-bearing Rocks

Ideally, the composition of jadeite should not depart greatly from $NaAlSi_2O_6$. In most natural jadeite, at least 80% of the pyroxene's M1 site is occupied by Al, and at least 80% of the M2 site is taken by Na (Deer et al., 1997). Omphacite, on the other hand, is chemically much more complex. It is essentially a solid solution of jadeite and diopside with some aegirine. Omphacite is simplistically defined as $Jd_{50}(Di+Hd)_{50}$, but may show a considerable range of jadeite, diopside and hedenbergite, and may also contain aegerine and kosmochlor components (see Morimoto et al., 1988; García-Casco et al., 2009). Following the classification of Morimoto et al. (1988; see Figure 6), the compositional ranges

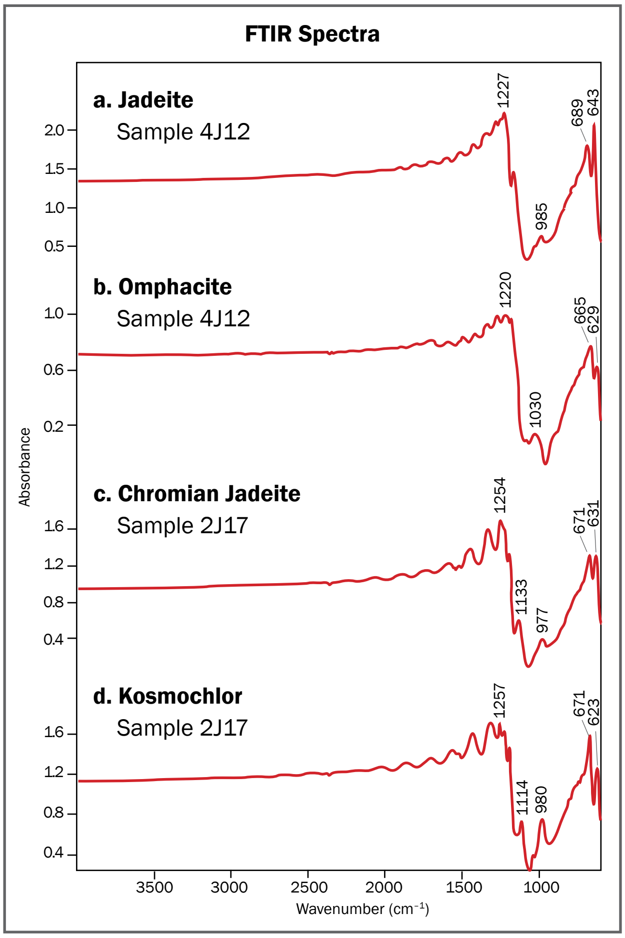

Figure 8: Representative FTIR spectra are shown for: (a) jadeite, (b) omphacite, (c) chromian jadeite and (d) kosmochlor.

of the quadrilateral (Ca-Mg-Fe) pyroxene, the Na-Al pyroxene (jadeite), and the Na-Fe^{3+} pyroxene (aegirine) are as follows: Omphacite lies within the area defined by $0.2 \leq Na/(Na+Ca) \leq 0.8$, and $Al/(Al+Fe^{3+}) \geq 0.5$, while jadeite lies in the field defined by $Na/(Na+Ca) \geq 0.8$ and $Al/(Al+Fe^{3+}) \geq 0.5$. If we follow this mineralogical classification strictly, a sample should not be called *jadeite* if it contains less than 80% Al as compared to Mg+Fe^{2+}, less than 50% Al as compared to Fe^{3+}, and less than 80% Na as compared to Ca. Furthermore, two temperature-dependent miscibility gaps between jadeite and Ca-Mg-Fe pyroxene have been described by several investigators (Davidson and Burton, 1987; Green et al., 2007; García-Casco et al., 2009; Harlow et al., 2011). At temperatures of 400°C, for example, they lie roughly between Na/(Na+Ca) ratios of 0.5–0.95 and between 0.2 and 0.4. This is also clearly visible in the ternary plots of Figure 6.

Apart from the chemical, and hence mineralogical, differences between omphacite and jadeite, there are also differences in the crystal structures of the two minerals, due to the differences in pressure and temperature of their formation. Although both minerals are clinopyroxenes crystallized in the monoclinic system, jadeite belongs only to one space group (C2/c), while omphacite has three polymorphs with symmetry C2/c, P2/n and P2 (Gaines et al., 1997). The crystallographic differences between jadeite and omphacite justify using separate terms (*jadeite jade* and *omphacite jade*) for referring to rocks composed predominantly of each mineral (see also Ou Yang et al., 2011).

The investigation of thin sections for this study has revealed the following facts: Several samples showed indications of pre- and syn-crystallization folding (i.e. polygonal arc textures, mineral alignment and micro-folds). Other samples had randomly oriented, decussate textures and lacked any tectonic overprint. Coarse-grained jadeitites with recrystallized textures (as described by Shi et al., 2009) were not observed in this study, which may be due to our randomly acquired samples. While the omphacitites often showed a monomineralic composition, the jadeitites mostly displayed complex mineral associations that usually included sodic and sodic-calcic amphiboles (e.g. arfvedsonite, richterite and katophorite). In some samples, both jadeite and omphacite were present; in many cases (e.g. samples 4J12 and 1J05), the jadeite appears to be the older phase, because it was rimmed by omphacite. In some samples (e.g. 4J39), the presence of omphacite next to clinoamphibole (richterite) created macroscopically clearly visible, millimetre-sized green spots in a white matrix consisting of jadeite. Omphacite also occurred as prismatic crystals in foliated layers, in shear bands and in fractures, which points to late metasomatic processes (addition of Ca) along the foliation and shear zones. A compelling feature of most of the investigated rocks was the marked chemical zonation of jadeite and omphacite, indicating rapid growth of these minerals at relatively low temperatures (cf. Shi et al., 2003; 2005b; 2012; Oberhänsli et al., 2007). According to Harlow et al. (2014), jadeitite in Myanmar occurs along the intersection of the Burmese Western and Eastern provinces along an offset of the Sagaing Fault. The primary occurrences of jadeitite consist of dykes or veins within serpentinites, which formed by crystallization from fluids during high-pressure metamorphism (Harlow and Sorensen, 2005; Shi et al., 2005b; Yi et al., 2006; Nyunt, 2009). Investigations of Goffé et al. (2000) on jadeitites from northern Myanmar point to subduction-related metamorphic conditions of approximately 400°C at 1.5 GPa. Due to these relatively low temperatures and the short time of the metamorphic overprint during the subduction process, mineral homogenization by diffusion was not possible.

Gemmological Identification of Burmese Jadeite-bearing Rocks

The identification of these Burmese rocks simply by their appearance is problematic. Omphacitite tends to be darker in appearance than jadeitite, although some jadeitite can be dark (as seen in Figure 9 and noted in Harlow et al., 2014) and omphacite jade also may have a lighter tone resembling jadeite jade (McClure, 2012). However, compared to jadeitite, omphacitite typically appears less transparent when viewed with transmitted light and tends to be greyish green.

A short summary of the gemmological properties of jadeite, omphacite and kosmochlor jades is given in Table II. Our findings confirm that it is sometimes possible to separate jadeite- from omphacite-dominant rocks using basic

Figure 9: The translucent medium-dark green carvings in this diamond necklace are jadeite jade (spot RI readings of 1.65–1.66), while those in the earrings had a higher RI of 1.67. This, combined with their slightly darker appearance, suggests the presence of an omphacite component. All of the carvings are 2–3 mm thick, and the largest ones measure 2.7 cm long. Photo by Tay Thye Sun.

gemmological properties such as RI, SG and the 437 nm absorption line. However, the samples analysed in this study reveal that Burmese jadeitites are not so pure after all, as they contain various modal proportions of clinoamphibole, kosmochlor, omphacite and other minerals. Our investigations show some similarities to the grouping by Htein and Naing (1994), who describe monomineralic (pure) and polymineralic (impure) jade, although some additional accessory minerals such as rutile and ilmenorutile were found by those authors (see also Htein and Naing, 1995). Predominantly monomineralic samples can be inhomogeneous due to solid solution and solvi, as well as chemical zoning. While some high-quality jadeitites are homogeneous and monomineralic, a large number of greyish, greenish and dark stones sold as jadeite jade have a complex polymineralic composition. Our studies reveal that in other than pure jadeitite, clinoamphibole or omphacite also contribute to variable RI and SG. Therefore, the use of RI spot readings and SG values does not lead to a rigorous identification. This is particularly true for the SG of jadeitite samples containing abundant clinoamphibole (e.g. 1J02 and 1J04), which had much lower values of 3.16 and 3.25, respectively. However, the RI values of both these samples were still within the typical jadeite jade range of 1.65–1.66. Nevertheless, the 437 nm absorption line was not detected, in contrast to pure jadeitite.

Among the more advanced methods available in a well-equipped gemmological laboratory, Raman micro-spectroscopy is the best technique for jade identification. With an appropriate database it is possible to non-destructively analyse spot-by-spot the composition of a rock being tested. In addition, micro-FTIR spectroscopy can provide a good distinction between jadeite, chromian jadeite, omphacite and kosmochlor. A high-resolution analytical apparatus like the Bruker Lumos micro-FTIR spectrometer should be used. Our FTIR

*Table II: Gemmological properties of jadeite, omphacite and kosmochlor jades from Myanmar.**

	Jadeite jade	**Omphacite jade**	**Kosmochlor jade**
Colour	Colourless, white, lavender, brown, yellow, green and dark green	Dark green to black	Green to black; uneven
Transparency	Transparent to opaque	Translucent to opaque	Opaque
RI	1.65–1.67	1.66–1.68	1.68–1.75
SG	3.25–3.40	3.30–3.45	3.35–3.50
Magnification	Fine-to-coarse grained, granular to fibrous texture	Fine grained, fibrous texture	Fibrous and radiating aggregates
Absorption spectrum	437 nm line; chromian jadeite shows lines at 630, 655 and 690 nm	No 437 nm line or Cr^{3+} absorption	None observed

* Data from this study, Webster (1995), and www.gahk.org/attachment/fcteststd2.pdf.

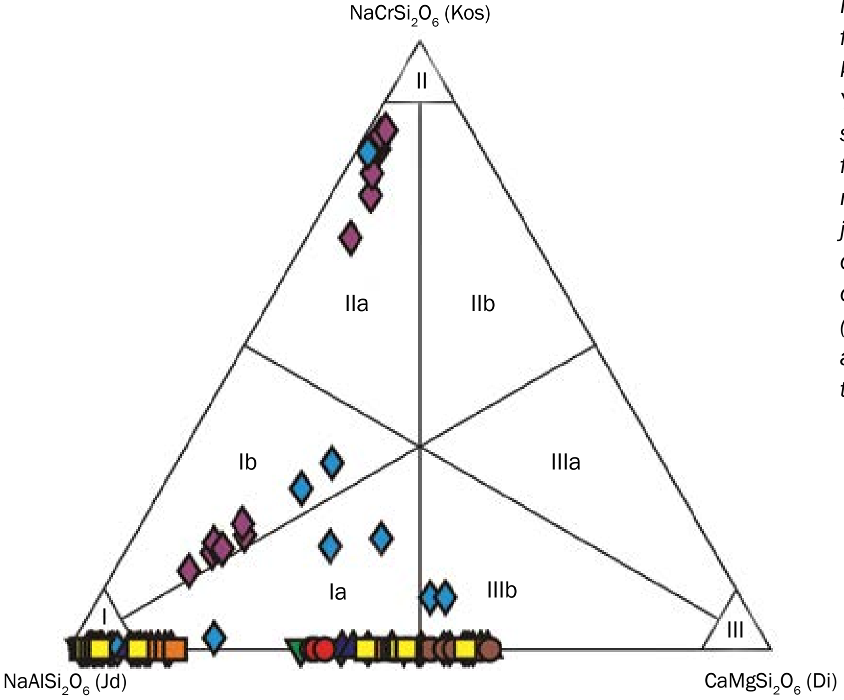

Figure 10: Electron microprobe analyses from this study are plotted in the kosmochlor-jadeite-diopside diagram of Ou Yang and Ng (2012). In the classification scheme proposed by those authors, the fields define pure jadeite (I), jadeite with minor omphacite (Ia), chromium-containing jadeite (Ib), pure kosmochlor (II), jadeite-containing kosmochlor (IIa), diopside-containing kosmochlor (IIb), pure diopside (III), kosmochlor-containing diopside (IIIa) and jadeite-containing diopside (IIIb). For the key to symbols, see Figure 6.

spectra gave equally satisfactory identifications as Raman spectroscopy and the electron microprobe. With these micro-analytical methods, tiny grains down to 1 µm (Raman) or 5 µm (FTIR) can be investigated. Raman or FTIR spectroscopy of larger analytical areas may yield mixed spectra that are not useful for identification, especially for samples that were not previously investigated microscopically and with microprobe analysis.

Current Classification/Nomenclature and Proposal for a New System

As a consequence of the results of this study, the present terminology of jadeitic gem materials should be seriously reconsidered. Such rigid schemes as the ternary jadeite–diopside–kosmochlor diagram of Ou Yang and Ng (2012) may be applied to monomineralic samples with a homogeneous mineral composition, but they are not appropriate for polymineralic samples. This becomes evident from Figure 10, in which we have plotted our microprobe analyses using the classification diagram of Ou Yang and Ng (2012). Jadeitites with kosmochlor fall into a large area ranging from the jadeite field (I) to the jadeite-containing kosmochlor field (IIa), while jadeitites, albite-bearing jadeitites and jadeitites with clinoamphibole plot in the fields for pure jadeite (I), jadeite with minor omphacite (Ia) and jadeite-containing diopside (IIIb). Due to their mineral chemical variability, even the monomineralic omphacitites cover a broad field from jadeite-containing diopside (IIIb) to jadeite with minor omphacite (Ia). Furthermore, the scheme does not consider minerals like clinoamphibole, albite or phlogopite, which are common constituents of the jade rocks.

Similarly, Hänni (2007) started from the assumption of a monomineralic composition, which may be true for some pure-appearing green jadeitites (e.g. Figure 11). However, as demonstrated in this investigation, many jadeitites and kosmochlor-bearing jadeitites from Myanmar are polymineralic and extremely inhomogeneous due to their textures and complex mineral zonation patterns. Furthermore, such observations have also been made for jadeitites from Kenterlau-Itmurundy (Lake Balkhash, Kazakhstan; Ernst et al., 2013) and a number of other locations (for an overview, see Harlow et al., 2014). In many cases, the rocks display strong compositional variability with complex mineral intergrowths of micrometre size. Common gemmological methods of investigation like RI, SG and energy-dispersive X-ray fluorescence spectroscopy (EDXRF) are not applicable to such small-scale structures. The rigorous identification of all the phases present is only possible using polarization microscopy of

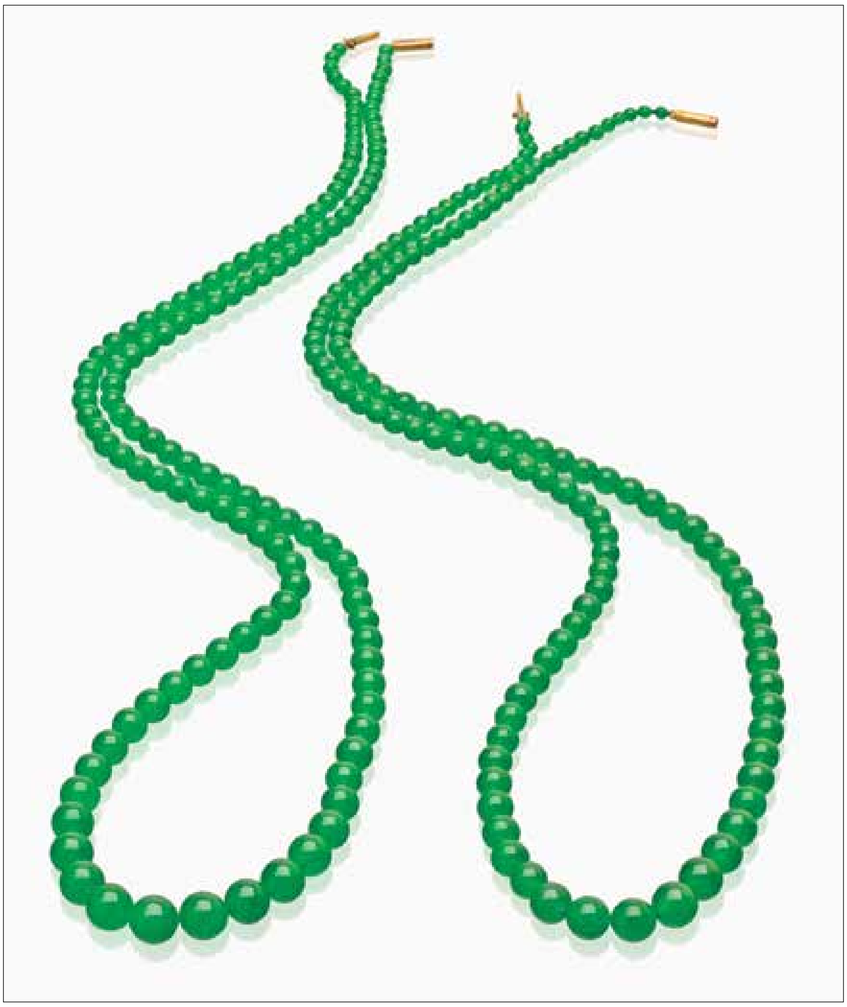

Figure 11: The pure, translucent appearance and high quality of the beads in these necklaces suggests that they consist only of jadeite with little or no impurities. Each of the necklaces is composed of 127 Imperial jadeite beads in graduated sizes ranging from 3.45 to 10.15 mm in diameter. They are approximately 75.5 and 79.5 cm long, and sold for HK$42,680,000 at the Sotheby's Hong Kong auction in October 2013. Photo by Luc Phan, © Swiss Gemmological Institute SSEF.

thin sections and electron microprobe analysis, which is unfeasible for gem samples.

An appropriate non-destructive approach used by gemmological laboratories should employ Raman or FTIR analysis to assess the composition of jadeite-bearing rocks and identify them correctly. As an example, we suggest that 20 spots on the surface of a medium-grained sample should be analysed. (The total number of analysed points should, of course, depend on the texture and grain size of the sample, with more points necessary for heterogeneous and finer-grained samples and fewer points needed for coarse-grained specimens.) When the same result is obtained for 15 of these spots (75%), this should be used to name the sample. Therefore, if 15 out of 20 analysed points were jadeite and the remaining spots were kosmochlor or omphacite, the rock should be called kosmochlor-jadeite jade or omphacite-jadeite jade, respectively. We propose that *jade* should be used as part of the name, as this word has traditionally been used for the classification of such polymineralic rocks.

The International Mineralogical Association (IMA) has already established a nomenclature framework that has been useful for mineralogists worldwide since 1988, and jadeite, kosmochlor and omphacite are all mineral names that are accepted by the IMA. According to the nomenclature given by CIBJO, we suggest using the terms *jadeite jade, kosmochlor jade* and *omphacite jade* to describe gems that consist predominantly of these constituents. As described above, we propose analysing a grid on a sample, with the most abundant mineral used to determine the name. This method would provide a simple and helpful tool for jade dealers and gemmologists who have some basic training to understand the complexity of jade classification. It is hoped that such a practical classification will be widely accepted, thus making the trading of jade easier.

Fei Cui and Jade Terminology

The use of the term *fei cui* by the Hong Kong government to refer to a granular to fibrous polycrystalline aggregate composed of jadeite, omphacite and/or kosmochlor is in accordance with Chinese tradition. However, we feel that the terms *jadeite jade, kosmochlor jade* and *omphacite jade* are more in-line with the mineralogical and scientific nomenclature of jade identification. Nevertheless, the term *fei cui* can be added as an optional modifier. In such a case, an example of this terminology would be 'jadeite jade *(fei cui)*'—rather than the wording '*fei cui* (jadeite jade)' that is currently used in Hong Kong. In English, the latter format could imply that all *fei cui* is jadeite jade, which would be misleading.

Conclusion

This study shows a wide diversity in the jadeite-bearing rocks from Myanmar that are used for decorative and jewellery purposes. Petrographic and micro-chemical studies reveal that these rocks exhibit extensive chemical and textural inhomogeneities, which render a classification by common gemmological methods rather difficult. With the help of thin-section investigations in combination with electron microprobe analysis, five different groups of jadeitite and omphacitite rocks were recognized. These rocks display a wide range of mineral content and rock fabric, resulting in quite a variable macroscopic and microscopic appearance.

With the recognition of this diversity, and with more advanced instrumentation available in gemmological laboratories, there is a call for revising the former jade nomenclature. We propose analysing a sample using Raman or FTIR spectroscopy on a point grid, with the most abundant mineral giving the name (i.e. *jadeite jade, omphacite jade* or *kosmochlor jade*).

References

Bender F., 1983. *Geology of Burma—Beiträge zur Regionalen Geologie der Erde.* Gebrüder Bornträger, Berlin, Germany, 293 pp.

Chhibber H.L., 1934. *The Mineral Resources of Burma.* Macmillan, London, 320 pp.

CIBJO, 2013. *The Gemstone Book.* Coloured Stone Commission 2013-1, 67 pp., www.cibjo.org/download/13-10-26%20Official%20CIBJO%20Gemstone%20Book.pdf.

Damour A.A. 1863. Notice et analyse sur le jade vert: Réunion de cette matière minérale à la famille des wernerites. *Comptes Rendus des Séances de l'Académie des Sciences,* **56**, 861–865.

Davidson P.M. and Burton B., 1987. Order-disorder in omphacitic pyroxenes: A model for coupled substitution in the point approximation. *American Mineralogist,* **72**(3–4), 337–344.

Deer W.A., Howie R.A. and Zussman M.A., 1997. *Rock-Forming Minerals—Single Chain Silicates,* Vol. 2A. The Geological Society, London, 668 pp.

Downs R.T., 2006. The RRUFF Project: An integrated study of the chemistry, crystallography, Raman and infrared spectroscopy of minerals. *Program and Abstracts of the 19th General Meeting of the International Mineralogical Association,* Kobe, Japan, 23–28 July, Abstract O03-13, 117.

Droop G.T.R., 1987. A general equation for estimating Fe^{3+} concentrations in ferromagnesian silicates and oxides from microprobe analyses, using stoichiometric criteria. *Mineralogical Magazine,* **51**, 431–435, http://dx.doi.org/10.1180/minmag.1987.051.361.10.

Ernst K., Franz L., Krzemnicki M.S., Harlow G.E., De Capitani C. and Kouznetsov N., 2013. A new occurrence of kosmochlor in Cr-jadeite rocks from Kenterlau-Itmurundy (Lake Balkhash, Kazakhstan). *Abstract Volume—11th Swiss Geoscience Meeting,* Lausanne, Switzerland, 15–16 November, 96–97.

Foshag W.F., 1957. Mineralogical studies on Guatemalan jade. *Smithsonian Miscellaneous Collections,* **135**(5), Publication 4307, 60 pp.

Gaines R.V., Skinner H.C.W., Foord E.E., Mason B. and Rosenzweig A., 1997. *Dana's New Mineralogy,* 8th edn. John Wiley & Sons Inc., New York, New York, USA, 1,872 pp.

García-Casco A., Rodríguez Vega A., Cárdenas Párraga J., Iturralde-Vinent M.A., Lázaro C., Blanco Quintero I., Rojas Agramonte Y., Kröner A., Núñez Cambra K., Millán G., Torres-Roldán R.L. and Carrasquilla S., 2009. A new jadeitite jade locality (Sierra del Convento, Cuba): First report and some petrological and archeological implications. *Contributions to Mineralogy and Petrology,* **158**, 1–16, http://dx.doi.org/10.1007/s00410-008-0367-0.

Goffé B., Rangin C. and Maluski H., 2000. Jade and associated rocks from jade mines area, northern Myanmar as record of a polyphased high pressure metamorphism. *Eos, Transactions American Geophysical Union,* **81**(48), Fall Meeting Supplement, Abstract V21E-10, http://abstractsearch.agu.org/meetings/2000/FM/sections/V/sessions/V21E/abstracts/V21E-10.html.

Green E.C.R., Holland T.J.B. and Powell R., 2007. An order-disorder model for omphacitic pyroxenes in the system jadeite-diopside-hedenbergite-acmite, with applications to eclogite rocks. *American Mineralogist,* **92**(7), 1181–1189.

Gübelin E.J., 1964–1965. Maw-sit-sit: A new decorative gemstone from Burma. *Gems & Gemology,* **11**(8), 227–238.

Gübelin E.J., 1965. Maw-sit-sit—A new decorative gemstone from Burma. *Journal of Gemmology,* **9**(10), 329–344, http://dx.doi.org/10.15506/jog.1965.9.10.329.

Hänni H.A., 2007. A European gemologist's thoughts on jadeite jade. *Journal of the Gemmological Association of Hong Kong,* **28**, 25–29.

Hänni H.A. and Meyer J., 1997. Maw-sit-sit (kosmochlor jade): A metamorphic rock with a complex composition from Myanmar (Burma). *Proceedings of the 26th International Gemmological Conference,* Idar-Oberstein, Germany, 27 September–3 October, 22–24.

Harlow G.E. and Olds E.P., 1983. Terrestrial ureyite: Occurrence and significance. *Eos, Transactions American Geophysical Union,* **64**, 353.

Harlow G.E. and Olds E.P., 1987. Observation on terrestrial ureyite and ureyitic pyroxene. *American Mineralogist,* **72**(1–2), 126–136.

Harlow G.E. and Sorensen S.S., 2005. Jade (nephrite and jadeite) and serpentinite: Metasomatic connections. *International Geology Review,* **47**, 113–146 , http://dx.doi.org/10.2747/0020-6814.47.2.113.

Harlow G.E. and Shi G., 2011. An LA-ICP-MS study of lavender jadeite from Myanmar, Guatemala, and Japan. *Gems & Gemology,* **47**(2), 116–117.

Harlow G.E., Sisson V.B. and Sorensen S.S., 2011. Jadeitite from Guatemala: New observations and distinctions among multiple occurrences. *Acta Geologica,* **9**(3–4), 363–387.

Harlow G.E., Sorensen S.S., Sisson V.B. and Shi G.H., 2014. Chapter 10: The Geology of Jade Deposits. In L.A. Groat (Ed.), *The Geology of Gem Deposits,* 2nd edn., Short Course Handbook Series **44**, Mineralogical Association of Canada, Quebec, 305–374.

Hawthorne F.C., Oberti R., Harlow G.E., Maresch W.V., Martin R.F., Schumacher J.C. and Welch M.D., 2012. Nomenclature of the amphibole supergroup. *American Mineralogist,* **97**(11-12), 2031–2048, http://dx.doi.org/10.2138/am.2012.4276.

Hibbard M.J., 1995. *Petrography to Petrogenesis.* Prentice Hall, Upper Saddle River, New Jersey, USA, 587 pp.

Htein W. and Naing A.M., 1994. Mineral and chemical compositions of jadeite jade of Myanmar. *Journal of Gemmology,* **24**(4), 269–276, http://dx.doi.org/10.15506/JoG.1994.24.4.269.

Htein W. and Naing A.M., 1995. Studies on kosmochlor, jadeite and associated minerals in jade of Myanmar. *Journal of Gemmology,* **24**(5), 315–320, http://dx.doi.org/10.15506/JoG.1995.24.5.315.

Hughes R.W., Galibert O., Bosshart G., Ward F., Oo T., Smith M., Sun T.T. and Harlow G.E., 2000. Burmese jade: The inscrutable gem. *Gems & Gemology,* **36**(1), 2–26, http://dx.doi.org/10.5741/GEMS.36.1.2.

Leake B.W., Woolley A.R., Arps C.E.S., Birch W.D., Gilbert M.C., Grice J.D., Hawthorne F.C., Kato A., Kisch H.J., Krivovichev V.G., Linthout K., Laird J., Mandarino J., Maresch W.V., Nickel E.H., Rock N.M.S., Schumacher J.C., Smith D.C., Stephenson N.C.N., Ungaretti L., Whittaker E.J.W. and Youzhi G., 1997. Nomenclature of amphiboles. Report of the subcommittee on amphiboles of the International Mineralogical Association Commission on new minerals and mineral names. *European Journal of Mineralogy,* **9**, 623–651, http://dx.doi.org/10.1127/ejm/9/3/0623.

Liddicoat R.T., 1981. *Handbook of Gem Identification,* 11th edn. Gemological Institute of America, Santa Monica, California, USA.

McClure S., 2012. The jadeite/omphacite nomenclature question. GIA News from Research, Gemological Institute of America, Carlsbad, California, USA, 10 April, www.gia.edu/gia-news-research-nr41012.

Misch P., 1969. Paracrystalline microboudinage of zoned grains and other criteria for synkinematic growth of metamorphic minerals. *American Journal of Science,* **267**, 43–63, http://dx.doi.org/10.2475/ajs.267.1.43.

Morimoto N., Fabries J., Ferguson A.K., Ginzburg I.V., Ross M., Seifert F.A., Zussman J., Aoki K. and Gottardi G., 1988. Nomenclature of amphiboles. *American Mineralogist,* **73**, 1123–1133.

Nyunt T.T., 2009. Petrological and Geochemical Contribution to the Origin of Jadeitite and Associated Rocks of the Tawmaw Area, Kachin State, Myanmar. Ph.D. dissertation, Institut für Mineralogie und Kristallchemie, University of Stuttgart, Germany, 176 pp.

Oberhänsli R., Bousquet R., Moinzadeh H., Moazzen M. and Arvin M., 2007. The field of stability of blue jadeite: A new occurrence of jadeite from Sorkhan, Iran, as a case study. *Canadian Mineralogist,* **45**, 1501–1509, http://dx.doi.org/10.3749/canmin.45. 6.1501.

Okano M., Kitawaki H., Abduriyim A. and Kawano J., 2009. Natural omphacite. *GAAJ-Zenhokyo Lab Report* **6**, 12 March.

Ou Yang C.M., 1984. A terrestrial source of ureyite. *American Mineralogist,* **69**(11–12), 1180–1183.

Ou Yang C.M., 1999. How to make an appraisal of jadeite. *Australian Gemmologist,* **20**, 188–192.

Ou Yang C.M. and Li P.C., 1999. Review of recent studies on black jadeite jade. *Journal of Gemmology,* **26**(7), 417–424, http://dx.doi.org/10.15506/JoG.1999.26.7.417.

Ou Yang C.M. and Qi L.J., 2001. Hte Long Sein – A new variety of chrome jadeite jade. *Journal of Gemmology,* **27**(6), 321–327, http://dx.doi.org/10.15506/JoG.2001.27.6.321.

Ou Yang C.M. and Ng M., 2012. Nomenclature and classification of *fei cui* (pyroxene jade).

Proceedings of the 3rd International Gem and Jewelry Conference (GIT 2012), 12–16 December, Bangkok, Thailand, 240–243.

Ou Yang C.M., Li J.Q., Li H. and Kwok B., 2003. Recent studies on inky black omphacite jade, a new variety of pyroxene jade. *Journal of Gemmology,* **28**(6), 337–344.

Ou Yang C.M., Yen H.K., Ng M.F.Y. and Chan S.Y., 2011. Nomenclature and classification of *fei cui* (pyroxene jade). *Proceedings of International Symposium on Jade,* Peking University, Beijing, 1–2 September, 23–34.

Prosperi L., Adamo I., Bocchio R., Diella V. and Pavese A., 2011. Italian gemstones: Peridot from Sardinia, demantoid garnet from Val Malenco, omphacite "jade" from the Po Valley, Piedmont, amber from Sicily. *32nd International Gemmological Conference,* Interlaken, Switzerland, 13–17 July, 114–117.

Shi G.-H., Cui W., Tropper P., Wang C., Shu G.M. and Yu H.X., 2003. The petrology of a complex sodic and sodic-calcic association and its implications for the metasomatic processes in the jadeitite area in northwestern Myanmar, formerly Burma. *Contributions to Mineralogy and Petrology,* **145**, 355–376, http://dx.doi.org/10.1007/s00410-003-0457-y.

Shi G.H., Stöckhert B. and Cui W.Y., 2005a. Kosmochlor and chromian jadeite aggregates from Myanmar jadeitite area. *Mineralogical Magazine,* **69**, 1059–1075, http://dx.doi.org/10.1180/0026461056960308.

Shi G., Tropper P., Cui W., Tan J. and Wang C., 2005b. Methane (CH_4)-bearing fluid inclusions in the Myanmar jadeite. *Geochemical Journal,* **39**, 503–516.

Shi G., Wang X., Chu B. and Cui W., 2009. Jadeite jade from Myanmar: Its texture and gemmological implications. *Journal of Gemmology,* **31**(5–8), 185–195.

Shi G., Harlow G.E., Wang J., Wang J., Ng E., Wang X., Cao S. and Cui W., 2012. Mineralogy of jadeitite and related rocks from Myanmar: A review with new data. *European Journal of Mineralogy,* **24**, 345–370, http://dx.doi.org/10.1127/0935-1221/2012/0024-2190.

Spry A., 1969. *Metamorphic Textures*. Pergamon Press, Oxford, 350 pp.

Webster R., 1994. *Gems,* 5th edn., revised by P.G. Read. Butterworth-Heinemann, Oxford, 267–279.

Werner A.G., 1774. *Von den äusserlichen Kennzeichen der Fossilien [On the External Characters of Fossils, or of Minerals]*. Leipzig, Germany, 302 pp.

Whitney D.L. and Evans B.W., 2010. Abbreviations for names of rock-forming minerals. *American Mineralogist,* **95**(1), 185–187, http://dx.doi.org/10.2138/am.2010.3371.

Yardley B.W.D., MacKenzie W.S. and Guilford C., 1990. *Atlas of Metamorphic Rocks and their Textures*. John Wiley & Sons, New York, New York, USA, 120 pp.

Yi X., Shi G. and He M., 2006. Jadeitized omphacitite from Myanmar jadeite area. *Acta Petrologica Sinica,* **22**(4), 971–976.

The Authors

Prof. Dr Leander Franz and Prof. Dr Christian de Capitani
Mineralogisch-Petrographisches Institut,
Universität Basel, Bernoullistrasse 30,
CH-4056 Basel, Switzerland
E-mail: leander.franz@unibas.ch

Tay Thye Sun
Far East Gemological Laboratory,
12 Arumugam Road #04-02, Lion Building B,
Singapore, 409958

Prof. Dr Henry A. Hänni
Swiss Gemmological Institute SSEF,
Falknerstrasse 9, CH-4001 Basel, Switzerland

Theerapongs Thanasuthipitak
Department of Geological Science,
Chiang Mai University, Thailand

Wilawan Atichat
The Gem & Jewelry Institute of Thailand (GIT),
ITF Tower, Silom Road, Bangrak, Bangkok
10500

Acknowledgements

Tay Thye Sun sincerely thanks Emeritus Reader Dr Tony Barber (Geology Department, Royal Holloway, University of London) for his constant guidance. Also Ms Swae Swae Aye, Ms Ma Gjam, Mr Nyi Nyi Aung and Mr Tin Kyaw Than are thanked for helping to procure jade samples for this research and obtain information for this project. Willi Tschudin, technician at the Institute for Mineralogy, Earth Science Department of Basel University, provided the polished thin sections. Ms Yang Qiu Jing helped translate an article (in Mandarin) on jadeite jade by Prof. C. M. Ou Yang. H. Orsini-Rosenberg of Bruker (Fällanden, Switzerland) is acknowledged for giving access to their FTIR spectrometers on a trial basis. We gratefully acknowledge the helpful reviews of Dr Guanghai Shi, Dr George Harlow and an anonymous reviewer.

The Discoverer of Tsavorite—Campbell Bridges—and His Scorpion Mine

Bruce Bridges and Jim Walker

Geologist Campbell Bridges was the first to discover gem-quality green grossular in Tanzania in 1967 and in Kenya in 1970. In 1973, Campbell collaborated with Tiffany & Co. in New York, USA, to develop a trade name for this garnet, which they called *tsavorite*—in reference to the nearby Tsavo National Park in Kenya. In 1980, the Scorpion mine, located in the Taita-Taveta District of south-east Kenya, was developed by Campbell and his team into the world's most important consistent and long-term producer of tsavorite. Operations at this mine continued until the tragic murder of Campbell in 2009. His death has had a profound effect on tsavorite production in the region, and activities at all of the Bridges' mining operations have been suspended until a protracted court case is resolved for prosecuting the accused murderers. This article describes the history of the Scorpion mine and the unique geology of the deposit that makes it so productive. Also discussed is the planned reopening of the mine in the near future.

The Journal of Gemmology, 34(3), 2014, pp. 230–241, http://dx.doi.org/10.15506/JoG.2014.34.3.230

Introduction

Campbell Bridges (1937–2009; Figure 1) was a visionary geologist, miner, and entrepreneur, who lived and worked in Tanzania and Kenya for over 40 years. His mother was of Scottish descent and his English father was a geologist who lived and worked in Africa since before Campbell's birth. Campbell grew up in southern Africa and moved to East Africa in the mid-1960s, shortly before discovering important deposits of the green grossular (coloured by V ± Cr) that became known as *tsavorite* (e.g., Figures 2 and 3). Many in the gem and jewellery industry consider tsavorite to be the finest green gemstone that is commercially available in the marketplace.

Campbell and his team consistently produced commercial quantities of tsavorite from his Scorpion mine for nearly 30 years. Then, on 11 August 2009, Campbell, his son Bruce (author BB) and four of Bridges' employees were ambushed on their own mining concession by a group of 35 assailants. Tragically, Campbell was murdered in the premeditated attack. Bruce and his employees fought back with such force and determination that they drove off the attackers—despite sustaining severe injuries—and due to their resolve they prevented the attackers from desecrating Campbell where he had fallen. International media coverage was extensive, and news of the murder spread rapidly throughout the

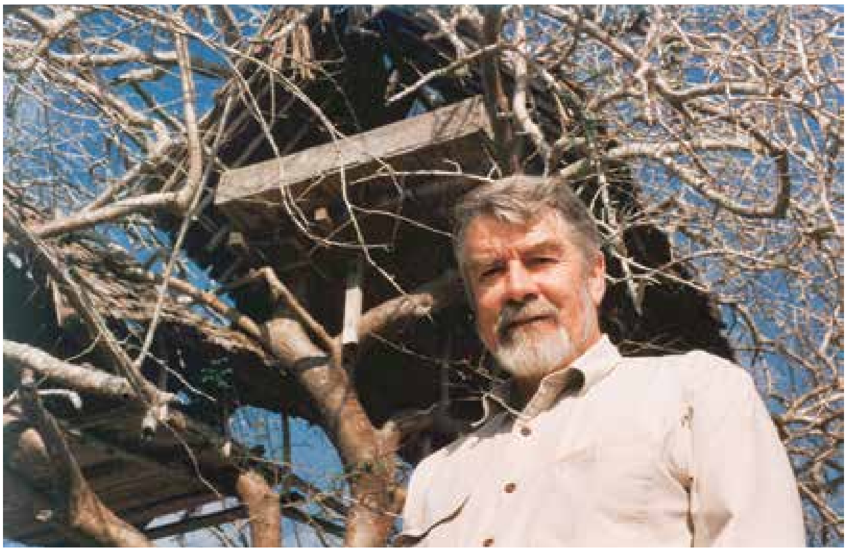

Figure 1: Campbell Bridges stands in front of his first tree house, where he and his wife Judith lived for several years during the period when he discovered and initially mined tsavorite in Kenya. Photo by Judith Bridges, 1993.

gem industry. The Bridges have been inundated with emails of condolence and outrage from over 40 different countries. The international gem community continues to show solidarity and support (e.g. www.thepetitionsite.com/130/justice-for-campbell-bridges), which has been most comforting and humbling to Campbell's family.

In this article, we examine the importance of the Scorpion mine as an historical source of tsavorite. We also look at the impact of Campbell's death on overall tsavorite production from Kenya, and discuss plans for the re-opening of the Scorpion mine, which has the potential to once again become the world's leading source of tsavorite.

Brief History of the Discovery and Naming of Tsavorite

The story of tsavorite's discovery and naming is best described in Campbell's own words, in the following excerpt from an interview with author BB:

> I initially discovered tsavorite in 1961 in Zimbabwe (then Rhodesia) while working for the United Kingdom Atomic Energy Authority. We were locating and assessing beryl deposits, as beryllium was thought at the time to be the best metal for lining atomic reactors. A geological map showed that a range of hills near my camp contained an interesting combination of different rock types

Figure 2: This platinum ring contains a 3.28 ct antique cushion tsavorite from the Scorpion mine surrounded by 0.52 carats of diamonds. The band is set with 1.16 carats of tsavorite. Named 'Eternity', the ring is part of the Bridges Collection jewellery line. Photo by B. Bridges.

Figure 3: These fine-quality tsavorites from the Komolo and Scorpion mines weigh 5.22–12.46 ct. Photo by B. Bridges.

that could well have resulted in the formation of gemstone or other mineral deposits. So one Sunday, when I was off duty, I set out to explore an area near the top of these hills. As I was making my way up the edge of a steep gully, an old rogue buffalo charged out of the bush at me. I jumped down into the gully. The buffalo followed me in a menacing manner along the edge of the ravine for a while, then gave up and went off into the bush. I continued upward, inspecting the rock exposures in the bottom and sides of the gully. Where it neared the top of the hill, I found an outcrop that contained small bright green crystals. This was my first encounter with green garnet.

My second discovery of green grossularite garnet occurred in northern Tanzania in 1967. It occurred in a small hidden valley in a low range of hills just over 100 km south-west of Mt. Kilimanjaro, about 13 km south-east of the village of Komolo. Between Komolo and these hills lies a belt infested with tsetse fly. Sansivera (wild elephant sisal) was abundant in this valley, and because of this ready food supply, a large rhinoceros had made this area his home. The following morning after we had dug a new pit in our search for the green gem, we would find the rhino's tracks firmly implanted in the soil on the edge of the pit. For this reason he came to be known as 'The Mining Inspector' and a sharp eye was always kept out for him as we walked along the narrow trails through the sword-tipped elephant sisal.

A characteristic inclusion of the green garnet from this area was open capillary tubes (sometimes containing gypsum) and when abundant, they resembled a bank of reeds within the body of the stone.

Subsequently, this deposit yielded for a short time some of the largest tsavorites ever found, including one beauty weighing just under 35 ct. But that was long after I had lost the mine due to nationalization by the Tanzanian government and moved to Kenya. The colour of the grossular at this location ranged from pale to a fine rich 'grass'-green.

Toward the end of 1970, I had located a small range of grey, humpbacked hills in southeast Kenya, 135 km south-east of Mt. Kilimanjaro, not unlike the hills of Komolo in appearance. More important, these hills formed part of a belt of similar rock types to those in which the green garnet of Tanzania occurred. Before the end of 1970 I had found my first Kenyan green garnet in these hills, and in 1971 I pegged the first blocks of mineral claims. The area was uninhabited and comprised Hunting Block No. 64. Lying close to the border with Tsavo National Park, elephant, lion and other wild game were abundant. To keep cool during the scorching days of the hot summer months, we constructed a sturdy tree-house in a large gamble flam tree on the side of a hill with a magnificent panoramic view out over the plains to the east. At various times, the flam tree would blossom and surround the tree-house with beautiful orchid-like flowers.

Between the tree-house and the coast, the skyline is broken by the great mountain of Kasigau, rising sheer out of the plain for more than 1,000 m. Each morning the sun rises in a blaze of glory behind this mountain, and as the shimmering air cools towards evening a little cloud appears and lands like a flying saucer on top of Kasigau.

When we were away from the tree-house for any length of time, one of the two leopards that inhabited the range would drag its kill (usually a lesser kudu) up the tree and eat it on my bed. For a short while after our return he would express his displeasure by walking around the tree at night, growling and clawing at the bark, though he still had the benefit of drinking water from the tsavorite-studded bird bath at the bottom of the tree.

In late 1973, Henry B. Platt [then president of Tiffany & Co.; Figure 4], who had taken a keen interest in my discoveries right from the start, decided that it was time to give this gem a trade name. Modern mineralogical convention suggests that the naming of a mineral should end with *-ite*. As Tsavo was the obvious locality choice, Mr Platt and I named the magnificent fiery green gemstone *tsavorite*, while the Germans proposed the name *tsavolite*. My wife had been pushing for *campbellite*—but I had staunchly refused to consider it—I felt very strongly the gem needed to be named for Tsavo.

Figure 4: In 1973, green grossular was given the trade name tsavorite *by Campbell Bridges and Harry Platt, president of Tiffany & Co. Photo by Judith Bridges.*

> CIBJO, a European confederation originally founded in 1926 as 'BIBOA', was expanded in 1961 and renamed CIBJO (Confederation Internationale de la Bijouterie, Joaillerie, et Orfevrerie). Among other purposes, it cements nomenclature and sets 'best practice' guidelines to better engender consumer confidence. CIBJO made a ruling to accept the name 'tsavorite'. The rest is history.

General Geology

The geology of the Scorpion mine area is well understood as a result of observations by Campbell (e.g. Bridges, 1974, 1982) and the present authors, and has been corroborated in several reports by other researchers (Gübelin and Weibel, 1975; Pohl and Niedermayr, 1978; Key and Hill, 1989; Suwa et al., 1996; Keller, 1992; Hauzenberger et al., 2007; Feneyrol et al., 2013). Tsavorite deposits in East Africa are hosted by metamorphic rocks of the Mozambique Belt. The protoliths of these rocks were deposited in a shallow marine environment and subsequently metamorphosed during the East African Orogeny between 650 and 550 million years ago (Feneyrol et al., 2013). Bituminous black shales that were deposited in the marine basins were metamorphosed to form graphite gneiss. Black shales are typically enriched in V, the colouring agent (sometimes with Cr) in tsavorite. The basement rocks in the Scorpion mine area consist primarily of gneisses that are interbedded with mica, kyanite and graphite schists, as well as lesser amounts of quartzites, calc-silicate rocks and marbles. Tsavorite mineralization is hosted by graphite gneisses, which are typically interlayered with schists and bands of marble ranging from 10 cm to 2 m thick. The graphitic gneisses consist of quartz, alkali feldspar, biotite and graphite. Sillimanite, epidote, allanite, titanite, zircon, apatite, hematite and magnetite are also common accessory minerals.

Location and Access

The Scorpion mine and other nearby tsavorite deposits (Figure 5) are located in the Taita/Taveta District of south-eastern Kenya, approximately

Figure 5: The map shows the Bridges' tsavorite mines, which are located near Mindi Hill and the Mgama Ridge in the Mwatate area of south-eastern Kenya.

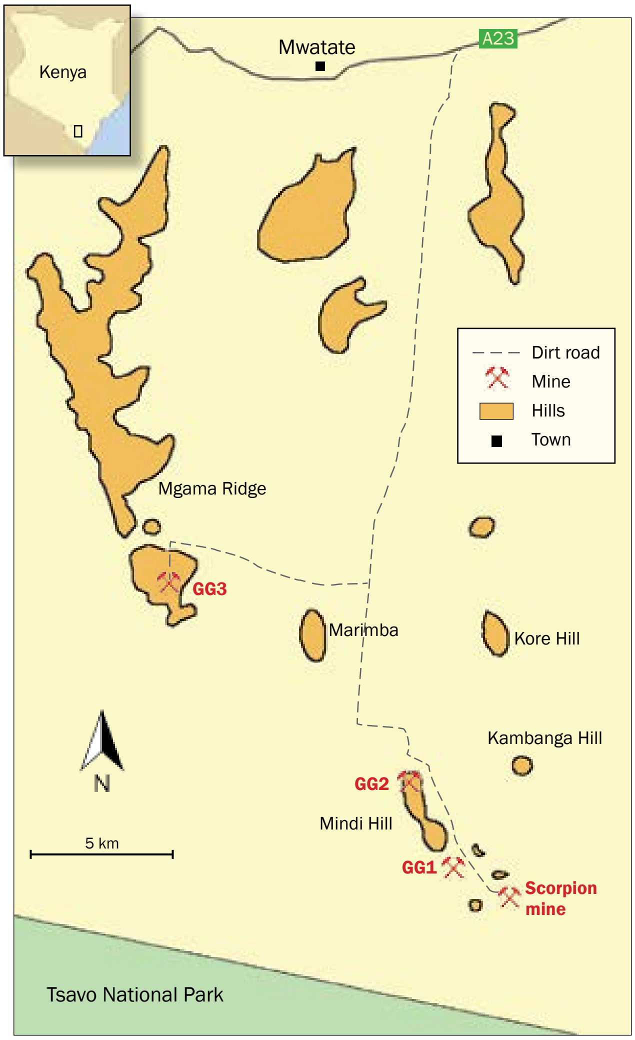

Figure 6: This 1998 photo of the Scorpion mine shows the team opening up a side cut along the No. 4 decline. Photo courtesy of J. Walker.

30 km south of the town of Mwatate, and 5 km outside Tsavo National Park. From Nairobi, this area is accessed by driving south on highway A109 for 329 km to the town of Voi. Then, the route turns west on highway A23, continuing approximately 20 km to Mwatate. This was originally a small bush town inhabited by sisal workers, shopkeepers, small-time mechanics, bar owners, prostitutes, *zurura* (wanderers), gem dealers and *waganga* (medicine men or witch doctors). From Mwatate, the mines are accessed via dirt tracks that lead roughly 30 km south, through rocky outcrops and African savannah that hosts umbrella acacias and *ngoja kidogo* (wait-a-bit) bushes. The tracks are well maintained by the Bridges, but during the rainy season they can become extremely difficult to traverse and in some places impassable.

Early Tsavorite Mining in Kenya

From 1970 to 1979, Campbell worked on what was then called Exclusive Prospecting License No. 164 and surrounding claims. His main operations were called GG1, GG2 and GG3 (GG = green garnet). GG1 is located at the southern end of Mindi Hill, just south of his original tree-house. GG2 is situated on top of the northern-most section of Mindi Hill. GG3 is positioned at the southern end of Mgama Ridge, approximately 7 km north-north-west of Mindi Hill. Both GG1 and GG3 produced tsavorite in a variety of green shades, but most of the material was of a lighter tone, and the cut gems very rarely exceeded 3 ct. Material from GG2 exhibited a variety of tones, and this deposit eventually produced large stones in lighter shades. However, during the 1970s these latter gems were not well accepted in the market. This, of course, has changed today.

When Campbell started working in this area, it was still uninhabited. As news of his discoveries spread, and he gained recognition for his geological knowledge and ability to find gem material, he started seeing more and more people prospecting and staking surrounding claims. As tsavorite continued to gain acceptance in the gem industry, primarily as a result of Campbell's tireless efforts of education and promotion, he realized that he needed to find a deposit that would consistently produce material with a richer colour and in larger sizes. In 1980, approximately 1.5 km to the south-east of GG1, he found exactly what he was looking for. This deposit came to be known as the Scorpion mine, due to the numerous and large scorpions found at the site.

The Scorpion Mine

The Scorpion mine (e.g., Figure 6) is located a few kilometers south-east of Mindi Hill, at a position where the general trend of the rocks turns northward. This general bending of the rocks created a series of tight recumbent folds. This fold structure created an environment in which the hydrothermal solutions needed to form tsavorite collected in channels along the crests and troughs of the folds (Figures 7 and 8a). These 'saddle reefs' at Scorpion were easier to follow than the planar reef structures of

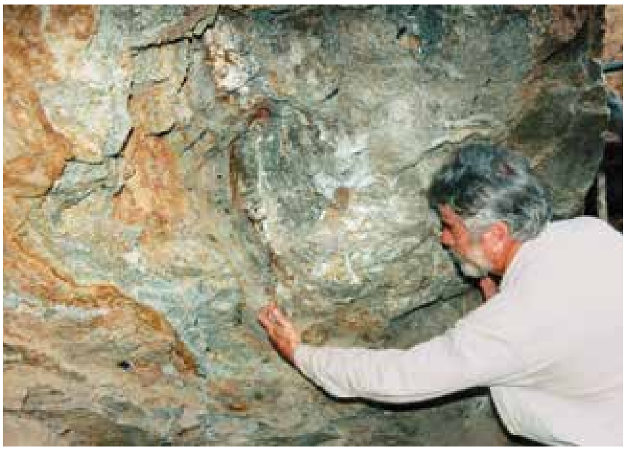

Figure 7: Campbell Bridges indicates the gem-bearing reef in the hinge of a syncline in the No. 2 tunnel of the Scorpion mine. Photo by J. Walker, 1997.

GG1 and GG3, resulting in a larger, more consistent gem production. Campbell strategically engineered his mining tunnels to follow these folds so that the tsavorite mineralization along the crests and troughs could be easily extracted from the ceiling, floor or sidewalls. The folds are tight enough that there commonly are two or more ore shoots containing tsavorite nodules within a single tunnel. The nodules are situated between boudins (i.e., sausage- or barrel-shaped structures formed when a rigid body is stretched and deformed amidst less competent rocks; Figure 8b). The boudins acted as catalysts for tsavorite formation by promoting the formation of conduits for the hydrothermal solutions moving along the fold hinges (Figure 8c). During the mining process, the boudins help mark the locations of the fold hinges, making the ore zones easier to follow than the 'warp zones' in a planar reef. The structure of mineralization in a planar reef is analogous to a plastic pool cover, with air pockets forming in areas where the plastic is warped. The hydrothermal solutions collected in the warp zones between layers of graphite gneiss and marble. Tsavorite mineralization in such zones is inconsistent in frequency—in sharp contrast to saddle reefs. While a saddle reef structure does not assure production at every metre, it does make following the mineralization easier and allows for a more regular formation of tsavorite nodules. Scorpion's reef structure thus combines conditions ideal for both the consistent production of tsavorite and cost-effective mining: by following the hinge of a fold, a relatively steady production of tsavorite is likely.

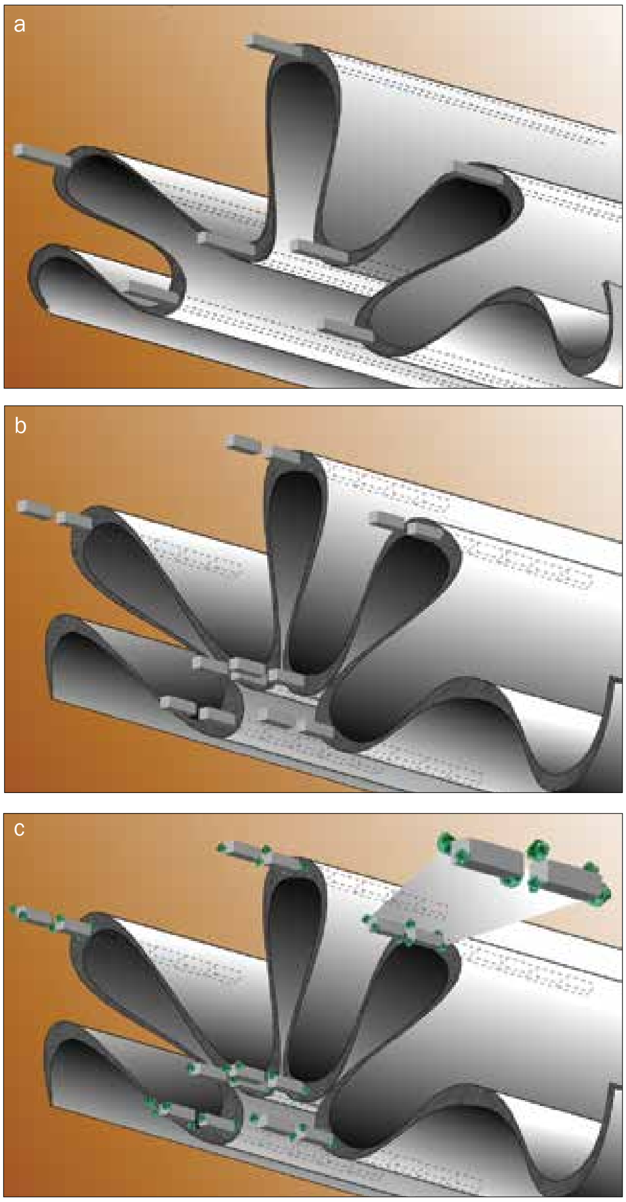

Figure 8: The host rocks at the Scorpion mine were initially deformed into a series of tight recumbent folds (a). With further compression, competent rock units along the hinges of the folds were stretched apart to form boudins (b). Hydrothermal solutions were channelled along the fold axes and boudins, leading to the formation of tsavorite nodules between the boudins (c). Drawings by J. Walker, 2009, not to scale.

In one part of the Scorpion mine (No. 4 tunnel), the nodules were rimmed by blue zoisite (fractured tanzanite). Tsavorite and tanzanite have similar chemical compositions, and Campbell believed the zoisite shell was due to a secondary influx of hydrothermal solutions that reacted with the tsavorite nodule, but at lower temperature and pressure. This was confirmed by Feneyrol et al. (2013), who indicated that zoisite formed during retrograde metamorphism at ~500°C and ~2 kilobars. In another part of the mine (No. 2 tunnel), the rims surrounding the tsavorite nodules consist of kaolinite, epidote and scapolite.

Mining and Production

From the earliest beginnings of the Scorpion mine, Campbell knew he had found a deposit with tremendous potential. He established four declines (tunnels), and kept track of each one's productivity. Ultimately, the No. 2 and No. 4 tunnels proved most productive, and each is now more than 150 m long. The tunnels have proper supports, ventilation, electrical power, and plumbing for water and/or compressed air (e.g., Figure 9).

The No. 2 and No. 4 declines were worked in rotation by three specialized teams (i.e. blasting, jackhammering and pocketing). Since the tunnels penetrate well below the weathered horizon (Figure 10), the rock is extremely hard and therefore requires drilling and blasting. The blasting team marks the face for drilling so that the gem-bearing reef will be undercut by the explosive charge. Depending on the rock conditions, holes are drilled to a depth of 0.5–1.5 m with a burden of 10–15 inches (25–38 cm; the burden is the distance between rows of holes). The holes are charged with gelignite and ammonium nitrate, and the explosives are set off with detonating cord. After the tunnel is cleared of the blasted waste rock, the jackhammer team moves in to 'square up' the face and remove any remaining country rock, while being careful not to disturb the gem-bearing reef. Again the waste rock is removed, in preparation for the pocketing team. This team utilizes hand tools to minimize damaging the gem rough in any unexposed

Figure 9: The tunnels at the Scorpion mine have been properly outfitted for a safe and efficient mining operation, with timbering, ventilation, electricity, a concrete floor and a water line, as shown here in the No. 2 decline. Photo by B. Bridges, 2008.

Figure 10: Here the team uses an 80 lb (36 kg) jackhammer to break up the country rock in the weathered horizon, at a depth of ~30 feet (9.1 m) from the surface. At greater depths, the unweathered rock is extremely hard and requires blasting with explosives. Photo by J. Walker, 1997.

Figure 11: A portion of a tsavorite nodule is shown right after it was extracted from the working face of the No. 2 tunnel of the Scorpion mine. Photo by J. Walker, 1997.

nodules. Hammers and chisels are employed for the majority of the work until a nodule is located. Then smaller hammers, fine chisels and even nails are used to carefully extract the gem material. The nodules initially appear intact, but they are quite fractured (Figure 11). By first removing the surrounding host rock, the gem material can be extracted without damage (Figure 12).

The No. 4 tunnel follows a curved lenticular-shaped saddle reef positioned at the nose of a recumbent fold. In its early days, tunnel No. 4 proved so rich that it became known as the Bonanza Reef, since the quality and quantity of the tsavorite it produced was unlike anything Campbell had ever seen before. The colour was consistently medium-to-deep 'grass' green, sometimes with a slight blue secondary modifying hue (Figure 13).

Figure 13: This tsavorite gem rough from the Scorpion mine ranges from pure green to slightly bluish green. From left to right, the pieces weigh 26 g, 15 g and 9 g. Photo by B. Bridges.

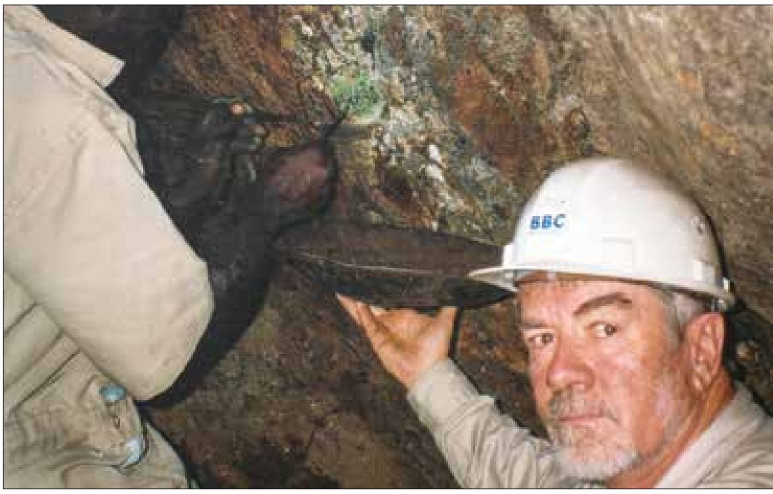

Figure 12: Campbell Bridges supervises the extraction of a tsavorite nodule from the No. 2 tunnel of the Scorpion mine. Lightweight hand tools are utilized to minimize damage to the gem material. Photo by J. Walker, 2003.

The No. 2 decline follows the hinge of a syncline. Its production increased gradually until reaching a maximum in the 1990s. Tsavorite from this tunnel showed a wide colour range, from a vivid medium-light 'spring' green to a vibrant medium-dark 'forest' green. It has also produced some of the largest concentrations of fine tsavorite ever recovered, including one nodule in 2005 that contained over 5 kg of top gem-grade rough. The most impressive stone cut from this production was the Scorpion King, a beautiful medium-dark cushion-shaped gem weighing 20.20 ct (Figure 14).

The most recent production from the Scorpion mine occurred in the No. 2 tunnel in April 2010, when author JW supervised the removal of a section of reef that Campbell and Bruce had prepared for extraction just one day before the attack. The team mined two nodules of tsavorite that yielded beautiful medium to medium-dark material, and cutting of this rough produced a few stones between 2 and 6 ct.

For nearly 30 years, from the time the Scorpion mine was opened until the day Campbell was murdered, the deposit yielded a consistent supply of tsavorite in terms of both quality and quantity.

Figure 14: The Scorpion King is an exceptional 20.20 ct cushion-shaped tsavorite. It was cut from rough material that was recovered in 2005 from a large nodule in the No. 2 tunnel at an approximate depth of 155 m. It is laser inscribed on the girdle with serial number 001 of the Campbell Bridges Signature Collection (see inset, photo by Martin Fuller). Photo by B. Bridges.

This long-term production makes the Scorpion mine the most prolific tsavorite deposit known. While other mines in both Kenya and Tanzania have had productive periods, the planar structure of those deposits has resulted in more sporadic yields of tsavorite.

Marketing and Pricing

During the early years following Campbell's discovery, it was hard to convince anyone to buy tsavorite due to a general lack of awareness. Campbell received comments such as "What is it?", "It's just a garnet" and "The only precious green gemstone is emerald". In response to these and numerous other such remarks, Campbell would cheerfully reply, "Tsavorite is the king of green gemstones, and one day people will be clamouring for it. It will be so popular that there won't be enough supply to meet the demand." Though he is not here to witness it, the present-day tsavorite market is the fulfilment of this prophecy, and supply is indeed struggling to meet demand. In fact, since Campbell's death, tsavorite production has fallen dramatically while the demand for tsavorite has skyrocketed, and prices have leapt to keep pace.

There are a number of reasons for these developments. The Bridges have closed all of their tsavorite mining operations pending the resolution of the trial of Campbell's accused murderers, and this has led to a marked decrease in tsavorite inventory. Production from surrounding tsavorite miners also plummeted after Campbell's passing, since he regularly provided them with guidance in mining techniques and in finding their ore shoots after they pinched or shifted. In addition, many of the miners have redirected their efforts to the low-cost recovery of chrome tourmaline from alluvial deposits that are found in abundance in the 'tsavorite belt' of Kenya and Tanzania; such tourmaline is in strong demand in China. Lastly, continued security problems in the tsavorite-mining area of Kenya have caused many of the legitimate miners to cease operations.

In 1974, when Tiffany & Co. debuted tsavorite to the world, a fine-quality 1 ct stone wholesaled for approximately US$150/ct. Such a gem now sells for between $750/ct and $1,250/ct wholesale. It is important for the gem trade to make the distinction between tsavorite and lighter green grossular (marketed under such names as *mint garnet, mint green grossular, Merelani mint,* etc.). This distinction is akin to the difference between emerald and green beryl. Tsavorite exhibits a richer and deeper colour, whereas green grossular is lighter in tone. The deeper green coloration is produced by higher V and/or Cr (Switzer, 1974), and the availability of green grossular in large sizes appears to correlate with lower concentrations of these chromophoric elements.

In the opinion of the present authors, green grossular should be priced at approximately 20–25% of tsavorite of similar size, shape and clarity. Throughout its short history, tsavorite has witnessed a steady increase in value, even during the U.S. stock market crash in the late 1980s when the prices of the majority of other gemstones fell.

Tsavorite's Unique Properties

The properties of tsavorite were studied by Campbell (e.g. Bridges, 1974) and added to by others (Switzer, 1974; Gübelin and Weibel, 1975; Pardieu and Hughes, 2008–2009). Tsavorite typically is not treated in any way to enhance its colour or clarity.

A well-cut tsavorite is remarkably brilliant. Its bright appearance is due to its relatively high RI of 1.74 and its considerable dispersion of 0.028. Its hardness is substantial, at 7¼–7½ on the Mohs scale, and tsavorite is a tough and durable gemstone with no cleavage. Tsavorite is considerably rarer than emerald, especially in larger sizes (i.e. 3+ ct), and is unique to East Africa in terms of commercial production of gem-quality material.

Being an isotropic gem, the purity of tsavorite's green colour is a defining characteristic. Yet, tsavorite can exhibit a wide range of green hues and tones, from a medium-light yellowish green, to a vibrant bluish green, to a deep 'forest' green (again, see Figure 14). The middle tones (i.e. medium to medium dark) are most sought after, while over-light or over-dark stones are of less value. The most valuable hue is a pure green (Figure 15), or green with a bluish secondary hue. Stones showing the latter coloration are typically more included than those without the bluish hue, which is believed by the authors to be due to a higher Cr content. Indeed, a clean, bright, pure green to bluish green tsavorite weighing more than 2 ct is extremely rare and a gemstone to be prized.

Present and Future of the Scorpion Mine

Since Campbell's murder in 2009, the Scorpion mine and the Bridges' surrounding tsavorite claims have been placed on 'care-and-maintenance' status while the family endures a protracted court process (Pike, 2012). The court case does not have any bearing on the ownership of the mine, but is focused on prosecuting the accused murderers. The Bridges family and their employees continue to receive death threats, so they have decided to minimize any further incidents by keeping a low profile and a smaller work force. The Bridges currently employ 20–30 local people, while in the past they had more than 50 employees. Some of these workers have been with the Bridges' company for 20+ years, and the family feels an acute sense of responsibility towards them and their dependents—all of whom would suffer extreme hardship if the Bridges were to permanently cease operations in Kenya. In addition, by eventually reopening the mine, the Bridges family will continue Campbell's legacy as the founding father of tsavorite and life-long promoter of East African gemstones.

Figure 15: The tsavorites in these platinum earrings show a vibrant pure green colour. Named 'Papillon' in the Bridges Collection jewellery line, the earrings contain 8.34 carats of tsavorite from the Scorpion mine and 0.67 carats of diamonds. Photo by B. Bridges.

To keep their concessions and employees secure, a private security team funded by the Bridges has been placed at the Scorpion mine and elsewhere on their claims until the court case is resolved. The Bridges family and their security staff (assisted by high-level Kenyan government authorities) have been able to identify the majority of the conspirators involved in planning and perpetrating Campbell's murder (Mwaura, 2013). The witnesses have all given testimony in the court case, and the judge should give a final ruling in the near future. In anticipation of this, preparations are currently being made to reopen the Bridges' mining claims.

The present authors strongly believe there is excellent potential for further sustained commercial production of tsavorite from the Scorpion mine. As the tunnels have been mined at depth, multiple additional ore shoots have

Figure 16: Campbell Bridges enjoys the view from his 'luxury edition' tree-house at the Scorpion mine. His legacy of bringing the beautiful green gemstone tsavorite to the gem trade lives on. Photo by B. Bridges, 2008.

been encountered, and these should continue to considerable depth unless they are truncated by faulting or other structural features in the area, which have not been observed. Also, in late 2010, a geophysical survey was conducted to help identify new tsavorite targets in the area formerly known as Exclusive Prospecting License No. 164. The results of this study were favourable, with the survey verifying what Campbell had intuitively already known to be true. As such, this survey will help guide mining efforts in the future.

Conclusion

Pioneers, adventurers and discoverers throughout history have often received their greatest accolades after they have passed from this Earth. This also can be said for Campbell Bridges (Figure 16). Since his tragic murder, tsavorite has seen a dramatic increase in public awareness and appreciation. This, combined with limited additional production, has helped push the price of tsavorite to levels never seen in its approximately four decades on the market. It is most regrettable that the man who moved people with his love of Africa and its gems is not here to see his dream come true. His vision is now inherited by those he loved and inspired.

On her desk, Judith Bridges has a bronze cast from a scorpion that her husband found in the red-gold earth of Tsavo. Campbell encountered the scorpion when they were young and the mining camp was just starting. Their children were young, too, and Tsavo was still very wild. Judith remembers the stories her husband would tell their children at bedtime in the tent by the light of the hurricane lantern—stories of mighty scorpions named 'Crusher' and 'Smasher', 'Steel Claw' and 'Fire Sting'. It was in honour of these warriors that Campbell gave the Scorpion mine its name. When Judith is asked why she fights on to retain control of the mine, although she is so much the underdog, the words of the scorpion in the fable 'The Scorpion and the Frog' come to her…"it is my nature".

The Scorpion mine was instrumental to the emergence and promotion of tsavorite in the global gem industry. It was the first mine to produce tsavorite in consistent quantity and quality due to the structure of its gem-bearing reef. The importance of this mine—and of Campbell's activities in the area—is poignantly demonstrated by the abrupt decrease in tsavorite production since his death. It is the hope of the Bridges family, the friends and colleagues of Campbell and the international gem community, that justice will be served and that security will be restored to the area so that legitimate tsavorite mining can resume. With the court case coming to completion in the near future and the planned reopening of the Bridges' mines, tsavorite production is projected to increase and the Scorpion is set to reassert itself as Africa's premier tsavorite mine once again.

Dedication

This article is dedicated to Campbell Bridges, who shall live forever through his discovery of tsavorite and the love he shared with family and friends. The Bridges family expresses a heartfelt thanks to all those who have supported us in our most trying times and enabled Campbell's legacy and dream for tsavorite to live on.

References

Bridges C.R., 1974. Green grossularite garnets ("tsavorites") in East Africa. *Gems & Gemology,* **14**(10), 290–295.

Bridges C.R., 1982. Gemstones of East Africa. In D.M. Eash (Ed.), *International Gemological Symposium Proceedings,* Gemological Institute of America, Santa Monica, California, USA, 263–275.

Feneyrol J., Giuliani G., Ohnenstetter D., Fallick A.E., Martelat J.E., Monié P., Dubessy J., Rollion-Bard C., Le Goff E., Malisa Q.E., Rakotondrazafy A.F.M., Pardieu V., Kahn T., Ichang'i D., Venance E., Voarintsoa N.R., Ranatsenho M.M., Simonet C., Omito E., Nyamai C. and Saul M., 2013. New aspects and perspectives on tsavorite deposits. *Ore Geology Reviews,* **53**, 1–25, http://dx.doi.org/10.1016/j.oregeorev.2013.01.016.

Gübelin E.J. and Weibel M., 1975. Green vanadium grossular garnet from Lualenyi, near Voi, Kenya. *Lapidary Journal,* **29**, 402–414 and 424–426.

Hauzenberger C.A., Sommer H., Fritz H., Bauernhofer A., Kroner A., Hoinkes G., Wallbrecher E. and Thoni M., 2007. SHRIMP U-Pb zircon and Sm-Nd garnet ages from the granulite-facies basement of SE Kenya: Evidence for Neoproterozoic polycyclic assembly of the Mozambique Belt. *Journal of the Geological Society, London,* **164**, 189–201, http://dx.doi.org/10.1144/0016-76492005-081.

Keller P.C., 1992. *Gemstones of East Africa*. Geoscience Press, Tucson, Arizona, USA, 73–93.

Key R.M. and Hill P.G., 1989. Further evidence for the controls on the growth of vanadium grossular garnets in Kenya. *Journal of Gemmology,* **21**(7), 412–422, http://dx.doi.org/10.15506/jog.1989.21.7.412.

Mwaura M., 2013. Kenya: Eight on trial over Scot's murder. *The Star,* 10 May, http://allafrica.com/stories/201305101762.html.

Pardieu V. and Hughes R.W., 2008-2009. Tsavorite—The untamed beauty. *InColor,* Fall-Winter, 12–20.

Pike S., 2012. Murder, corruption, and greed—The Bridges' continuing fight for justice. *JEA News,* **4**(16), www.palagems.com/bridges.htm.

Pohl W. and Niedermayr G., 1978. *Geology of the Mwatate Quadrangle (Sheet 195/2) and the Vanadium Grossularite Deposits of the Area*. Kenya-Austria Mineral Exploration Project, 1975–1978. Ministry of Natural Resources, Kenya.

Suwa K., Suzuki K., Miyakawa K. and Agata T., 1996. Vanadium grossular from the Mozambique metamorphic rocks, south Kenya. *Journal of Southeast Asian Earth Sciences,* **14**(3/4), 299–308, http://dx.doi.org/10.1016/s0743-9547(96)00066-9.

Switzer G.S., 1974. Composition of green garnet from Tanzania and Kenya. *Gems & Gemology,* **14**(10), 296–297.

The Authors

Bruce Bridges
Bridges Tsavorite, Tucson, Arizona, USA
brucebridges@tsavorite.com

Jim Walker
Bridges Exploration Ltd., Nairobi, Kenya

Emeralds Partially Coated with Amorphous Carbon

Gagan Choudhary

Recently, nine faceted emeralds submitted to the Gem Testing Laboratory, Jaipur, India, were identified as coated owing to the metallic to sub-metallic reflections on their pavilion facets. The coated surfaces did not show any diagnostic features with routine EDXRF and Raman spectroscopy. However, some samples had concentrations of the coating substance in surface cavities, and Raman analysis of those areas revealed the presence of amorphous carbon. Specifically, a broad feature at ~1550 cm^{-1} with a shoulder at ~1360 cm^{-1} identified the coating substance as an 'a-C' type film. Microscopic observation showed that the coating was damaged and removed from several areas, suggesting its instability to normal wear and tear.

The Journal of Gemmology, 34(3), 2014, pp.242–246, http://dx.doi.org/10.15506/JoG.2014.34.3.242

Introduction

The coating of gems is one of the oldest forms of enhancement, and is done to improve the appearance and/or durability of the stone, and thereby its value. The use of traditional coating materials such as paint, ink, plastic or coloured polymers still continues today (e.g. Choudhary, 2011, 2013), but they have been largely replaced by more sophisticated coatings. With advances in technology, improved coating methods have been developed to provide a wider range of colours and optical effects with better durability. During the past several years, a variety of gem materials such as diamond, topaz, quartz, beryl and cubic zirconia have been coated with metals (gold, silver, etc.), oxides (of aluminium, silicon, zirconium, etc.), or fluorides (of calcium, magnesium, etc.), and many of these have been described in the literature (e.g. McClure and Smith, 2000; Evans et al., 2005; Shen et al., 2007; Schmetzer, 2008). In addition, treaters have claimed using other types of films—such as diamond-like carbon (DLC) and nanocrystalline synthetic diamond—to reportedly modify the colour, appearance and/or durability of diamonds and coloured gemstones (e.g. McClure el al., 2010; Shigley et al., 2012). Serenity Technologies (www.serenitytechnology.com), one of the companies that performs such treatments, claims to use a nanocrystalline diamond coating process to improve surface wear resistance of various 'soft' gem materials, including emerald, apatite, tanzanite and others. A Japanese company, Apple Green Diamond Inc., is marketing various synthetic coloured gemstones

Figure 1: These nine faceted emerald samples (3.54–33.64 ct) proved to be coated with an ultrathin carbon-based film on their pavilion facets. Composite photo by G. Choudhary.

(as well as cubic zirconia) that also reportedly have nanocrystalline diamond coatings (http://diamondlite.co.jp).

Although coloured gemstones supposedly coated with DLC have been available in the trade for years (Koivula and Kammerling, 1991), no detailed documentation of these materials is available to the author's knowledge. Recently, the author examined nine faceted emeralds (Figure 1) at the Gem Testing Laboratory, Jaipur, that were identified as coated with an amorphous carbon film. According to the client, these stones made their way to Jaipur from Hong Kong. This article provides a brief characterization of these coated emeralds.

Background on Carbon Film Coatings

Broadly, carbon films have been divided into three types: amorphous carbon (a-C), nanocrystalline and microcrystalline. In materials science, *diamond-like carbon* is defined as amorphous carbon containing an unstructured mixture of sp^2 (as in graphite) and sp^3 (as in diamond) bonds, resulting in variable hardness, chemical inertness, transparency, colour, etc. (e.g. Robertson, 2002; Filik, 2005). The higher the sp^3 content, the greater the hardness and durability of the material. DLC films exist in various sub-forms, depending on their structure and method of production; a few examples are 'a-C:H', 'ta-C', 'ta-C:H' and 'polymeric a-C:H' (e.g. Chu and Li, 2006). However, in the gem industry, treaters frequently claim they use a 'diamond-like-coating' rather than amorphous carbon. Members of the gem trade commonly associate such coatings with diamond and simply call the gems 'diamond coated', but these amorphous carbon or diamond-like carbon films do not have the hardness or durability associated with diamond. Nano-crystalline and micro-crystalline carbon films have quite different structures and properties than amorphous carbon films, and are more closely related to diamond (e.g. Chu and Li, 2006).

Samples and Methods

Nine emeralds, weighing 3.54–33.64 ct (Figure 1), were submitted to the Gem Testing Laboratory, Jaipur, for routine identification without any prior information. Standard gemmological testing was performed to establish their identity. Qualitative energy-dispersive X-ray fluorescence (EDXRF) chemical analyses of all samples were conducted using a PANalytical MiniPal 2 instrument under two different conditions: elements with a low atomic number (e.g. Si) were measured with a tube voltage of 4 kV and current of 0.850 mA, while transition and heavier elements were measured at 15 kV and 0.016 mA. Raman spectra in the region 2000–200 cm^{-1} were collected from all samples using an Airix Corporation – TechnoS Instruments STR 300 confocal microspectrometer with 532 nm laser excitation, an exposure time of 10 seconds per scan, and 10 scans per spot.

Figure 2: The pavilion facets of this 13.45 ct emerald show a golden metallic to sub-metallic lustre that indicates the presence of a coating. Also note the chip in the coating near the keel of the pavilion toward the upper left. Photo by G. Choudhary.

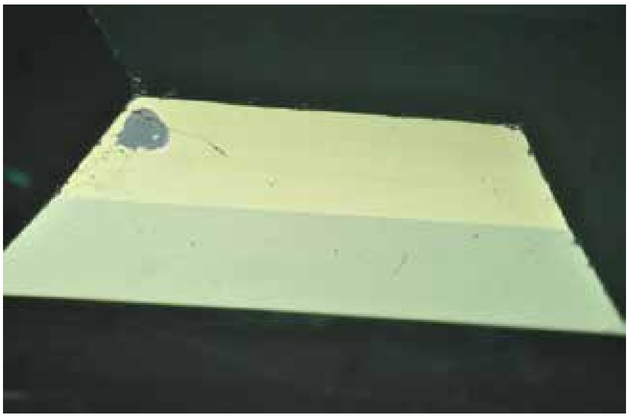

Figure 3: The chipped areas on the pavilion of the 13.45 ct emerald show the duller lustre of the underlying emerald against the bright metallic lustre of the coated facets. Also note the dark line corresponding to a surface-reaching fracture that cross-cuts the large chip. Photomicrograph by G. Choudhary; reflected light, magnified 24×.

Results and Discussion

Visual Observations

When viewed face up, all samples displayed a similar green colour with a slight yellowish tint and moderate saturation (again, see Figure 1) that is typically associated with emeralds. The samples appeared transparent with minor to significant inclusions visible to the unaided eye, and had a vitreous lustre. These initial observations suggested the samples were natural emeralds. However, when their pavilion side was viewed, a golden metallic to sub-metallic lustre was apparent (Figure 2), which raised the suspicion that a surface-related treatment, such as coating, was present on those facets.

Gemmological Properties

All the measured gemmological properties were consistent with emerald. Although it would not have been surprising to find some difference in refractive indices between the crown and pavilion surfaces due to the coating on the pavilion, identical RI values were obtained with similar sharpness of the shadow edges on the refractometer scale.

Microscopic Features

Viewed with the gemmological microscope, all the emeralds displayed typical liquid films, 'fingerprints' and prominent jagged three-phase inclusions along with growth and colour zoning, confirming them as natural and of probable Colombian origin (see e.g. Gübelin and Koivula, 1997). In addition, all the emeralds had been clarity enhanced using a colourless resin, in amounts ranging from minor to significant. The presence of resin was suggested by golden/blue colour flashes along the fractures, and this was later confirmed by infrared spectroscopy (cf. Kiefert et al., 1999).

Viewed with reflected light, even at higher magnification, the crown sides of the emeralds did not display any features related to surface coating, while all the pavilions showed the golden metallic to sub-metallic lustre that was visible with the unaided eye; some chipped areas displayed the vitreous lustre of the underlying emerald (Figures 2 and 3). In addition, some surface-reaching fractures stood out as highly contrasting dark lines against the bright surrounding facet. When the samples were observed in diffused transmitted light, the coating substance appeared brown (Figure 4), particularly where it was more visible around the chipped areas, enabling a comparison between the coated surface and the underlying emerald. Some of the cavities and/or surface-reaching tubules appeared darker than the rest of the coated surfaces, suggesting a thicker concentration of the coating substance in those areas (Figure 5). Under oblique fibre-optic lighting, some of the facets also displayed a strong blue iridescence along with fine lines that appeared to be polishing marks (again, see Figure 5). The coating substance apparently scattered the white light from the polishing lines/grooves, resulting in the blue iridescence.

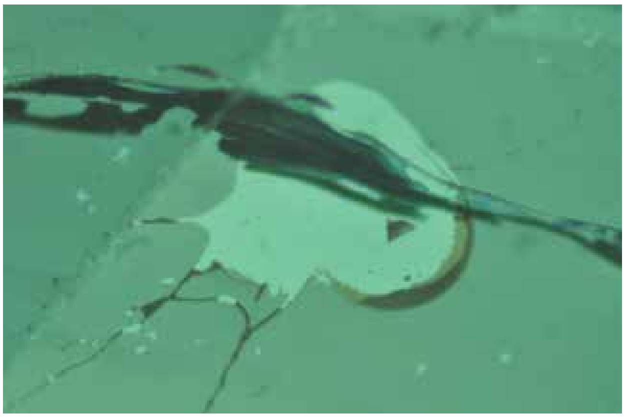

Figure 4: Under diffused transmitted light, the coating layer appears brown, particularly around the chipped areas. Note the difference in colour between the underlying emerald and the surrounding coated surface. Also, the underlying fracture contains some subtle bluish flashes suggesting the presence of resin filler. Photomicrograph by G. Choudhary; magnified 64×.

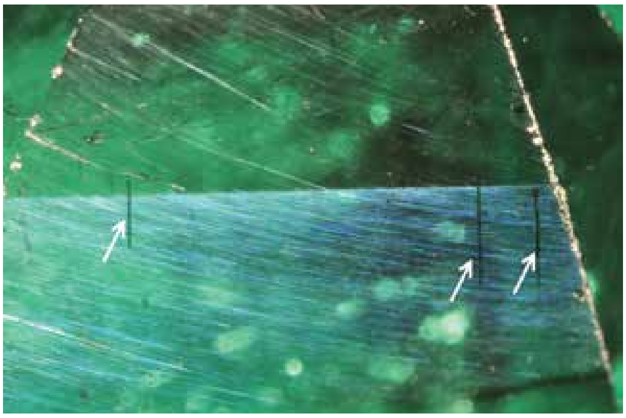

Figure 5: Surface-reaching tubules (see arrows) appear darker than the rest of the coated surface of this emerald, suggesting a thicker concentration of the coating substance within these cavities. In addition, oblique fibre-optic lighting shows an area of blue iridescence that apparently corresponds to light scattering from coated polish marks. Photomicrograph by G. Choudhary; magnified 32×.

EDXRF Analysis

Although the metallic to sub-metallic lustre of the coating suggested the presence of some metallic oxide, EDXRF spectroscopy revealed only those elements associated with emerald: impurities of Ca, V, Cr and Fe were present along with Al and Si. Traces of Ti, which provide one of the key identifying features of the coating process associated with Diamantine (Shigley et al., 2012), were not detected in these samples.

Raman Analysis

Raman spectroscopy of a typical coated surface did not produce any features besides those associated with the underlying emerald, but this was not surprising considering the extremely thin nature of some coating materials. However, Raman analysis of surface-breaking cavities and growth tubes that displayed concentrations of the coating substance showed a broad feature at ~1550 ± 5 $\mathrm{cm^{-1}}$ with a shoulder at ~1360 ± 5 $\mathrm{cm^{-1}}$ (Figure 6). The band at ~1550 $\mathrm{cm^{-1}}$ is designated as the 'G' peak for graphite, while that at ~1360 $\mathrm{cm^{-1}}$ is a 'D' (disorder) peak (e.g. Mednikarov et al., 2005; Chu and Li, 2006); both of these features are due to sp^2 bonding of carbon atoms. Further, the Raman spectral pattern observed for this coating substance was consistent with that reported for a-C films (i.e. softer carbon films formed without hydrogen, usually at low energy or higher temperature; Chu and Li, 2006). The characteristic strong peak of diamond at 1332 $\mathrm{cm^{-1}}$ was completely missing from the coating substance.

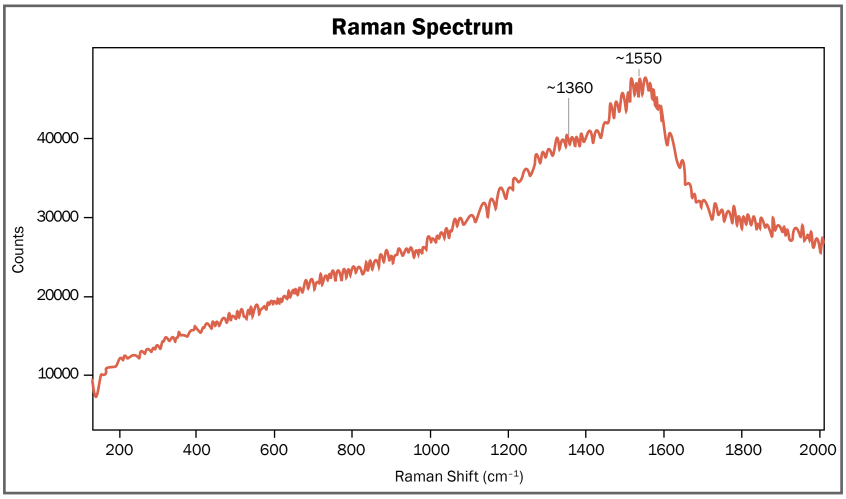

Figure 6: Raman analysis of surface-breaking growth tubes (see Figure 5) containing thicker concentrations of the coating substance produced a broad feature at ~1550 $\mathrm{cm^{-1}}$ with a shoulder at ~1360 $\mathrm{cm^{-1}}$. This spectral pattern is consistent with amorphous carbon films and is due to sp^2 bonding of the carbon atoms.

Conclusions

The identification of these emeralds as coated was quite straightforward because of the presence of metallic to sub-metallic surface reflections on the pavilion facets. However, determining the nature of the coating substance was more challenging, as reported previously for ultrathin carbon-based coatings (e.g. McClure et al., 2010; Shigley et al., 2012). Fortunately, four samples had concentrations of the coating substance in surface features, and Raman spectroscopy of these areas identified the coating as amorphous carbon. Although technically such coatings may be referred to as 'diamond-like carbon', in the gem trade this terminology is often falsely equated to diamond (i.e. 'diamond coated'). However, these coatings do not possess the hardness and durability associated with diamond, and therefore must not be called 'diamond coated'.

Gemstones are typically coated to improve their appearance and/or durability, but in this case a lot has been left for assumption regarding the improvement of either of these factors. These emeralds were coated only on their pavilion facets, which implies that the treatment was intended to improve their brilliance. In a stone like emerald, which is rarely inclusion-free, such a coating will hardly make an impact. Further, the coating on these emeralds had been chipped from several areas, suggesting its instability to normal wear and tear.

References

Choudhary G., 2011. Gem News International: Plastic coated quartz, imitating emerald. *Gems & Gemology,* (**47**)1, 71–72.

Choudhary G., 2013. Violet and pink coated opals. *Australian Gemmologist,* **25**(2), 55–57.

Chu P.K. and Li L., 2006. Characterization of amorphous and nanocrystalline carbon films. *Materials Chemistry and Physics,* **96**, 253–277, http://dx.doi.org/10.1016/j.matchemphys.2005.07.048.

Evans D.J.F., Fisher D. and Kelly C.J., 2005. Coated pink diamond—A cautionary tale. *Gems & Gemology,* **41**(1), 36–41, http://dx.doi.org/10.5741/gems.41.1.36.

Filik J., 2005. Raman spectroscopy: A simple, non-destructive way to characterise diamond and diamond-like materials. *Spectroscopy Europe,* **17**(5), 10–17.

Gübelin E.J. and Koivula J.I., 1997. *Photoatlas of Inclusions in Gemstones.* ABC Edition, Zurich, Switzerland, 249–250.

Kiefert L., Hänni H.A., Chalain J-P. and Weber W., 1999. Identification of filler substances in emeralds by infrared and Raman spectroscopy. *Journal of Gemmology,* **26**(8), 501–520, http://dx.doi.org/10.15506/jog.1999.26.8.501.

Koivula J.I. and Kammerling R.C., 1991. Gem News: Faceted gems coated with diamond-like carbon. *Gems & Gemology,* **27**(3), 186.

McClure S.F. and Smith C.P., 2000. Gemstone enhancement and its detection in the 1990s. *Gems & Gemology,* **36**(4), 336–359, http://dx.doi.org/10.5741/gems.36.4.336.

McClure S.F., Kane R.E. and Sturman N., 2010. Gemstone enhancement and its detection in the 2000s. *Gems & Gemology,* **46**(3), 218–240, http://dx.doi.org/10.5741/GEMS.46.3.218.

Mednikarov B., Spasov G., Babeva Tz., Pirov J., Sahatchieva M., Popov C. and Kulisch W., 2005. Optical properties of diamond-like carbon and nanocrystalline diamond films. *Journal of Optoelectronics and Advanced Materials,* **7**(3), 1407–1413.

Robertson J., 2002. Diamond-like amorphous carbon. *Materials Science and Engineering,* **37**, 129–281, http://dx.doi.org/10.1016/S0927-796X(02)00005-0.

Schmetzer K., 2008. Surface treatment of gemstones, especially topaz—An update of recent patent literature. *Journal of Gemmology,* **31**(1/2), 7–13, http://dx.doi.org/10.15506/jog.2008.31.1.7.

Shen A.H., Wang W., Hall M.S., Novak S., McClure S.F., Shigley J.E. and Moses T.M., 2007. Serenity coated colored diamonds: Detection and durability. *Gems & Gemology,* **43**(1), 16–34, http://dx.doi.org/10.5741/GEMS.43.1.16.

Shigley J.E., Gilbertson A. and Eaton-Magaña S., 2012. Characterization of colorless coated cubic zirconia (Diamantine). *Gems & Gemology,* **48**(1), 18–30, http://dx.doi.org/10.5741/GEMS.48.1.18.

The Author

Gagan Choudhary FGA is deputy director of the Gem Testing Laboratory, Rajasthan Chamber Bhawan, Mirza Ismail Road, Jaipur, India 302 003.
Email: gagan@gjepcindia.com

Acknowledgements

The author is grateful to Dr Tarun Sharda of Jaipur for helpful discussions on diamond films, to the anonymous reviewers for their help with nomenclature of carbon-based coating materials and to Sandeep Vijay of the Gem Testing Laboratory for recording Raman data.


PARAIBA
Powerful Colours

The 'Sleeping Lion' Baroque Pearl: An Update

J. C. (Hanco) Zwaan, Dirk M. van der Marel and Herman A. Dommisse

The Sleeping Lion is one of the largest-known nacreous pearls and has an interesting history. Newly discovered early references indicate that soon after the pearl was sold in Amsterdam in 1778, it was offered for sale in St. Petersburg in 1779. The pearl was recently removed from its setting, allowing its weight to finally be determined at 2,373 grains (593 ct or 118.65 grams). High-resolution X-ray micro-CT scanning revealed the inner structure of the pearl in much greater detail than could be seen during a previous study, and together with Raman spectroscopy, confirmed that the Sleeping Lion is a natural blister pearl. As properties presented in a previous study indicate that this pearl has a freshwater origin, it can be reaffirmed that this is the largest natural freshwater blister pearl documented to date.

The Journal of Gemmology, 34(3), 2014, pp. 248–253, http://dx.doi.org/10.15506/JoG.2014.34.3.248

Introduction

Five years ago, two of the present authors described the properties and history of one of the largest-known nacreous pearls (Zwaan and Dommisse, 2009; Figure 1). At the time we had to estimate the weight of the pearl because it was tightly mounted on a gold rod that was used to set the pearl in the centre of a stylized Lotus bud (Figure 1, inset). However, this rod was removed after the owner decided to show the pearl loose, in order to showcase its 'sleeping lion' appearance when presented on its original display box (described in Zwaan and Dommisse, 2009; see Figure 2). This gave us the opportunity to weigh the loose pearl, and also to examine it with high-resolution X-ray computed microtomography (micro-CT). This short note gives additional historical information and also updates the properties of this remarkable pearl.

History

From historical accounts, Zwaan and Dommisse (2009) reported that the pearl was sold in Amsterdam in 1778, as "a large pearl, of 578 carats, visualizing a sleeping lion…". After it was sold, the pearl's history was unknown until 1865, when the second-known owner from Poland appeared, shortly before the return of the pearl to Amsterdam around 1868.

New information on the history of the pearl was found in an old recipe book for edible molluscs (Lovell, 1867), and kindly brought to our attention by Dr Jack Ogden. It reveals that the pearl probably left Amsterdam shortly after it was

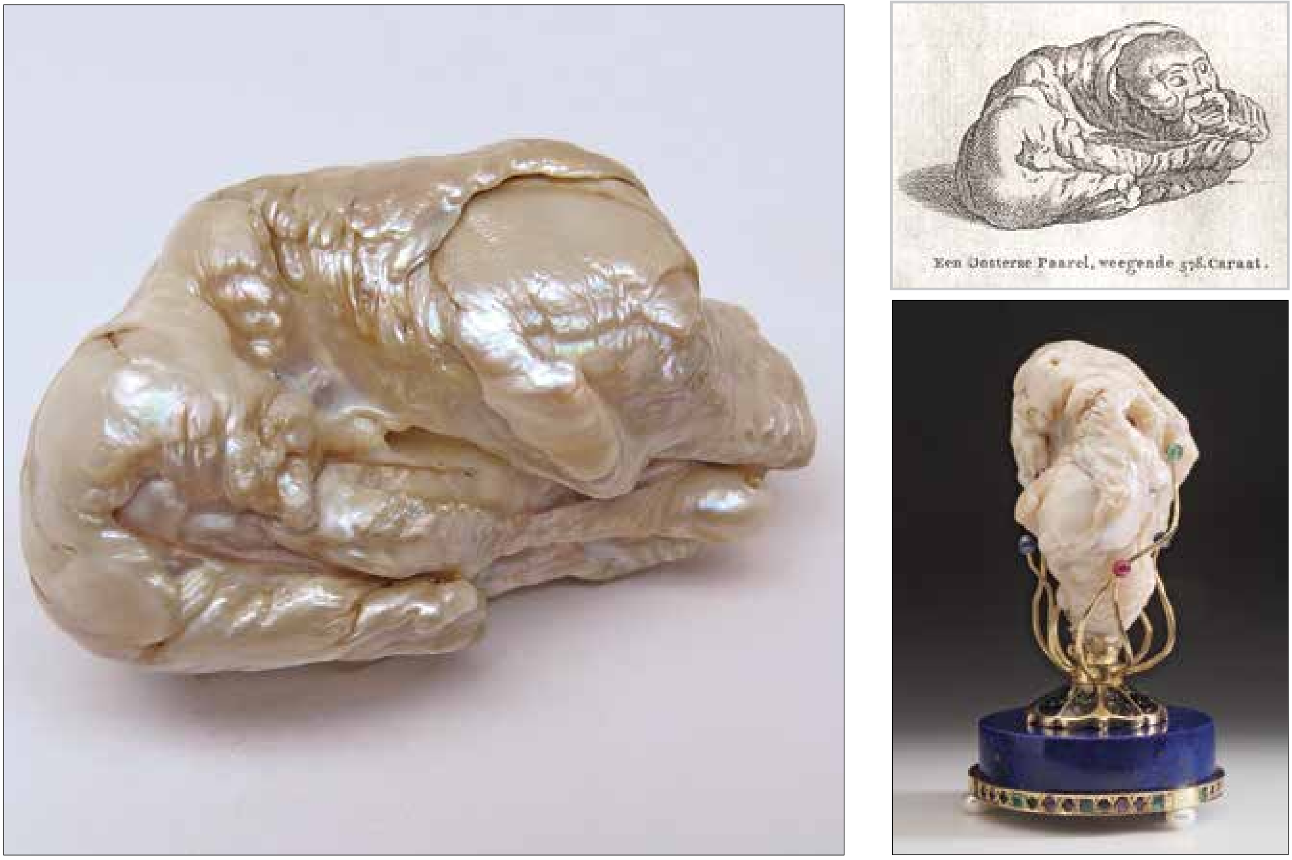

Figure 1: The Sleeping Lion Pearl, which measures approximately 70 × 43 × 39 mm, has been removed from its former setting in the centre of a stylized lotus bud (lower right, photo © Amsterdam Pearl Society). It is now displayed as a loose pearl, as drawn in 1778 (upper right); photo by J. C. Zwaan.

auctioned in 1778, to be sold in St. Petersburg, Russia, the following year: "In 1779 a pearl, which from its shape was called the Sleeping Lion, was offered for sale at St. Petersburg by a Dutchman; it weighed 578 carats, and was bought in India for £4500" (Lovell, 1867, p. 60). Further, Dr Ogden indicated that this information was evidently taken from Nicholson (1808, unpaginated, from the section 'Pearls'): "A pearl, called from its figure the sleeping lion, that weighed 578 carats, was offered for sale at Petersburg in 1779 by a Dutchman. On one side, which was flattish, it was beautifully striped. It was bought in India for 4500*l*." The young Nicholson (1753–1815), a scientist and inventor, arrived in Amsterdam in the summer of 1777 as a sales representative for the English pottery firm of Wedgwood & Bentley (Lamp, 2004). For three years he worked in the old town centre, a few steps away from the Munt tower where the Sleeping Lion Pearl would be auctioned on 26 August 1778. His quote strongly suggests that he had seen the pearl and had

Figure 2: The Sleeping Lion Pearl is displayed on the gilded copper box (approximately 74 × 54 × 47 mm) that was originally manufactured for it. Photo by Tom Haartsen, © Amsterdam Pearl Society.

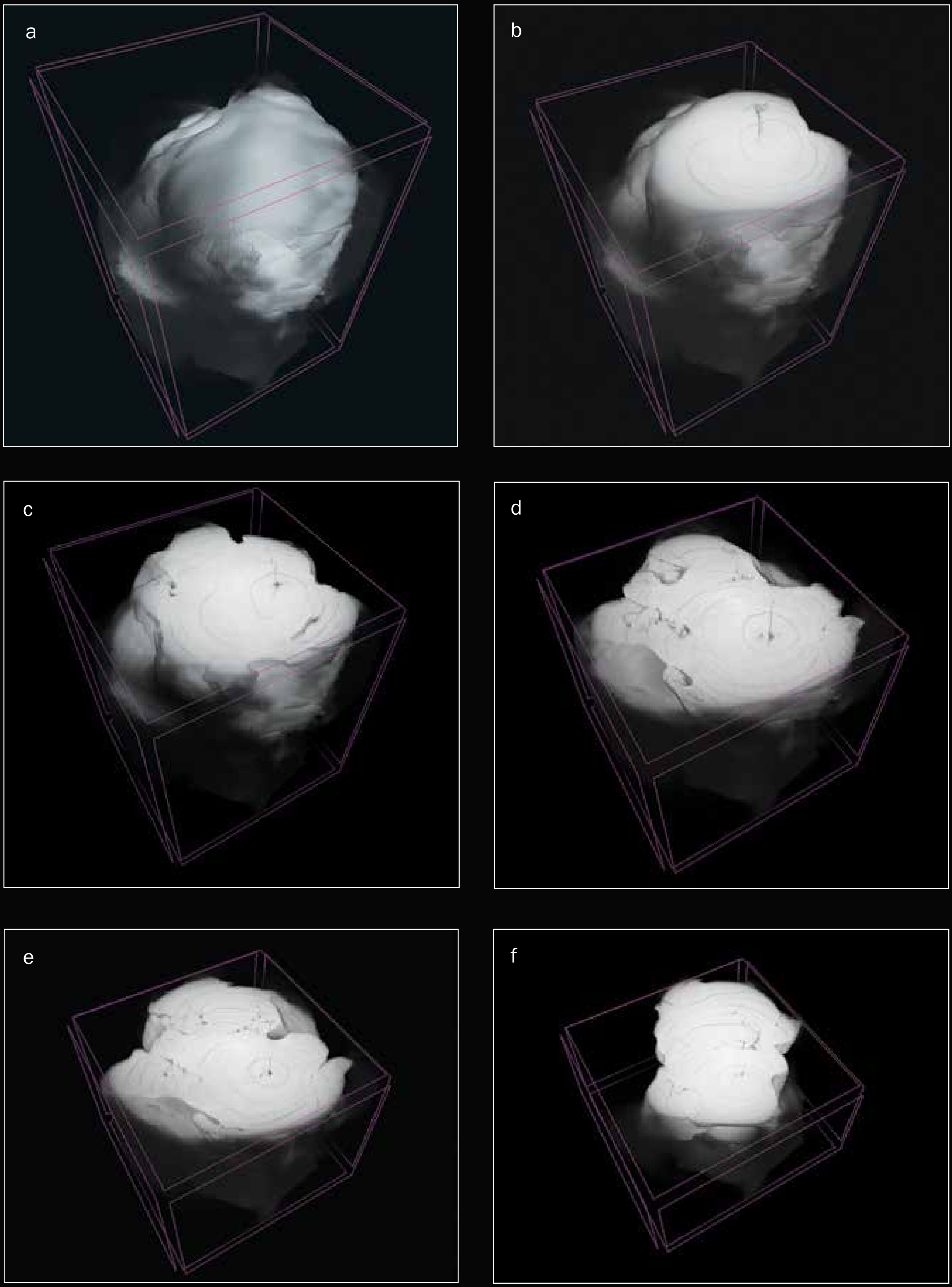

Figure 3: A 3D model of the Sleeping Lion Pearl (a) was reconstructed from X-ray micro-CT scans. Concentric layering is seen in the five scans shown here that were taken along the length of the pearl, from top to bottom (b–f).

carefully observed it himself (the pearl indeed has a rather flat 'striped' reverse side; compare with Figure 4 in Zwaan and Dommisse, 2009). Otherwise he must have taken these observations from somewhere else, but then there would have to be another (slightly older, Dutch?) reference which, to date, has not been found.

This new piece of information, stating that the pearl was bought in India, does not contradict a Far East (or Chinese) origin, as postulated earlier; it also indicates that the pearl probably went to Russia twice, as the previous Dutch owner Louk van Kooten stated that his grandfather Louis van Kooten took the pearl to Fabergé in St. Petersburg, sometime between 1910 and 1914 (Zwaan and Dommisse, 2009).

Weight

The weight of the pearl immediately after the removal of the mounting rod was 593.29 ct (2373.16 grains). Subsequently, the small and narrow drill hole was filled with a mixture of mother-of-pearl grit and glue. The weight of the pearl including this filling is 593.43 ct (2373.72 grains). Thus we have confirmed that the actual weight of the pearl is 2373 grains (118.65 grams), which is 0.6 grams lower than the weight estimated by Zwaan and Dommisse (2009).

Comparing this weight with the 578 ct mentioned by Nicholson (1808) and Lovell (1867), the carat weight used at the time (before the standardization of the metric carat in the early 20th century) must have been around 0.2053 grams, which is exactly the value of the London carat and close to the value of the Amsterdam carat of 0.2057 grams at the end of the 19th century, according to the values given by Lenzen (1970).

Inner Structure and Composition

With the pearl unmounted, we also had the opportunity to study its internal structure with high-resolution X-ray micro-CT scanning, without having to deal with interference problems due to the presence of a metal rod. A Skyscan 1172 micro-CT scanner was used for this purpose. The operating conditions were set at 100 kV and 100 μA, using both Al- and Cu-foil filters and an exposure time of 5,500 milliseconds for each image. Due to its large size, the pearl was divided into five parts that were separately scanned, with the camera offset turned on. For each scan, the pearl was rotated 180° in steps of 0.30°. For each position, three frames were averaged. The five separate scans were stitched together, and after reconstruction a total of 5,325 images were processed. The camera pixel size was fixed at 8.70 μm; after reconstruction, the image pixel size was 13.17 μm. From the reconstructed three-dimensional (3D) model of the pearl, a video was made to show the internal structures along almost the entire length of the pearl, and then going into the pearl from its reverse side (available in an online data depository on *The Journal*'s website).

The high-resolution X-ray micro-CT scans (Figure 3) provide much more detail than the original CT scans (compare with Figure 6 of Zwaan and Dommisse, 2009). Although the shape of the pearl is highly irregular, it shows remarkably consistent concentric layering—typical of natural pearls—that is oriented perpendicular to the long axis of the pearl. The scans also confirm that the pearl is solid throughout, without any substantial hollow cavities. Where cavities are present, they are small and very shallow or thin. When the pearl was viewed from its reverse side (Figure 4; compare with Figure 4 of Zwaan and Dommisse, 2009), parallel growth lines were observed on and near the surface, indicating that this side of the pearl was attached to the shell of the host mollusc. These properties indeed confirm that this is a natural blister pearl.

Raman spectroscopy, using a Thermo DXR Raman microscope with 532 nm laser excitation, was employed to analyse five randomly chosen spots at and slightly underneath the surface of the pearl. The Raman spectra revealed that the white surface consisted of aragonite, with main bands at 1085, 706 and 701 cm^{-1}. The strongest band, at 1085 cm^{-1}, derives from the symmetric stretching mode (ν_1) of the carbonate ion; the doublet at 706 and 701 cm^{-1} corresponds to in-plane bending (ν_4) of the carbonate ion, which is in contrast to the single band at ~711 cm^{-1} found in Raman spectra of calcite (compare, e.g., Urmos et al., 1991; Wehrmeister et al., 2010). Therefore, Raman analysis confirms the nacreous nature of this pearl, as already concluded by Zwaan and Dommisse (2009) on the basis of its

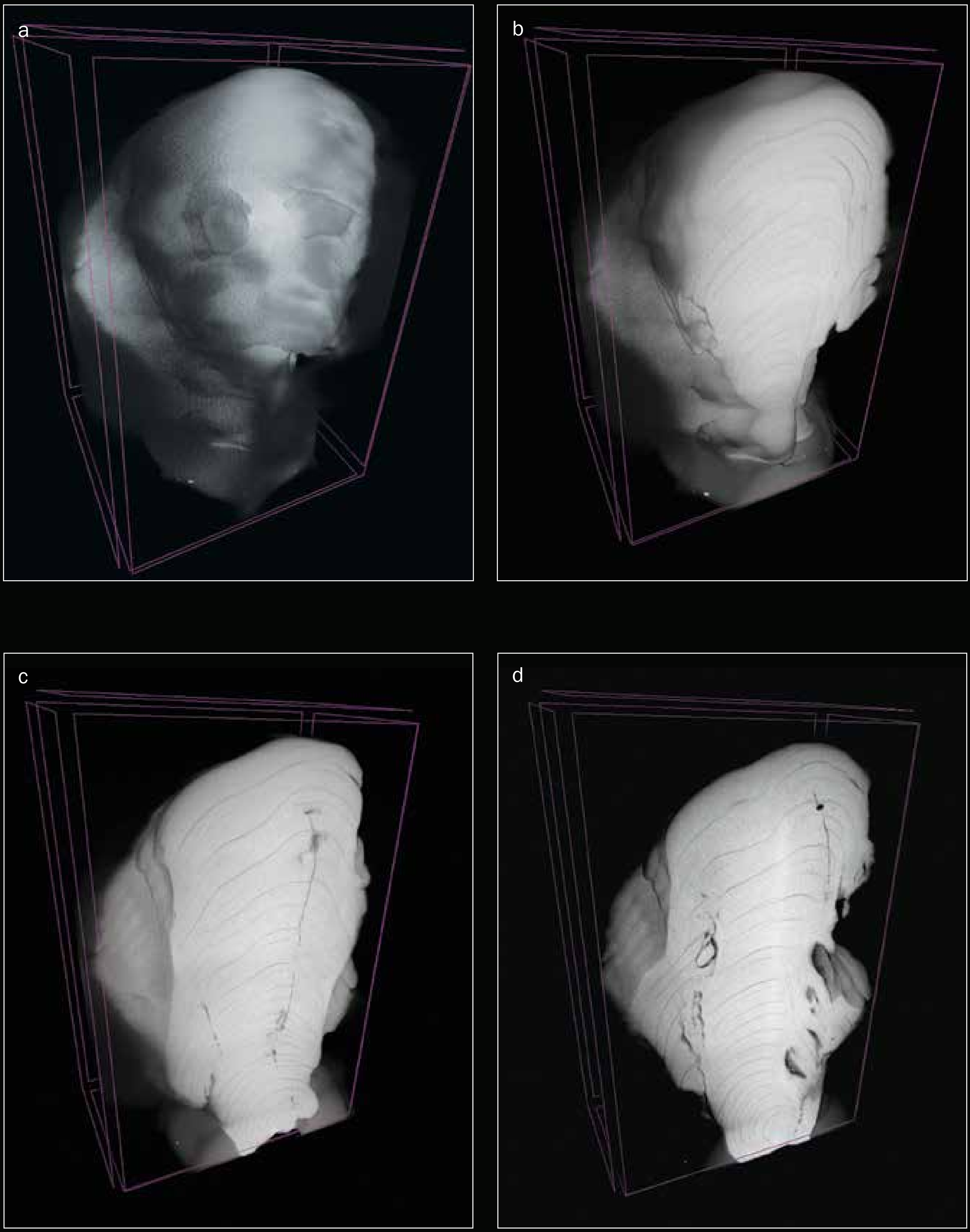

Figure 4: Viewed from its reverse side, the Sleeping Lion Pearl is shown as a 3D model (a) and also in slices (b–d) that reveal parallel growth lines which are oriented roughly parallel to the orientation of the pearl's attachment with the shell of its host mollusc.

optical features. A small, slightly brownish area near the borehole did not reveal bands related to a particular pigment; the Raman spectrum was influenced by relatively strong fluorescence instead. It is possible that this slight coloration formed during the drilling of the borehole.

Conclusion

New evidence shows that soon after the Sleeping Lion Pearl was auctioned in Amsterdam in 1778, it was then offered for sale in St. Petersburg in 1779.

The measured weight of the pearl is 2,373 grains; it is therefore confirmed to be one of the largest-known nacreous pearls, slightly less in weight than the Pearl of Asia (2,420 grains) and slightly greater than the Arco Valley Pearl (2,300 grains; cf. Table II of Zwaan and Dommisse, 2009).

High-resolution X-ray micro-CT scanning and Raman analysis confirmed that this is a naturally formed nacreous blister pearl without any substantial hollow cavities.

References

Lamp P., 2004. *Drie eeuwen Wedgwood en Nederland*. Damon BV, Amsterdam, The Netherlands, 221 pp.

Lenzen G., 1970. *The History of Diamond Production and the Diamond Trade*. Transl. by F. Bradley, Barrie and Jenkins, London, 230 pp.

Lovell M.S., 1867. *The Edible Mollusks of Great Britain and Ireland, with Recipes for Cooking Them*. Reeve & Co., London, 207 pp., http://tinyurl.com/4477n5d.

Nicholson W., 1808. *A Dictionary of Practical and Theoretical Chemistry, with its Application to the Arts and Manufactures, and to the Explanation of the Phaenomena of Nature; Including throughout the Latest Discoveries, and the Present State of Knowledge on those Subjects*. Richard Phillips, London, 826 pp., http://tinyurl.com/3ceawbd.

Urmos J., Sharma S.K. and Mackenzie F.T., 1991. Characterization of some biogenic carbonates with Raman spectroscopy. *American Mineralogist*, **76**(3–4), 641–646.

Wehrmeister U., Soldati A.L., Jacob D.E. and Häger T., 2010. Raman spectroscopy of synthetic, geological and biological vaterite: A Raman spectroscopic study. *Journal of Raman Spectroscopy*, **41**, 193–201, http://dx.doi.org/10.1002/jrs.2438.

Zwaan J.C. and Dommisse H.A., 2009. A description and history of one of the largest nacreous pearls in the world. *Journal of Gemmology*, **31**(5-8), 196–202, http://dx.doi.org/10.15506/jog.2009.31.5.196.

The Authors

Dr J. C. (Hanco) Zwaan and
Dirk M. van der Marel
Netherlands Gemmological Laboratory/
Naturalis, P.O. Box 9517, Leiden,
The Netherlands
E-mail: hanco.zwaan@naturalis.nl

Herman A. Dommisse
Amsterdam Pearl Society, Amsterdam,
The Netherlands; owner of the Sleeping Lion
Pearl.

Acknowledgements

Dr Jack Ogden is thanked for pointing us to the historical references mentioned.

GIT 2014

December 8-9, 2014, Chiang Mai, Thailand

The Exquisite Gem Connectivity

Keynote Speakers:

- **Prida Tiasuwan**
  Board Chairman of Pranda Jewelry Group
  "The Role of AEC in Global Gem and Jewelry Market"
- **Jean Claude Michelou**
  ICA Vice President
  "Past, Present and Future Prospects of World's Colored Stones"
- **Lutz Nasdala**
  Head of Mineralogy and Spectroscopy,
  Institute of Mineralogy and Crystallography.
  University of Vienna
  "Raman Micro-spectroscopy of Diamond"
- **Burak Cakmak**
  Vice President of Corporate Responsibility,
  Corporate Communication and Design Services.
  Swarovski
  "CSR in Gem and Jewelry Business"
- **Thomas Nyborg**
  Managing Director, Pandora Thailand
  "Developing at 10,000 Pieces of Jewelry per Hour"
- **Franco Pianegonda**
  CEO of Franco Pianegonda
  "Jewelry Designs: Creativity In Action"

Conference Dates:

December 8-9, 2014: Technical Sessions, Oral and Poster Presentations

December 3-7, 2014: Pre-Conference Excursion: Mogok, Myanmar, co-organized by AIGS

December 10-12, 2014: Post-Conference Excursion: Phrae - Sukhothai gems field' Northern Thailand

Venue:

Holiday Inn Chiang Mai, Northern Thailand
Accommodations: Hotels in the conference vicinity with special rates to be announced in the 2nd Circular in October 2014

Registration Fees:

- Early bird USD 170, after Oct 31 USD 270
- Student USD 100, after Oct 31 USD 150
- On-Site USD 320
- Pre-Conference Excursion USD 1,180
  (Air ticket and visa to Myanmar excluded)
- Post-Conference Excursion USD 350
  (Limited seats available on first come first serve basis)

Secretariat Office:

Tel: +66 2634 4999 ext. 438
Email: git2014@git.or.th
Pre-Conference Excursion
Contact person: Ho Yu
E-mail: fieldtrip@aigsthailand.com
Facebook: http://www.facebook.com/GITConference2014Thailand

Field Studies in Sri Lanka by GIT

April 2014

Pornsawat Wathanakul

The Gem and Jewelry Institute of Thailand (GIT) recently visited Sri Lanka with the aim of educating five young Thai academic staff from three universities in Thailand about the geology of gem deposits in that country. The trip was accomplished with the technical cooperation of Sabaragamuwa University in Balangoda, Sri Lanka. GIT provided academic support with the participation of associate professor Dr Visut Pisutha-Arnond and this author. The young Thai researchers are all PhD university lecturers in geology, earth sciences and gemmology, namely Drs Krit Won-In, Bhuwadol Wanthanachaisaeng, Somruedee Satitkune, Prayath Nantasin and Pitsanupong Kanjanapayont. Also in attendance was GIT research staff member Ms Nadya Nilhad. The group was led by Gamini Zoysa, a renowned authority on Sri Lankan gems and good friend of GIT.

From Colombo, our route followed highway A26 northeast to the Elahera gem area in Central Province. From Elahera we visited gem deposits in the Kaluganga and Hassalaka areas. We then proceeded southwest through the core terrane of the Sri Lankan highland, and overnighted in the holy city of Kandy before proceeding to the Avissawella gem area in Western Province. Then, on the way to the great gem town of Ratnapura, we visited

The team poses with local Sri Lankan leaders at Mahiyangana quarry in north-western Uva Province, which provides a good exposure of hornblende-biotite-garnet gneiss of the Highland Complex. Photo by C. Wathanakul.

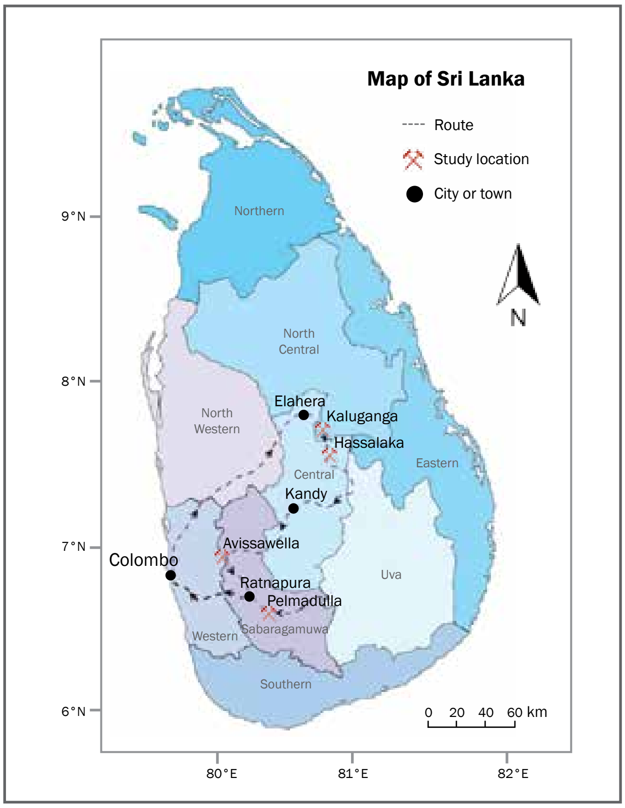

Our route followed a clockwise loop from Colombo, proceeding to Elahera and gem deposits in the Kaluganga and Hassalaka areas, then to the holy city of Kandy, and onward to mines near Avissawella, Ratnapura and Pelmadulla.

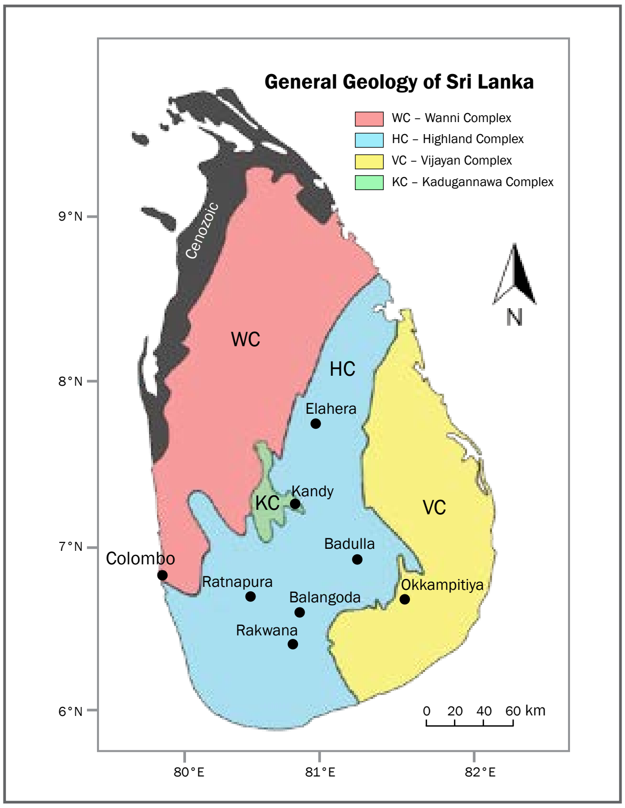

The rocks of Sri Lanka are composed of various Precambrian metamorphic complexes, as well as Cenozoic limestones. Redrawn after Chandrajith et al. (2001) and Zoysa (2013).

Sabaragamuwa University. We studied many gem mines in the Ratnapura area and also near Pelmadulla. We then returned to Colombo, having covered nearly 800 km.

Geology: Sri Lanka consists mainly of three metamorphic rock units called the Wanni, Highland and Vijayan Complexes; there is also a small unit named the Kadugannawa Complex in the Kandy area. The island is composed mostly of metamorphic and sedimentary rocks, as well as igneous rocks including pegmatites of granitic or syenitic derivatives. The metamorphic rocks are mainly made up of charnockite, charnockitic gneisses, quartzo-feldspathic gneiss, calc-gneiss and granulite (Zoysa, 2013). Sri Lanka produces various gems, notably blue sapphire, 'geuda' corundum, chrysoberyl (including cat's eye), kornerupine, several varieties of garnet, topaz, tourmaline, aquamarine and more. Although some primary gem deposits are known on the island, most of the mining exploits gravels, which reflect the original rock types and various gem origins that existed prior to their erosion.

Central and North Central Provinces: The Elahera gem mining area is known for producing good-quality sapphires. Here square-pit mining is done with simple hand tools to access the gem-bearing gravels at depths of about 5–20 m depending on the topography. (Sri Lankan mining law allows the use of mechanised equipment only by special permission.) Gem panning is done directly in the pits, using water pumped from a nearby stream. Fortunately, during our visit a few sapphires were collected together with other gems (garnet, chrysoberyl and tourmaline).

Mining with hand tools is also done around the village of Kaluganga. Here, the eluvial and residual deposits are explored using shovels and iron bars. The miners find residual rock fragments by feeling and listening as they drive the bars into the ground. These rocks and soils are carried to a nearby stream for panning. Our

(A) Miners pan gems within a pit at Dasgiriya, south of Elahera (7°38′13.49″ N, 80°49′20.58″ E). (B) This sapphire was recovered from the Dasgiriya pit during our visit. (C) Also produced from the Dasgiriya pit was this assortment of gem rough. (D) Dr Krit Won-In gets a lesson on gem panning from an experienced miner. (E) In Thorapitiya village near Hassalaka, this pit is being dug in a rice field (7°22′10.24″ N, 80°56′36.81″ E). (F) A fruit plantation hosts this gem mining pit in Thorapitiya village (7°22′07.25″ N, 80°56′48.45″ E). Photos by S. Satitkune (A, B and C), P. Wathanakul (D) and N. Nilhad (E and F).

(A) Gems have been concentrated in this bend of the Seethawaka River near Avissawella (6°57'11.93" N, 80°13'12.32" E). (B) Material from the Seethawaka River is washed and sorted using simple equipment. Photos by P. Wathanakul (A) and K. Won-In (B).

staff was trained in local panning techniques, but we usually kept the sand and threw the concentrates away! Correct panning involves knowing how to move both the pan and your body.

In the Hassalaka area, gems are also mined from compact soil, particularly near Thorapitiya village. The gem pits are dug in all possible areas such as in rice fields and fruit plantations.

Almost at the apex of the highland core is situated the famous holy city of Kandy, where there is a temple that houses Sri Lanka's most important Buddhist relic—a tooth of the Buddha. We witnessed a ceremony with people lined up to pray at the relic, carrying beautiful flowers such as lotus and wild jasmine.

Western Province: In the Avissawella area, we saw gem mining along the Seethawaka River. According to the National Gem & Jewellery Authority of Sri Lanka, this deposit reportedly earned around US$8 million (River bank gem mining projects…, 2014) and produced over 5,000 g of sapphire rough (G. Zoysa, pers. comm., 2014). Mining takes place where the river makes a 90° turn, resulting in the concentration of heavy minerals (including gems) in the river bed.

Sabaragamuwa Province: The Sabaragamuwa region is situated in an intermontane basin within the highland mountains of Sri Lanka. Here lie the great placer deposits of the Ratnapura area, where gems have been derived from rocks of the Highland Complex.

At Sabaragamuwa University, the Sri Lankan government recently established programmes covering the management of gem mining and the gem industry. GIT has been invited to engage in academic cooperation with the university.

On the way to our next destination, we detoured from our route to take a closer look at some outcrops near Pelmadulla. We then noticed a mining pit in a nearby paddy field. While the square pits in Sri Lanka are normally 3×3 m, this one was twice as large (3×6 m). The miners were competing against the seeping groundwater, and they had to work quickly to reach the gem-bearing gravels without the need for a pump to remove water from the pit.

To mine gems in areas of soft wet soil such as paddy fields, the miners have developed a clever method to keep the pits from collapsing. They support the pit walls with wooden timbers together with local plants (such as ferns) to retain the soil between the timbers. This allows only water to seep into the pit.

We obtained a variety of sapphire samples from the Ratnapura area.

Gem Deposit Types: In summary, most of the gem deposits we visited were associated with gravel beds, in which mineral density controls the assemblages that are deposited. A good

(A) Miners search for gems in a paddy field at Migahagoda near Pelmadulla (6°37′00.30″ N, 80°33′30.80″ E). (B) This square pit at Migahagoda employs timbers and local fern vegetation to support the pit walls. (C) Another pit at Migahagoda uses a water pump in addition to structural support of the pit walls. (D) Well-formed, slightly rounded sapphire crystals (here, up to 13.5 mm long) are mined from the Ratnapura area. (E) A variety of colours is seen in these sapphires (up to 12.0 mm) from the Ratnapura area. Photos by P. Wathanakul (A), P. Nantasin (B), V. Pisutha-Arnond (C), P. Kanjanapayont (D) and G. Zoysa (E).

example of this is provided by deposits along the Seethawaka River. Other geological types noted from previous visits to Sri Lanka include the primary deposit of pink sapphires hosted by metamorphic rocks at Wellawaya, as well as gems hosted by pegmatites and skarns.

A wide diversity of rocks of the Highland Complex provided the sources of gems in the gravels. Contact metasomatism is an important mechanism for producing good-quality gem corundum. In addition, various gem minerals can originate from shear zones in the metamorphic host rocks.

References

Chandrajith R., Dissanayake C.B. and Tobschall H.J., 2001. Application of multi-element relationships in stream sediments to mineral exploration: A case study of Walawe Ganga Basin, Sri Lanka. *Applied Geochemistry*, **16**(3), 339–350, http://dx.doi.org/10.1016/s0883-2927(00)00038-x.

River bank gem mining projects gain big profit, Sri Lanka authority said, 2014. ICA Newsletter, May/June, http://tinyurl.com/lfq2lod.

Zoysa G., 2013. Sapphire deposits of Sri Lanka—Past & present. 33rd International Gemmological Conference, Hanoi, Vietnam, 12–16 October, 143–146.

Acknowledgements

GIT thanks Gamini Zoysa for being an excellent field leader, and is grateful to the friendly local miners for showing us their mining techniques. Special thanks are also due to Mr Amitha Gamage, Chairman of the National Gem & Jewellery Authority of Sri Lanka, for permission to export samples. We also acknowledge Mr Padon Tangulrat for drafting the location map.

Dr Wathanakul is Director of GIT, 140 ITF Tower, Silom Road, Bangkok 10500, Thailand, and is an assistant professor in mineralogy and geology of mineral deposits, Department of Earth Sciences, Kasetsart University, Bangkok.
E-mail: pwathanakul2@gmail.com

Gem-A Notices

GIFTS AND DONATIONS TO THE ASSOCIATION

The Association is most grateful to the following for their gifts and donations for research and teaching purposes:

Maggie Campbell Pedersen FGA, London, for back issues of *Gems & Gemology,* the *Goldsmiths' Review* and *Jewellery Studies.*

Prof. Dr Henry A. Hänni FGA, Basel, Switzerland, for a beryl, a synthetic ruby and a rock crystal fashioned as spheres for viewing interference figures with the polariscope.

Liu Hongwei FGA, Tianjin, P.R. China, for a monetary donation.

Miranda E. J. Wells FGA DGA, Ironbridge, Shropshire, for a large collection of garnet-topped doublets in various colours.

MEMBERSHIP

At a meeting of the Council of the Association held on 3 September 2014, Jessica Cadzow FGA was appointed to serve on the Council. The following were elected to membership:

Fellowship and Diamond Membership (FGA DGA)

Onnink, Janneke, *Abbotsford, British Columbia, Canada*
Lowther, Joan, *Stockholm, Sweden*

Fellowship (FGA)

Buis, Jan, *Lopik, Utrecht, The Netherlands*
Chui, Chun Hin, *Shatin, Hong Kong*
Donaldson, Gillian, *Toronto, Ontario, Canada*
Esterhuysen, Stephanus, *Viljoeskroon, South Africa*
Hsieh Chung-Wei, *Chung Ho, Taiwan, R.O. China*
Lee Hsiu Fen, *Leeuwarden, The Netherlands*
Leung Ying, *Tsing Yi, Hong Kong*
Ovesen, Hasanthi, *London*
Tong Xiaofei, *Shanghai, P.R. China*
Wong Ling Sum, Olivia, *Tuen Mun, Hong Kong*
Yang Qiujing, *Singapore*
Yiu King, *Tuen Mun, Hong Kong*

Diamond Membership (DGA)

Hartstone, Bradley, *New Barnet, Hertfordshire*

Associate Membership

Baker, Jan, *Rockhampton, Queensland, Australia*
Bromley, Matthew, *Leamington Spa, Warwickshire*
Carlillo, Antonio, *Ottaviano, Italy*
Davis, Lee, *Louisville, Kentucky, USA*
De Graw, Clare, *Tokyo, Japan*
Engelhard, Tzafrir, *Kfar Saba, Israel*
Frieden, Thomas, *Thun, Switzerland*
Gasimov, Jalal, *Baku, Azerbaijan*
Jakubovic, Deborah, *New York, New York, USA*
Khalsa, Nirinjan, *Beverly Hills, California, USA*
Khan, Amir, *Peshawar, Khyber Pakhtunkhwa, Pakistan*
Khan, Gul, *London*
Love, James, *Belleville, Ontario, Canada*
McAlpine, Ross, *Liverpool, Merseyside*
Matthews, Mark, *San Antonio, Texas, USA*
Moller, Katharina, *Toronto, Ontario, Canada*
Orcel, Riccardo, *London*
Pear, Bradley, *Bloomfield, Michigan, USA*
Prinsloo, Martha, *Gosport, Hampshire*
Proler, Rose, *Houston, Texas, USA*
Santarsiere, Miguel, *Folkestone, Kent*
Taylor, Maxwell, *Maddington, Western Australia, Australia*
Timanova, Desislava, *Sofia, Bulgaria*
Tkachenko, Yegor, *Manhattan, New York, USA*
White, Anthony, *Maldon, Essex*
Williams, Sean, *Stoke-on-Trent, Staffordshire*

Gold Corporate Membership

Wakefields Jewellers Ltd., *Horsham, West Sussex*

OBITUARY

Felix Sydney Cobden FGA (D.1970), Ramat Gan, Israel, died on 22 July 2014.

Network and learn from independent jewellers like you

"The retail jewellery industry is changing so quickly, it's vital to get a wider perspective through the CMJ".

SAMANTHA HANSARD, **CHARLES FISH**

"I'm impressed by the CMJ's vision for the independent retailer".

KARL MASSEY,
PRESTONS OF BOLTON

"When our Christmas marketing material was sent out, we could see a clear increase in the number of customers coming through the door. CMJ marketing really works".

MELANIE WAKEFIELD, **WAKEFIELDS JEWELLERS**

"I can't think of a good reason why any independent jeweller in the UK wouldn't join".

KEITH PERYER, **JOHN BULL & CO.**

"The CMJ is the UK's most professional buying group, offering a range of expertise and help to independents that no one else can provide".

HELEN CADDICK, **ACOTIS**

SEMPER SPLENDIDUS

THE COMPANY OF
MASTER JEWELLERS

Become part of a dynamic co-operative that exists to benefit the retail jeweller.

The CMJ is much more than a buying group offering preferential terms. It is a network of retail members across the UK and Ireland, who together with the CMJ's executive team, approved suppliers and professional experts can provide support, advice and friendship.

Call Lucy, our membership services manager, on **01788 540250** to find out how we can help you.

Learning Opportunities

CONFERENCES AND SEMINARS

Gem-A Conference 2014
1–2 November 2014
London
www.gem-a.com/news--events/gem-a-conference-2014.aspx

Geology and Medicine: Exploring the Historical Links and the Development of Public Health and Forensic Medicine
Geological Society, Burlington House, London
2–4 November 2014
http://tinyurl.com/mgr6cfo

GIT 2014: The 4th International Gem and Jewelry Conference
8–9 December 2014
Bangkok, Thailand
www.git2014.com

Jaipur Jewellery Show (JJS) Seminars
20–23 December 2014
Jaipur, India
www.jaipurjewelleryshow.org

ICDCMT 2015: XIII International Conference on Diamond, Carbon Materials and Technology
13–14 January 2015
Zurich, Switzerland
www.waset.org/conference/2015/01/zurich/ICDCMT

Antwerp Diamond Trade Fair
25–27 January 2015
Antwerp, Belgium
www.antwerpdiamondfair.com/EN/the-adtfnews.html

International Diamond School: The Nature of Diamonds and their Use in Earth's Study
27–31 January 2015
Bressanone-Brixen, Italy
www.indimedea.eu/diamond_school_2015.htm

The Original Miami Beach Antique Jewelry Series 2015
28–29 January 2015
Miami Beach, Florida, USA
www.originalmiamibeachantiqueshow.com/TheShow/JewelrySeries.aspx

AGA Tucson Conference
4 February 2015
Tucson, Arizona
http://accreditedgemologists.org/currevent.php

Hasselt Diamond Workshop 2015, SBDD XX
25–27 February 2015
Hasselt, Belgium
www.uhasselt.be/UH/SBDD-overview/SBDD-overview-SBDD-XX.html

AGS International Conclave
22–25 April 2015
New Orleans, Louisiana, USA
www.americangemsociety.org

Association for the Study of Jewelry and Related Arts 10th Annual Conference
2–3 May 2015
Chicago, Illinois, USA
www.asjra.net/event.html

2015 CIBJO Congress
4–6 May 2015
Salvador, Brazil
http://tinyurl.com/myp9fjv

ICA Congress
16–19 May 2015
Colombo, Sri Lanka
www.gemstone.org/index.php?option=com_content&view=category&layout=blog&id=53&Itemid=38

Society of North American Goldsmiths' 44th Annual Conference
20–23 May 2015
Boston, Massachusetts, USA
www.snagmetalsmith.org/conferences/impact-looking-back-forging-forward

9th International Conference on New Diamond and Nano Carbons
24–28 May 2015
Shizuoka, Japan
www.ndnc2015.org

Jewelry Camp: 2015 Antique Jewelry & Art Conference
30–31 July 2015
West Harrison, New York, USA
www.jewelrycamp.org

Compiled by Georgina Brown and Brendan Laurs

EXHIBITS

Asia

A Little Clay on the Skin: New Ceramic Jewellery
Until 9 November 2014
World Jewelry Museum, Seoul, South Korea
www.wjmuseum.com/eng/e_exhibition.html

Europe

L'Oro nei Secoli dalla Collezione Castellani
Until 2 November 2014
Basilica di San Francesco, Arezzo, Italy
www.museistataliarezzo.it/mostre-eventi

Shine 2014—Young Emerging Design Talent
Until 24 November 2014
The Goldsmiths' Centre, London
www.goldsmiths-centre.org/whats-on/exhibitions/shine-2014-young-emerging-design-talent

With their Heads Held High—Headgear from all over the World
30 November 2014–22 February 2015
Schmuckmuseum, Pforzheim, Germany
www.schmuckmuseum.de

Jewelry. Revisited
Until 31 December 2014
Pinakothek der Moderne, Munich, Germany
www.pinakothek.de/en/kalender/2014-03-15/42328/danner-rotunda-jewelry-revisited

Divine Jewellery: The Art of Joseph Chaumet (1852–1928)
Until 4 January 2015
Musée du Hiéron, Saône-et-Loire, France
www.musee-hieron.fr/expositions/exposition-2014

Splendor et Gloria: Five Exceptional 18th-century Jewels
Until 4 January 2015
Museu Nacional de Arte Antiga, Lisbon, Portugal
www.museudearteantiga.pt/exhibitions/splendor-et-gloria

Treasures of the Middle Ages: Archaeological Finds from Poland
Until 15 March 2015
Museen Stade, Germany
www.museen-stade.de/schwedenspeicher/vorschau-ausstellungen

Gold of the Gods from Java
Until 6 April 2015
Wereldmuseum, Rotterdam, The Netherlands
www.wereldmuseum.nl/en/tentoonstellingen/goud-der-goden.html

Iron Urge: Jewellery and Objects Made Out of Iron
Until 11 May 2015
The Estonian Museum of Applied Art and Design, Tallinn, Estonia
www.etdm.ee/en/exhibitions

An Adaptable Trade: The Jewellery Quarter at War
Until 27 June 2015
Museum of the Jewellery Quarter, Birmingham
www.bmag.org.uk/events?id=3307

North America

Treasures from India: Jewels from the Al-Thani Collection
28 October 2014–25 January 2015
Metropolitan Museum of Art, New York, New York, USA
www.metmuseum.org/about-the-museum/press-room/exhibitions/2014/treasures-from-india

Cycles of Life: Rings from the Benjamin Zucker Family Collection
31 October–6 December 2014
Les Enluminures, New York, New York, USA
http://tinyurl.com/k6lhw2o

Glittering World: Navajo Jewelry of the Yazzie Family
13 November 2014–11 January 2016
The National Museum of the American Indian New York, New York, USA
http://nmai.si.edu/explore/exhibitions/item/?id=890

Brilliant: Cartier in the 20th Century
16 November 2014–15 March 2015
Denver Art Museum, Colorado, USA
www.denverartmuseum.org/exhibitions/brilliant-cartier-20th-century

Ancient Luxury and the Roman Silver Treasure from Berthouville
19 November 2014–17 August 2015
The Getty Villa, Pacific Palisades, California, USA
www.getty.edu/visit/exhibitions/future.html

Kiff Slemmons
20–23 November 2014
Gallery Loupe for Contemporary Art Jewellery, Montclair, New Jersey, USA
www.galleryloupe.com/exhibitions.php?sn=0&exhibit=57

Remarkable Contemporary Jewellery
Until 30 November 2014
Montreal Museum of Fine Arts, Quebec, Canada
http://wsimag.com/fashion/9308-remarkable-contemporary-jewellery

Gems & Gemology celebrates 80 years, Featuring the Artistry of Harold and Erica Van Pelt
Until December 2014
Gemological Institute of America, Carlsbad, California, USA
www.gia.edu/gia-museum-gems-gemology-anniversary

From the Village to Vogue: The Modernist Jewelry of Art Smith
Until 7 December 2014
Dallas Museum of Art, Texas, USA
www.dma.org/art/exhibitions/Art-Smith

The Greeks—Agamemnon to Alexander the Great
12 December 2014–26 April 2015
Montréal Museum of Archaeology and History, Old Montréal, Québec, Canada
www.pacmusee.qc.ca

Cartier: Marjorie Merriweather Post's Dazzling Gems
Until 31 December 2014
Hillwood Estate, Museum & Gardens, Washington DC, USA
www.hillwoodmuseum.org/whats/exhibitions/cartier-marjorie-merriweather-posts-dazzling-gems

Blue Moon Diamond [12 ct blue diamond]
Until January 6, 2015
Natural History Museum of Los Angeles County, California, USA
www.nhm.org/site/research-collections/mineral-sciences/temporary-displays/blue-moon-diamond

Arts of Islamic Lands: Selections from the al-Sabah Collection, Kuwait
Until 4 January 2015
Museum of Fine Arts, Houston, Texas, USA
www.mfah.org/exhibitions/al-sabah-collection

René Lalique: Enchanted by Glass
Until 4 January 2015
The Corning Museum of Glass, Corning, New York, USA
www.cmog.org/collection/exhibitions/lalique

Hollywood Glamour: Fashion and Jewelry from the Silver Screen
Until 8 March 2015
Museum of Fine Arts, Boston, Massachusetts, USA
www.mfa.org/exhibitions/hollywood-glamour

Arthur Koby Jewelry: The Creative Eye
Until 5 October 2015
Kent State University Museum, Kent, Ohio, USA
www.kent.edu/museum/exhibits/exhibitdetail.cfm?customel_datapageid_2203427=3506741

Gold and the Gods: Jewels of Ancient Nubia
Until 14 May 2017
Museum of Fine Arts, Boston, Massachusetts, USA
www.mfa.org/exhibitions/gold-and-gods

Middle East

Urartian Jewellery Collection
Until 31 July 2015
Rezan Has Museum, Istanbul, Turkey
www.rhm.org.tr/en/event/rezan-has-museum-urartian-jewellery-collection

Australia and New Zealand

Afghanistan: Hidden Treasures from the National Museum, Kabul
Until 16 November 2014
Western Australian Museum, Perth, Australia
http://museum.wa.gov.au/museums/perth/afghanistan-hidden-treasures

A Fine Possession: Jewellery and Identity
Until 20 September 2015
Powerhouse Museum, Sydney, Australia
www.powerhousemuseum.com/exhibitions/jewellery

OTHER EDUCATIONAL OPPORTUNITIES

Gem-A Workshops and Courses
Gem-A, London
www.gem-a.com/education/course-prices-and-dates.aspx

Special Topics in 20th Century Jewelry
4–5 December 2014
Christie's, New York, New York, USA
www.christies.edu/new-york/courses/short-course-jewelry.aspx

Gemstone Safari
5–22 January and 13–30 July 2015
Tanzania
www.free-form.ch/tanzania/gemstonesafari.html

Montreal School of Gemmology Gem and Jewellery Appraisal Course
6–29 July 2015 (in English and French)
Montreal, Quebec, Canada
www.ecoledegemmologie.com/en/c/10

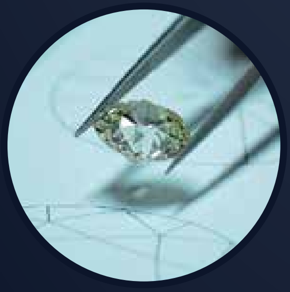

New Media

The Antoinette Matlins ‘Right Way’ Series on Using Gem Identification Tools

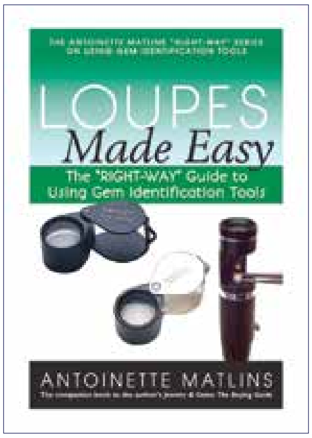

By Antoinette Matlins, 2013. GemStone Press, Woodstock, Vermont, USA, www.gemstonepress.com.

- *Loupes Made Easy,* 57 pages, ISBN 978-0943763941. US$9.99 eBook.
- *Dichroscopes Made Easy,* 52 pages, ISBN 978-0943763965. US$9.99 eBook.
- *Chelsea and Synthetic Emerald Filters Made Easy,* 45 pages, ISBN 978-0943763958. US$9.99 eBook.
- *Refractometers Made Easy,* 53 pages, ISBN 978-0943763989. US$9.99 eBook.
- *Ultraviolet Lamps Made Easy,* 57 pages, ISBN 978-0943763972. US$9.99 eBook.
- *SSEF Diamond-Type Spotter and Blue Diamond Tester Made Easy,* 47 pages, ISBN 978-0943763996. US$9.99 eBook.

The six publications in Antoinette Matlins’ ‘right way’ series are available as e-books. The aim of these guides is to introduce the layperson or novice gemmologist to the correct use of various gemmological tools, giving basic (and some more advanced) techniques, and also providing a reference for the results expected for various stones when tested with each tool.

In the loupe book, Matlins covers the key features to look for when purchasing this basic and essential instrument, including the style of casing, which can affect the colour of the stone under examination. Then basic techniques for good observation are provided, as well as examples of how inclusions can be indicative of certain gems.

From the loupe the series moves on to the dichroscope, and here again Matlins demonstrates, without resorting to scientific detail, how it is possible to obtain usable results. Although a dichroscope is seldom diagnostic on its own, the reader is shown how (in conjunction with other tools) it can help identify a gem.

Next to be considered is the Chelsea Colour Filter (developed by Gem-A), and it is covered in significant detail. After initially describing its correct use (and pitfalls), Matlins provides a comprehensive list of results for stones that the reader might encounter in the market. She also covers the ‘synthetic emerald support filter’, which provides additional information when evaluating whether an emerald is natural or synthetic.

The refractometer is next under the spotlight and, although this is an instrument that many students struggle with initially, the book provides clear instructions on how to obtain good data and interpret the results. The use of both white and monochromatic yellow light is covered, and the process of reading the measurement is clearly and concisely detailed. A comprehensive list of the RIs of the most common gems is provided in the latter section of the book, but this would benefit from a more tabular layout, with headings on each page. This is a minor point on what is otherwise a useful guide.

The gemmological uses of UV lamps are also given due consideration, and here Matlins is careful to emphasize the dangers associated with short-wave UV radiation, whilst still maintaining the enjoyment of seeing different reactions and colours produced by various gems. Some of the details provided on synthetic diamonds (both here and in the final book of the series on the SSEF Diamond Spotter) have been superseded by changes in technology and production methods, but generally the book provides a good reference to a wide range of fluorescent and phosphorescent effects that should satisfy any gemmologist.

The final book in this series deviates slightly from covering the more standard gemmological tools, insofar as it describes the Swiss Gemmological Institute SSEF’s Diamond Spotter. This instrument relies on the use of short-wave UV radiation to separate colourless diamonds into two categories: types IaA, IaAB and Ib (i.e. those not decolorized by HPHT treatment) and types IIa, IIb and rare IaB (i.e. those that may have undergone HPHT treatment). Again, Matlins is careful to remind the user of the dangers of short-wave UV radiation. Although not an everyday tool for most gemmologists, this, along with the Blue Diamond Tester (also from SSEF), is given the same level of detail as the other tools previously covered. Again, recent changes in technology and production techniques have affected some of the areas covered, but as a guide to get started using these instruments, this is a very good reference.

Although probably not a replacement for classroom training, these 'right way' guides provide a very good and understandable introduction to gem testing, and can, if used correctly, prevent costly gem identification mistakes.

Andrew S. Fellows

London's Lost Jewels: The Cheapside Hoard

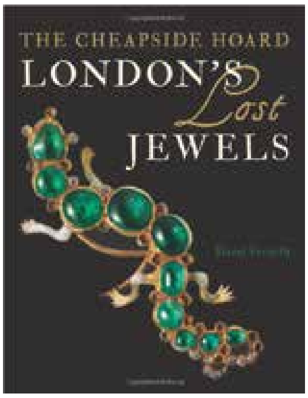

Hazel Forsyth, 2013. Philip Wilson Publishers, London, 248 pages, illus., softcover, www.museumoflondonshop.co.uk/store, ISBN 978-1781300206. £19.95.

Within its 248 pages, Hazel Forsyth has compiled more than one book. It is both history and mystery combined. The history covers the period up to the mid-17th century, a time that saw the plague, the overthrow of the British monarchy and the Great Fire of London. The mystery came to light in 1912 when buildings on the corner of Cheapside and Friday Street were to be demolished due to their subsidence and dangerous condition. They had stood there since 1667, the year after the Great Fire had razed much of the city. Although the name *Cheapside* seems far removed from the realm of precious jewels, in fact the whole area was a hive of industry—particularly for jewellery manufacturing.

With the prospect of redevelopment after the Great Fire, an unusual clause was inserted into the contract between the owners of the property (the Worshipful Company of Goldsmiths) and the building contractors and developers. It stated that any antiquities and articles or objects of interest or value should be preserved by the lessees and handed over to the lessors—the Worshipful Company. As the workmen began to break open the cellar floors, their picks uncovered the stock in trade of a 17th-century jeweller and the biggest cache of its kind in the world.

From the moment of discovery, there was a problem. The workmen did not hand over the jewels to the authorities, but took them to George Fabian Lawrence, better known as 'Stony Jack' (1862–1939): a pawnbroker, dealer, collector of antiquities and sometime employee of the Guildhall and London Museum. He cultivated the navvies of London and by gaining their confidence, was able to acquire 15,000 items in 15 years for what is now known as the Museum of London, which is located in the Barbican, close to Goldsmiths' Hall and the Cheapside Hoard site.

The workmen from the Cheapside site turned up at Stony Jack's office with 'many great lumps of caked earth which revealed intriguing gleams at various points'. The men thought they had unearthed a toyshop. Lawrence set about cleaning off the earth to reveal a treasure of tangled enamelled gold chains, cameos, intaglios, carbuncles, assorted gems and hard stones, rings, pendants and watches—a veritable fortune. Unique to the collection is a watch movement of the period which uses for its casing a Colombian emerald crystal!

The treasure was assembled in the Viscount Harcourt's house, where King George V and Queen Mary had a private viewing, and then was examined by the treasury solicitors on behalf of the crown. Surprisingly there was no treasure trove enquiry, and title to the entire collection of almost 500 pieces was granted to the London Museum.

This book was published on the occasion of an exhibition of the Cheapside Hoard that took place at the Museum of London from 11 October 2013 to 27 April 2014. It is filled with photos that explore and reveal the range of items in the Hoard. Regarding the date when the jewels were hidden, two pieces provide clues. One relic (a complicated timepiece with alarm and calendar) bears the name of the Swiss maker Gaultier Ferlite, which dates the watch to between 1610 and 1620. The other is a cornelian seal with the heraldic engraved swan of the Viscount Stafford. The intervention of King Charles I on his behalf points to a date close to 1640.

Hazel Forsyth has researched the Hoard and its history with extraordinary zeal and scholarship, and the reader is entertained with a wealth of fascinating information. The book is a must for anyone interested in gemstones, jewellery or history.

Alan Hodgkinson

Splendour and Science of Pearls

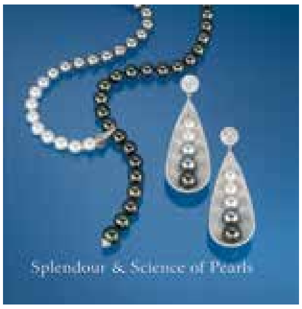

Dona Mary Dirlam and Robert Weldon (Eds.), 2013. Gemological Institute of America, Carlsbad, California, USA, 139 pages, illus., hardcover, http://store.gia.edu/product_p/0201055.htm, ISBN 978-0873110600. US$89.00.

My first impression of this attractive book was that it resembles an exhibition catalogue. After studying it in more detail, I became convinced that it would serve as a very good reference for anyone wanting to stage a comprehensive exhibition about pearls.

The book is divided into 11 chapters that cover a variety of topics, including the formation of pearls, their localities, pearl culturing, grading systems, treatments, identification procedures and fashion. The book excels in its superb photography that makes it pleasing to look at and renders it a *Bildband* (picture book in German), in the true sense of the word. There are 153 photos that show both rare old pearl jewels and creations by modern designers. Many types of pearls are documented, including traditional types of both saltwater and freshwater origin and exotic ones such as abalone, conch and Melo pearls.

Chapter 1, titled 'What is a Pearl?', deals with the formation and structure of pearls (what the authors call the 'nature of pearls'). Explanations are short and precise, and transmit rather complicated facts in a way that is easy to understand for the beginner, even sometimes putting too much emphasis on simplicity. In this context, I was grateful to see the authors speaking of 'molluscs' and not of 'oysters' (with a few exceptions), thus applying correct terminology. However, I would have liked to see pearls from bivalve molluscs other than *Pinctada* included in the chapter (e.g. Quahog or *Tridacna* pearls), as well as those from other gastropods like *Turbo* or *Cassis*.

Chapter 2, on 'Pearl History', consists of neatly arranged passages that explain the appreciation and evaluation of pearls in human history. An entire chapter (Chapter 3) is dedicated to the history of pearls in India, going from antiquity to the present day; pearls still play an important role in Indian culture. The chapter emphasizes the Mughal period, which has witnessed perhaps the most sumptuous use of pearls in history, and it is illustrated by equally sumptuous, beautiful photographs. Chapter 4, 'Natural Pearl Localities', lists the main pearling areas in order of their importance in history, starting with the Gulf (in the text, the authors speak of the Arabian Gulf while geographically speaking it is still the Persian Gulf), the Red Sea and the Strait of Manaar, and ending with river pearls from China, Europe and the United States. The paragraph on Europe seems rather short, as for example pearls from Bavaria or Saxony are not mentioned. I found it interesting that this chapter explains the ancient bow drill method, a topic that is often neglected in other books.

Chapter 5, 'Cultured Pearl Markets', covers the entire history from the beginnings in Japan to the modern markets for South Sea and Tahitian cultured pearls, as well as China with its varieties of cultured pearl shapes and colours, again illustrated by beautiful photographs (e.g. 'soufflé pearls' and 'fireballs'). Chapter 6, 'Pearl Farming', describes each individual step from collecting or growing the host molluscs to the first harvest. Chapter 7 provides a fine description of the advanced analytical methods that are available for pearl identification, like microradiography, X-ray computed microtomography, infrared spectroscopy, EDXRF and LA-ICP-MS. The chapter is based on a comparison study of Gulf saltwater pearls and Tennessee freshwater pearls, and is exemplary for the methods in pearl testing today that allow for the exact distinction of both natural vs. cultured and saltwater vs. freshwater pearls. The reader learns valuable information and inevitably wants to know more.

Chapter 8, 'How GIA Classifies Pearls', is valuable indeed as GIA was the first institution worldwide to introduce a pearl grading system (which still sets the standard today). The chapter nicely illustrates how size, shape, colour (including overtone and orient), lustre, surface characteristics and matching are determined. Chapter 9, 'Treatments and Identification', reviews dyeing, bleaching, heating, irradiation, coating, polishing and filling. Methods of detection are explained, and in addition to the advanced techniques described in Chapter 7, simple methods are also referred to. Chapters 10 and 11 focus on different types of pearl jewellery and on the influence of fashion and design. Again, the many photographs provide a delight for the reader's eyes.

Every chapter is preceded by a poem that the authors have carefully selected from the literature, going back as far as the Persian poet Saadi, which adds another sophisticated aspect to the significance of pearls as an object of culture.

I found *Splendour and Science of Pearls* to be a very pleasant book to read and look at. It is logically structured and conveys all the necessary basic information in a clearly arranged way.

Elisabeth Strack

Wonders within Gemstones II

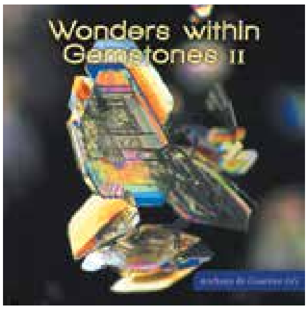

Anthony de Goutière, 2014. FriesenPress, Victoria, British Columbia, Canada, 72 pages, illus., softcover, http://anthonydegoutiere.com/the-book, ISBN 978-1460232774. US$23.99.

The new book by Anthony de Goutière is the most recent addition to many publications about the microscopic features of gem materials—in particular, inclusions and surfaces or fractures in gem crystals. This one is mainly artistic, and most of the photomicrographs can easily be viewed as abstract art. There are 60 pages of photos, containing 72 images of various sizes. The book is printed on matt rather than glossy paper, but the quality of the printing is very good. The most abundant gem materials featured in the book are topaz (24 pictures), beryl (17) and quartz (8).

I found a few errors in the descriptions of the photos. The origin of the moldavite on page 10 should be the Czech Republic, as Czechoslovakia has not existed since 1993, and moldavite comes from Bohemia, not Moravia. The 'silica outcrop' in moldavite on page 11 is formed by lechatelierite, which is the most diagnostic feature of genuine moldavite. The needles in a blue sapphire on page 16 are boehmite, not bhoemite. The inclusions in a topaz on page 38 are two-phase, not multi-phase. The red 'beetle-legs' on page 45 are described as lepidocrocite, but they are actually very thin hematite; true lepidocrocite has not been confirmed in quartz. The 'rutile' needles in quartz on page 54 are more probably tourmaline, as they are too white to be rutile. The hematite platelets on page 57 are most probably not in spectrolite (an almost opaque variety of labradorite), but rather are hosted by sunstone (a transparent variety of plagioclase).

However, none of the labelling errors diminish the overall quality of the photomicrography. Indeed, with this book, anybody—not only a gemmologist—can enjoy the beauty found in gems. The images are superb, and personally I would like to have some of them enlarged as posters to hang in my laboratory.

Jaroslav Hyršl

OTHER BOOK TITLES*

Coloured Stones

A Beautiful Hobby: Selecting, Salvaging, and Caring for Welo Ethiopian Opal
By Robert L. Nolan, 2014. Self-published, 160 pages, ISBN 978-0692234976. £14.63 softcover or £13.90 Kindle edition.

Geographic Origin Determination of Colored Gemstones
By Zhang Beili, Dietmar Schwarz and Taijin Lu, 2012. Geological Publishing House, Beijing, China, 330 pages, ISBN 978-7116808614 (in Chinese). ¥298.00 hardcover.

Kristallformen von Fluorit/Crystal Forms of Fluorite
By Eddy Van Der Meersche, 2014. Self-published, 296 pages, ISBN 978-9074669009 (in English/German). €45.00.

Organic Gems

Bone, Ivory, and Horn: Identifying Natural Materials
By Michael Locke, 2013. Schiffer Publishing, Atglen, Pennsylvania, USA, 320 pages, ISBN 978-0764343070. US$45.00 hardcover.

Pearl Gemology & Buying Guide: Everything You Need To Know About Pearl
By Milad Darejeh, 2013. Self-published, Notion Press, Chennai, Tamil Nadu, India, 114 pages, ISBN 978-9383185832. US$34.99 softcover.

Gem Localities

Fragile Black Heart—A Pictorial Journal of Lightning Ridge
By Lucy Di Paolo, 2014. Self-published, ISBN 978-1925086645. AU$41.95 hardcover, AU$24.95 DVD (30 minutes) or AU$12.00 eBook.

Lake Superior Agates: Identify Agates and Imposters
By James Magnuson and Carol Wood, 2013. Adventure Publications, Cambridge, Minnesota, USA, ISBN 978-1591934189. US$8.95 softcover.

Namibia Minerals and Localities
By Ludi von Bezing, Rainer Bode and Steffen Jahn, 2014. Bode Verlag GmbH, Salzhemmendorf-Lauenstein, Germany, 608 pages. €78.00 hardcover with DVD.

---

* Compiled by Georgina Brown and Brendan Laurs

Rockhounding New England: A Guide to 100 of the Region's Best Rockhounding Sites
By Peter Cristofono, 2014. FalconGuides, Guilford, Connecticut, USA, 320 pages, ISBN 978-0762783656. US$21.95 softcover.

Rockhounding New York: A Guide to the State's Best Rockhounding Sites
By Robert Beard, 2014. FalconGuides, Guilford, Connecticut, USA, 288 pages, ISBN 978-0762779000. US$19.95 softcover.

Sapphires in the Southwestern Part of the Rock Creek Sapphire District, Granite County, Montana
By Richard B. Berg, 2014. Montana Bureau of Mines and Geology Bulletin 135, Butte, Montana, USA, 86 pages. US$30.00 softcover.

General Reference

The Jeweler's Directory of Gemstones: A Complete Guide to Appraising and Using Precious Stones from Cut and Color to Shape and Settings
By Judith Crowe, 2012. Firefly Books, Richmond Hill, Ontario, Canada, 176 pages, ISBN 978-1770851085. £15.00 softcover.

Instruments and Techniques

Spectroscopic Methods in Mineralogy and Material Sciences
Ed. by Grant S. Henderson, Daniel R. Neuville and Robert T. Downs, 2014. *Reviews in Mineralogy and Geochemistry,* Vol. 78, Mineralogical Society of America, Chantilly, Virginia, USA, 800 pages, ISBN 978-1614517863. US$80.00 softcover or ebook.

Jewellery and *Objet d'Art*

20th Century Jewelry & the Icons of Style
By Stefano Papi and Alexandra Rhodes, 2013. Thames and Hudson Ltd., London, 272 pages, ISBN 978-0500516874. £35.00 hardcover.

Charles Edenshaw
By Dana Augaitis, Jim Hart and Robin K. Wright, 2013. Black Dog Publishing, London, 304 pages, ISBN 978-1908966209. £24.95 hardcover.

Da Gioielli ad Accessori Alla Moda [From Jewellery to Fashion Accessories]
By Barbara Bettoni, 2014. Marsilio Editori, Venice, Italy, 248 pages, ISBN 978-8831716161 (in Italian). €28.00 softcover.

Growing Talent: Jewellers and Silversmiths Nurtured by the Goldsmiths' Company
By The Goldsmiths' Company, 2013. The Goldsmiths' Company, London, 180 pages, ISBN 978-0907814320. £10.00 softcover.

Jewels and Jewellery
By Clare Phillips, 2014. V&A Publishing/Tokyo Bijutsu Co. Ltd., Tokyo, Japan, 176 pages, ISBN 978-4808709679. ¥3200 softcover.

***The Jewels of the Romanovs: Family & Court,* 2nd edn.**
By Stefano Papi, 2013. Thames and Hudson, London, 352 pages, ISBN 978-0500517062. £45.00 hardcover.

Mellerio dits Meller, Joaillier des Reines [Mellerio dits Meller, Jeweller to Queens]
By Vincent Meylan, 2013. Editions SW Télémaque, Paris, France, 448 pages, ISBN 978-2753301979 (in French). €27.00 softcover.

Out of this World! Jewelry in the Space Age
By Elyse Zorn Karlin, 2013. Flint Mine Press, New York, New York, USA, 52 pages, ISBN 978-0982520840. US$28.00 softcover.

Precious Materials in Asian History: Essays on Turquoise, Amber, Ivory, Diamond and Gold
By Berthold Laufer, 2014. Orchid Press, Hong Kong, 275 pages, ISBN 978-9745241091. US$45.00 softcover.

Vintage Jewellery Sourcebook
By Caroline Cox, 2014. Carlton Books, London, 64 pages, ISBN 978-1780974286. £5.99 softcover.

Social Studies

Dilemma of a Nation: Sierra Leone Blood Diamonds
By Alpha M. Barrie, 2014. CreateSpace Independent Publishing Platform, 122 pages, ISBN 978-1495296499. US$35.00 softcover.

Emerald City [Jaipur, India]
By Lawrence A. Babb, 2014. State University of New York Press, New York, USA, 232 pages, ISBN 978-1438445861. US$26.95 softcover or Kindle edition, or $80.00 hardcover.

Mining and Social Transformation in Africa: Mineralizing and Democratizing Trends in Artisanal Production
Ed. by Deborah Fahy Bryceson, Eleanor Fisher, Jesper Bosse Jønsson and Rosemarie Mwaipopo, 2014. Routledge, New York, USA, 248 pages, ISBN 978-0415709729. US$44.95 softcover.

Crown Color

Fine Rubies, Sapphires and Emeralds
Bangkok - Geneva - Hong Kong - New York

Crown Color is a proud supportor of the
Journal of Gemmology

Head Office: Crown Color Ltd., 14/F, Central Building, suite 1408
1-3 Pedder Street, Central Hong Kong SAR, Tel:+852-2537-8986
New York Office: +212-223-2363 | Geneva Office: +41-22-8100540

Stone Group Laboratories

Where technology and experience meet.

- Gem Identification
- Treatment Analysis
- Consultation
- Research

www.StoneGroupLabs.com

Gem-A
THE GEMMOLOGICAL ASSOCIATION
OF GREAT BRITAIN

Gem-A is getting social, so why not join us?

Gem-A is expanding its online activities – join us on Facebook, Twitter or LinkedIn.

fb.com/GemAofGB @GemAofGB

company/gem-a

Understanding Gems™

Visit www.gem-a.com

Think modular for your personal lab!

GEMMODUL®

New
MODUL 1
Polariscope and Docking Station for GemLED Refractometer

New
MODUL 2
Polariscope and Refractometer Illuminator Base

MODUL 3
Refractometer and Illuminator Base

MODUL 4
Polariscope

New
MODUL 5
Spectroscope and Coldlight Base

Modules combined into a GemLab at 2 1/2 feet

MODUL 6
UV LW/SW unit

www.eickhorst.com SYSTEM® EICKHORST Made in Germany

GEMMASTER®

ZEISS 10x – 80x

LEICA 10x – 48x/64x

Cool-touch LED daylight darkfield base

Examination of inclusions in immersion liquids

Hamburg / Germany · Tel. +49-40-514000-0 · Fax +49-40-514000-30 · info@eickhorst.com

Literature of Interest

Coloured Stones

Alien Sightings: Pallasite. B. Williams and C. Williams, *GemGuide,* March/April 2014, 7–9, http://gemguide.com/alien-sightings-pallasite.

Classification chimique des corindons par analyse factorielle discriminante: Application à la typologie des gisements de rubis et saphires [Chemical classification of corundum by discriminant analysis: Application to the type of ruby and sapphire deposits]. G. Giuliani, G. Caumon, S. Rakotosamizanany, D. Ohnenstetter and M. Rakotondrazafy, *Revue de Gemmologie,* **188**, 2014, 14–22 (in French with English abstract).

Comparative study on mineral components, microstructures and appearance characteristics of nephrite from different origins. L. Lu, Z. Bian, F. Wang, J. Wei and X. Ran, *Journal of Gems & Gemmology,* **16**(2), 2014, 56–64 (in Chinese with English abstract).

Exotic rocks in the jewellery trade: Dalmation Stone, Lotus Stone, Kabamba Stone. B. Bruder, *Gemmologie: Zeitschrift der Deutschen Gemmologischen Gesellschaft,* **63**(1/2), 2014, 35–42 (in German with English abstract).

Garnet: Common mineral, uncommonly useful. E.F. Baxter, M.J. Caddick and J.J. Ague, *Elements,* **9**(6), 2013, 415–419, http://dx.doi.org/10.2113/gselements.9.6.415.

Garnet: From stone to star. L. Galoisy, *Elements,* **9**(6), 2013, 453–456, http://dx.doi.org/10.2113/gselements.9.6.453.

Gemmological characteristics of light pink to pink beryls. B. Na, R. Sun, Z. Li and H. Liu, *Journal of Gems & Gemmology,* **16**(3), 2014, 32–37 (in Chinese with English abstract).

'Guaven-Quartz' – ein neuer pinkfarbiger Schmuckstein aus Brasilien ['Guava Quartz'—A new pink gemstone from Brazil]. U. Henn, R. Schultz-Güttler and T. Häger, *Gemmologie: Zeitschrift der Deutschen Gemmologischen Gesellschaft,* **63**(1/2), 2014, 43–47 (in German with English abstract).

Heat transport properties of cristobalite and discussion of "snowflake" formation. A.M. Hofmeister, *Canadian Mineralogist,* **51**, 2013, 705–714, http://dx.doi.org/10.3749/canmin.51.5.705.

Laser-induced time resolved luminescence of natural grossular $Ca_3Al_2(SiO_4)_3$. M. Gaft, H. Yeates, L. Nagli and G. Panczer, *Journal of Luminescence,* 137, 2013, 43–53, http://dx.doi.org/10.1016/j.jlumin.2012.11.015.

Is near-endmember birefringent grossular non-cubic? New evidence from synchrotron diffraction. S.M. Antao, *Canadian Mineralogist,* **51**, 2013, 771–784, http://dx.doi.org/10.3749/canmin.51.5.771.

A study of the inclusions in phenakite and the formation conditions of phenakite. G. Shijia and B. Feng, *Acta Petrologica et Mineralogica,* **32**(2), 2013, 180–188 (in Chinese with English abstract).

Three-phase inclusions in emerald and their impact on origin determination. S. Saeseaw, V. Pardieu and S. Sangsawong, *Gems & Gemology,* **50**(2), 2014, 114–132, http://dx.doi.org/10.5741/GEMS.50.2.114.*

The use of FTIR and Raman spectroscopy in the testing of *fei cui*: Jadeite, omphacite and kosmochlor. H.-P. Kan-Nyunt, B. Kwok and S.-L. Chan, *Journal of the Gemmological Association of Hong Kong,* **35**, 2014, 29–38, www.gahk.org/journal/GAHK_Journal_2014_v4.pdf.*

Diamonds

An analysis of the characteristics of brown diamonds from Mengyin in Shandong Province under transmission electron microscopy (TEM). G. Wu and X. Yu, *Acta Petrologica et Mineralogica,* **33**(2), 2014, 111–119 (in Chinese with English abstract).

Beyond Hope: Some other notable diamonds at the Smithsonian Institution—Part 3. R.C. Feather, *Rocks & Minerals,* **89**(5), 2014, 437–439, http://dx.doi.org/10.1080/00357529.2014.904667.

Botswana's scintillating moment. R. Weldon and R. Shor, *Gems & Gemology,* **50**(2), 2014, 96–113, http://dx.doi.org/10.5741/GEMS.50.2.96.

Morphology and spectral characteristics of octahedral diamond crystals from Yubileinaya diamond pipe (Yakutiya). L. Fang, *Journal of Superhard Materials,* **35**(4), 2013, 214–219, http://dx.doi.org/10.3103/S1063457613040023.

Reconstructing the Cullinan diamond. W.E. Wilson, *Mineralogical Record,* **45**(4), 2014, 457–463.

A study of the appearance of diamond: How human vision impacts brilliance and fire. Y. Shelementiev, G. Holloway, S. Sivovolenko, J. Mistry, R. Serov, G. Zhulin and K. Zipa, *Journal of the Gemmological Association of Hong Kong,*

Compiled by Brendan Laurs
* Article freely available for download, as of press time.

35, 2014, 48–56, www.gahk.org/journal/GAHK_Journal_2014_v4.pdf.*

Study on the evaluation of the crystal quality of diamonds. J. Liu, M. Chen, G. Wu and N. Gong, *Journal of Synthetic Crystals,* **43**(3), 2014, 559–564 (in Chinese with English abstract).

Fair Trade

Luxury and sustainable development: Is there a match? M.A. Achabou and S. Dekhili, *Journal of Business Research,* **66**(10), 2013, 1896–1903, http://dx.doi.org/10.1016/j.jbusres.2013.02.011.

Prospects for sustainability certification of metals. S.B. Young, Y. Zhe and G. Dias, *Metallurgical Research & Technology,* July 2014, http://dx.doi.org/10.1051/metal/2014008.

Films and Coatings

Diamond and diamond-like carbon. Z. Khalaj, M. Ghoranneviss, E. Vaghri and O. Ponta, in M.V. Diudea and C.L. Nagy (Eds.), *Diamond and Related Nanostructures,* Vol. 6 of *Carbon Materials: Chemistry and Physics 2013,* Springer, 2013, 29–47, http://dx.doi.org/10.1007/978-94-007-6371-5_2.

Hard graphite-like carbon coatings. L. Wang and Y. Wang, in Q.J. Wang and Y.-W. Chung (Eds.), *Encyclopedia of Tribology,* Springer, 2013, 1615–1619, http://dx.doi.org/10.1007/978-0-387-92897-5_1243.

Gem Localities

Colorful agate and jasper of southeastern Utah. R.D. Dayvault, *Rocks & Minerals,* **89**(4), 2014, 308–327, http://dx.doi.org/10.1080/00357529.2014.904661.

Gelber Mondstein aus Tansania [Yellow moonstone from Tanzania]. U. Henn and F. Schmitz, *Gemmologie: Zeitschrift der Deutschen Gemmologischen Gesellschaft,* **63**(1/2), 2014, 47–51 (in German with English abstract).

The gems of East Africa. R. Weldon, *GemGuide,* July/August 2014, 1–5, http://gemguide.com/the-gems-of-east-africa.

Is Myanmar jadeitite of Jurassic age? A result from incompletely recrystallized inherited zircon. T.-F. Yui, M. Fukoyama, Y. Iizuka, C.-M. Wu, T.-W. Wu, J.G. Liou and M. Grove, *Lithos,* 160–161, 2013, 268–282, http://dx.doi.org/10.1016/j.lithos.2012.12.011.

Quartz with sagenitic rutile inclusions from Myanmar. K. Schmetzer and M.P. Steinbach, *Australian Gemmologist,* **25**(5), 2014, 175–177.

Up from the depths: Underwater recovery of agates from Lake Superior, Keweenaw County, Michigan. T. Rosemeyer, *Rocks & Minerals,* **89**(4), 2014, 346–353, http://dx.doi.org/10.1080/00357529.2014.904668.

Instruments and Techniques

Raman spectroscopy as a tool for garnet analysis and investigation on samples from different sources. T. Ganetsos, T. Katsaros, P. Vandenabeele, S. Greiff and S. Hartmann, *International Journal of Materials and Chemistry,* **3**(1), 2013, 5–9.

La spectrométrie d'émission accessible à tous [Portable emission spectrometry]. D. Peyresaubes, M. Schoor and J.-C. Boulliard, *Revue de Gemmologie,* **188**, 2014, 24–28 (in French).

Miscellaneous

Duo valuation of an unusual ruby. S.M. Robertson, *GemGuide,* July/August 2014, 12–13, http://gemguide.com/duo-valuation-of-an-unusual-ruby.

Globalization, recession and the internationalization of industrial districts: Experiences from the Italian gold jewellery industry. V. De Marchi, J. Lee and G. Gereffi, *European Planning Studies,* **22**(4), 2014, 866–884, http://dx.doi.org/10.1080/09654313.2013.771624.

News Press

Cutting edge science used to ID natural pearls. S. Smith, *BBC News,* Science & Environment, 20 May 2014, www.bbc.com/news/science-environment-27374296.*

8.41-carat purple-pink diamond may fetch $15 million. A. DeMarco, *Forbes, Lifestyle,* 18 August 2014, http://lifeforb.es/1pqROI1.*

Global gold jewelry demand down 30% led by declines in China and India. A. DeMarco, *Forbes, Lifestyle,* 15 August 2014, http://tinyurl.com/mt9x6l3.*

Are museums selling out? E. Gamerman, *The Wall Street Journal,* Arts & Entertainment, 12 June 2014, http://online.wsj.com/articles/are-museums-selling-out-1402617631.

Rare 12-carat 'Blue Moon' diamond to be unveiled at L.A. Natural History Museum. A. DeMarco, *Forbes, Lifestyle,* 24 August 2014, http://lifeforb.es/1vLjnLR.*

Sparkling fall 2014 jewelry preview (Part 1). A. DeMarco, *Forbes, Lifestyle,* 25 August 2014, http://lifeforb.es/1vLjsPx.*

Organic Gems

Analysis of gemmological characteristics of Burma amber. Z. Bian, *China Gems & Jades,* May 2014 Supplement, 158–165 (in Chinese).

Analysis on organic elements and content variation of amber, treated ambers and copals from different producing areas around the world. Y. Wang, M. Yang and P. Niu, *Journal of Gems & Gemmology,* **16**(2), 2014, 10–16 (in Chinese with English abstract).

Color phenomena of blue amber. Y. Liu, G. Shi and S. Wang, *Gems & Gemology,* **50**(2), 2014, 134–140, http://dx.doi.org/10.5741/GEMS.50.2.134.

Experimental studies on the heat treatment of Baltic amber. Y. Wang, M. Yang and Y. Yang, *Gems & Gemology,* **50**(2), 2014, 142–150, http://dx.doi.org/10.5741/GEMS.50.2.142.

Pearls

A study of the Raman spectra of black natural and treated cultured pearls. G. Li and M. Zeng, *Acta Petrologica et Mineralogica,* **33**(2), 2014, 153–156 (in Chinese with English abstract).

Spectral identification characteristics of superficial-layer dyed golden seawater cultured pearls. D. Zhou and L. Li, *Journal of Gems & Gemology,* **16**(2), 2014, 71–77 (in Chinese with English abstract).

Variations in content of Mg, Fe, Zn and Mn in cultured seawater pearls and their influence on microstructure. L. Yang, Q.-Q. Ouyang, S.-D. Li, J. Chen and D.-N. He, *Acta Mineralogica Sinica,* **34**(3), 2014, 416–420 (in Chinese with English abstract).

Synthetics and Simulants

Analysis of CVD synthetic diamond by FTIR and Raman spectrometry. G. Wu, M. Chen, J. Liu, J. Liao and N. Gong, *Acta Mineralogica Sinica,* **34**(3), 2014, 411–415 (in Chinese with English abstract).

Mechanism and characteristics of synthetic diamond treated into red color. B. Cao, M. Chen, W. Hu and J. Zhang, *Journal of Gems & Gemology,* **16**(3), 2014, 24–31 (in Chinese with English abstract).

A tentative discussion on coloration genesis and color change mechanism of HPHT synthetic diamond. Y. Xue, X. He and T. Xie, *Acta Petrologica et Mineralogica,* **33**(2), 2014, 120–130 (in Chinese with English abstract).

Une méthod simple pour différencier les amétrines naturelles des amétrines synthetiques [A simple method to differentiate natural ametrines from synthetic ametrines]. F. Payette, *Revue de Gemmologie,* **188**, 2014, 4–12 (in French).

Treatments

Identification method of filled emerald: Taking DiamondView™ for example. X. Liu, H. Tang and C. Tu, *Journal of Gems & Gemology,* **16**(2), 2014, 17–26 (in Chinese with English abstract).

Issues with treated and natural green to greenish blue diamonds. F. Notari and T. Hainschwang, *GemGuide,* May/June 2014, 1–4, http://gemguide.com/issues-with-treated-and-natural-green-to-greenish-blue-diamonds.

A new enhancement method of gemstone ion implantation technique. Y. Cheng, H. Zhu, J. Li and C. Fan, *Journal of Gems & Gemology,* **16**(2), 2014, 6 5–70 (in Chinese with English abstract).

Compilations

Gem News International. Jadeite bangle with the appearance of polymer treatment • Prasiolite with inclusion influenced by Brazil-law twinning • Natural moissanite crystals from Israel • Unusual optical effect in blue sapphire • Assemblage of synthetic ruby in calcite matrix • Composite coral veneer glued to artificial matrix • Dyed bone as a red coral imitation • Bumble Bee 'jasper' from Indonesia • Pyrex bracelets • Shattuckite from the DRC • Shanghai jewellery show • Museum exhibits at GIA New York. *Gems & Gemology,* **50**(2), 2014, 158–169, www.gia.edu/gems-gemology.*

Gemmological Intelligence. Australian iris agate • Fungus-coated insect in Baltic amber • Zoned diamond slice with hollow tubules from Marange, Zimbabwe. *Australian Gemmologist,* **25**(5), 2014, 192–193.

Gemmologie Aktuell [Gemmology Up-to-date]. Corundum with coloured lead-glass fillings • Dyed labradorite • Dyed quartz passed off as jade • Smoked opal from Ethiopia • 'Alexite' glass as an imitation for colour-change diaspore ('zultanite') • 'Cherry quartz', 'pineapple quartz' and 'kiwi quartz' as well as 'pink amethyst'. *Gemmologie: Zeitschrift der Deutschen Gemmologischen Gesellschaft,* **63**(1/2), 2014 (in German and English).

Lab Notes. Chameleon diamond with Ni absorption band • Durability of CVD synthetic film on natural diamond • Star opal • Shell pearl as a pearl imitation • Yellow CVD synthetic diamond • Flux-grown synthetic ruby with hydrothermal synthetic seed crystal • Faceted wurtzite • Tenebrescent zircon. *Gems & Gemology,* **50**(2), 2014, 151–157, www.gia.edu/gems-gemology.*

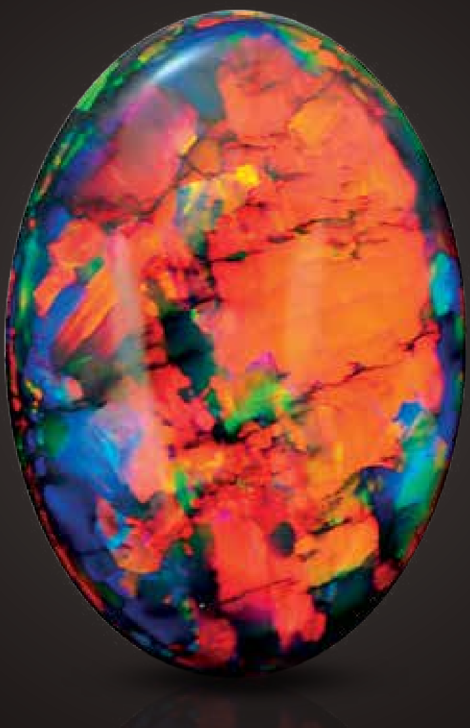

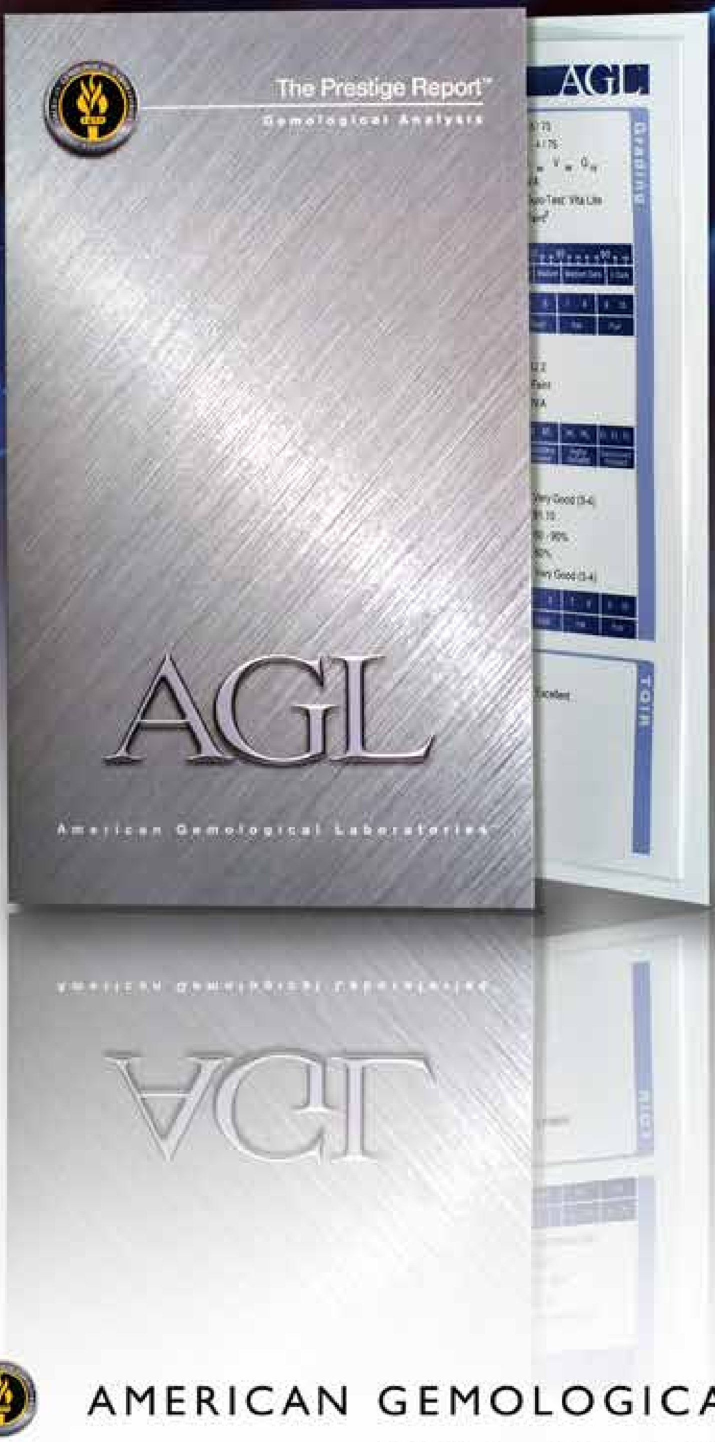
The Prestige Report™
Gemological Analysis
AGL
American Gemological Laboratories™
AGL
Grading

Gem-A
THE GEMMOLOGICAL ASSOCIATION
OF GREAT BRITAIN

Book now for the
Gem-A Conference 2014

SATURDAY 1 AND SUNDAY 2 NOVEMBER

Business Design Centre, Islington, London

Gem-A will host its internationally acclaimed annual conference from Saturday 1 to Tuesday 4 November. Welcoming a host of world-renowned speakers and delegates from across the globe, and with a reputation for tackling the most innovative and contemporary gem-related topics in the trade, this event is not to be missed!

On Saturday night there will be a dinner open to all delegates.

Saturday 1 November speakers

- **Bruce Bridges**
  The history of tsavorite and legacy of Campbell Bridges
- **Edward Boehm GG CG**
  Analyzing gems on the go: tips from the field
- **Dr Thomas Hainschwang FGA**
  The challenges faced by green to greenish blue diamonds coloured by natural or artificial irradiation
- **Alan Hart FGA DGA**
  Gems at the Natural History Museum: a review and a forward look
- **Dr Ulrich Henn**
  The different types of moonstone
- **Brian Cook**
  Paraíba tourmaline: an update
  Bahia golden rutilated quartz: an introduction
- **Vincent Pardieu GG**
  From Jedi to Windex: a quest to the origins of the ultimate red and blue spinels

Sunday 2 November speakers

- **Craig Lynch GG**
  The recovered jewellery of *RMS Titanic*
- **Dr Laurent Cartier FGA**
  An update on worldwide cultured pearl production
- **Chris Smith FGA GG**
  Ruby and sapphire source-type classification: an objective approach to help make country-of-origin determinations more consistent
- **Dr Menahem Sevdermish FGA**
  Further developments into digital colour analysis, grading, pricing and trading of gems
- **Terry Coldham FGAA**
  Australian sapphire — a forgotten foundation stone of Thailand’s gemstone industry
- **Richard Hughes FGA, with special guest John Saul**
  Heretical gemmology

MONDAY 3 NOVEMBER

Seminars

Gem-A Headquarters, 21 Ely Place, London EC1N 6TD

- **Richard Drucker FGA GG, President of GemWorld International Inc.**
  Coloured Stone Grading and Pricing Workshop
- **Mikko Åström FGA and Alberto Scarani GG, GemmoRaman**
  Applications of Raman and Photoluminescence Spectroscopy
- **Dr Franz Herzog** NEW
  A portable EDXRF device in gemmology: toy or dream?

TUESDAY 4 NOVEMBER

Visit to the Natural History Museum

FULLY BOOKED

Global ethical challenges within the industry

Gem-A Headquarters, Ely Place, London

Seminar with Greg Valerio, founder of CRED Jewellery and co-founder of Fair Jewellery Action, Vivien Johnston, trained goldsmith and founder of Fifi Bijoux, and Dana Schorr, coloured gemstone importer and president of Schorr Marketing.

Major sponsor
jewelry television
jtv.com

Sponsor
The Company of Master Jewellers
cibjo
The World Jewellery Confederation
GemmoRaman 532

Supporters
AnchorCert Gem Lab
Institute of Registered Valuers
GEMWORLD
Marcus McCallum FGA
C·W·SELLORS
Fine Jewellery

Associate Supporters
BJA
Apsara Gems
T.H.MARCH

Understanding Gems

Visit www.gem-a.com

To book contact
events@gem-a.com